

### **3. Experimentelle Arbeiten**

#### **3.1 Tierexperimentelle Studien zum geschlossenen Weichteiltrauma**

##### **3.1.1 In vivo Analyse der Mikrozirkulation im Skelettmuskel der Ratte nach geschlossenem Weichteiltrauma**

Im Zentrum der ersten Untersuchungen stand zunächst die Klärung der Frage, inwieweit eine traumatisch-induzierte mikrozirkulatorische Dysfunktion die Basis für den progressiven Verlauf schwerer geschlossener Weichteilschäden darstellt.

Aufgrund der Tatsache, dass bisher kein valides Tiermodell des geschlossenen Weichteilschadens beschrieben wurde, ist zunächst ein standardisiertes Tiermodell des traumatisch geschlossenen Weichteilschadens, welches eine *in-vivo*-Analyse und Quantifizierung der Mikrozirkulation erlaubt, etabliert worden (123, 150). Hierzu wurde die zur standardisierten Induktion schwerer Schädelhirntraumen entwickelte Computer-assoziierte Controlled-Impact-Injury-Technik (33, 100) für die Weichteiltraumatisierung der Extremitäten modifiziert. Mit Hilfe dieser standardisierten Technik konnte die klinische Situation einer durch ein Hochrasanztrauma induzierten schweren isolierten Weichteilverletzung (ohne Fraktur) im Tiermodell der Ratte realitätsnah und in Analogie zu einer humanen GII-III-Verletzung nach TSCHERNE (178) simuliert werden. Nach mikrochirurgischer Präparation des M. extensor digitorum longus (180) wurden mit Hilfe der intravitalem Fluoreszenzmikroskopie die posttraumatischen Veränderungen in der mikrovaskulären Perfusion und Entzündungsreaktion über einen Zeitraum bis zu 5 Tagen post Trauma analysiert und quantifiziert. Gleichzeitig wurde der intramuskuläre Druck und Wassergehalt zur Bestimmung des Ödems erfasst.

So war es bisher unklar, ob und in welchem Ausmaß ähnliche Mikrozirkulationsstörungen, wie sie für das Ischämie-/Reperfusionssyndrom pathognomonisch sind, auch beim traumatischen Weichteilschaden von pathophysiologischer Relevanz sind. Konkrete Ergebnisse in der Mikrozirkulationsanalyse des Skelettmuskels nach schweren, geschlossenen Weichteilschäden sind im folgenden aufgeführt:

- Die Mikrozirkulation des geschlossenen traumatisierten Skelettmuskels der Ratte lässt sich zuverlässig und mit sehr guter Bildqualität für einen Zeitraum von bis zu 5 Tagen nach Trauma mittels intravitale Fluoreszenzmikroskopie direkt quantitativ analysieren (123).
- Wie durch diese Studien gezeigt werden konnte, kommt es beim geschlossenen traumatisch bedingten Weichteilschaden zu protrahierten pathologischen Veränderungen der nutritiven Perfusion. Diese sind mit einer signifikanten Zunahme der mikrovaskulären Permeabilität (makromolekulare Leakage) als Anzeichen eines sich progressiv entwickelnden Endothelzellschadens vergesellschaftet. Weiterhin führt der geschlossene traumatische Weichteilschaden zu einer massiven traumatisch-induzierten Entzündungsreaktion, die durch eine drastische Zunahme der Akkumulation und Adhärenz von Leukozyten am mikrovaskulären Endothel postkapillärer Venolen gekennzeichnet ist. Das gleichzeitige posttraumatische Auftreten von mikrovaskulärem Perfusionsversagen, erhöhter mikrovaskulärer Permeabilität für plasmatische Makromoleküle, Leukozytenadhärenz und intramuskulärer Drucksteigerung sowie Ödem (Maximum erst 24-72h post Trauma) lässt somit auf eine kausale Bedeutung der Mikrozirkulationsstörung für die Entwicklung des Sekundärschadens schließen (123, 150).

## *In Vivo* Analysis of Microcirculation following Closed Soft-Tissue Injury

Klaus-D. Schaser, \*Brigitte Vollmar, \*Michael D. Menger,  
Lioba Schewior, †Stefan N. Kroppenstedt, Michael Raschke,  
‡Andreas S. Lübbe, Norbert P. Haas, and Thomas Mittlmeier

*Departments of Trauma and Reconstructive Surgery and †Neurosurgery, Charité, Campus Virchow-Clinic, Humboldt-University of Berlin, Berlin; \*Institute for Clinical and Experimental Surgery, University of Saarland, Homburg/Saar; and ‡Department of Oncology, Cecilien-Clinic, Bad Lippspringe, Germany*

---

**Summary:** Major loss of tissue is an almost invariable consequence of severe closed soft-tissue injury. Clinically, the extent of soft-tissue trauma determines the outcome of complex injuries and significantly influences bone healing. With use of a new animal model, this study quantitatively analyzed microcirculation, i.e., nutritive perfusion and leukocyte-endothelial cell interaction, in skeletal muscle after standardized closed soft-tissue injury. By means of a computer-assisted controlled-impact technique, a severe standardized closed soft-tissue injury was induced in the left hindlimb of 28 rats. The rats were assigned to four experimental groups (n = 7 per group) that differed by time of analysis (1.5, 24, 72, and 120 hours after injury); rats that were not injured served as controls (n = 7). Intramuscular pressure was measured, and microcirculation in the rat extensor digitorum longus muscle was analyzed by *in vivo* fluorescence microscopy, which allowed assessment of microvascular diameters, functional capillary density, number of rolling and adherent leukocytes in venules, and microvascular permeability. Edema weight gain was quantified by the ratio of wet to dry weight of the extensor digitorum longus muscle. Microvascular perfusion of the skeletal muscle was characterized by a significant reduction in functional capillary density, which was paralleled by an increase in capillary diameter throughout the 120 hours of observation when compared with the controls. Trauma-induced inflammatory response was reflected by a markedly increased rolling and adherence of leukocytes, primarily restricted to the endothelium of postcapillary venules; this was accompanied by increased microvascular permeability, indicative of a substantial loss of endothelial integrity. The microcirculation surrounding the core of the damaged tissue area resembled that of ischemia-reperfusion injury in skeletal muscle, i.e., heterogeneous capillary perfusion, pronounced microvascular leakage, and adherence of leukocytes. Enhanced vascular leakage and leukocyte adherence (24-72 hours after injury) coincided with the maximum intramuscular pressure (which was not indicative of compartment syndrome) and edema formation. These results demonstrate that initial changes, leading to ultimate tissue death, after closed soft-tissue injury are caused on the microcirculatory level. This standardized model provides further insight into microvascular pathophysiology and cellular interactions following closed soft-tissue injury. Thus, it is an adequate tool for testing novel therapeutic interventions.

---

Among the many factors that determine the outcome of complex injuries, the role of closed soft-tissue damage remains only partly understood. Clinically, the extent of soft-tissue damage significantly determines the process of bone healing, the guidance of fracture management, and patient prognosis. The underlying pathophysiological mechanisms of closed soft-tissue damage are just now being understood (4,20,42,48). Factors limiting our understanding of

closed soft-tissue injury include (a) difficulties, due to the lack of specific and noninvasive diagnostic tools, in evaluating the extent of the injury, (b) a limited number of clinical trials, (c) the absence of appropriate, standardized animal models of clinical relevance, and (d) unidentified pathways triggering the prolonged propagation and progressive course of the injury as noted clinically. Despite these limitations, management of severe closed soft-tissue injury is an exceptional clinical challenge (11,26,36,37,45). There is clear evidence that specific and efficient therapeutic interventions must be directed to early stages of the injury because the end stage, which is complicated by infected hematoma or extensive myonecrosis, responds minimally to treatment (25-27,37,45). Under-

---

Received June 15, 1998; accepted March 22, 1999.

Address correspondence and reprint requests to K-D. Schaser at Unfall- und Wiederherstellungschirurgie, Charité, Medizinische Fakultät der Humboldt, Universität zu Berlin, Campus Virchow Klinikum, Augustenburger Platz 1, D-13353 Berlin, Germany. E-mail: kschaser@charite.de

standing why initially viable tissues become necrotic over time in closed soft-tissue injury may therefore assist in improving therapeutic regimens aimed at restricting tissue damage. However, a valid and clinically relevant model of standardized closed soft-tissue injury, caused by high-velocity trauma without induction of fracture or compartment syndrome, remains to be established. The significance of high-velocity injuries to the limbs is of particular importance because most severe soft-tissue injuries occur in high-energy accident victims.

With injury, ischemia, or infection, inflammatory reactions in severely damaged and necrotic skeletal muscle can destructively affect the surrounding tissue (43). These deleterious changes, in conjunction with the progressive course of closed soft-tissue injury, may be caused and preceded by microcirculatory alterations below the level of compartment syndrome. Therefore, this study evaluates the hypothesis that progressive tissue damage following severe closed soft-tissue injury is secondary to delayed and prolonged microvascular perfusion failure (decreased nutritive perfusion independent of its cause) or increased leukocyte recruitment (leukocyte rolling and adherence to the microvascular endothelium as a prerequisite for transendothelial emigration and extravasation of these cells [2] to the focus of inflammation), or both. To test this hypothesis, the present study aimed to quantitatively analyze, with use of a new animal model, the microcirculation, i.e., nutritive perfusion and leukocyte-endothelial cell interaction, in skeletal muscle following standardized closed soft-tissue injury.

## MATERIAL AND METHODS

### Animal Model, Impact Device, and Surgical Preparation

All experimental procedures were performed with ethical permission from the local animal rights protection authorities and followed the National Institutes of Health guidelines for the use of laboratory animals.

After 3 days of acclimatization to the laboratory, 35 male Sprague-Dawley rats (weight: 250-300 g) were anesthetized with intraperitoneal injections of ketamine (90 mg/kg body weight, Ketavet; Pharmacia and Upjohn GmbH, Erlangen, Germany) and xylazine (10 mg/kg body weight, Rompun; Bayer, Leverkusen, Germany). Additional doses of ketamine and xylazine were given to maintain anesthesia throughout the experiment. This anesthesia was chosen because ketamine has been shown to depress the cardiovascular and respiratory systems and deregulate capillary perfusion of skeletal muscle to a lesser extent than pentobarbital or propofol (14).

Before surgical preparation, the rats underwent a tracheotomy and were intubated to maintain open airways. A venous catheter (0.58-mm inner diameter, polyethylene 50 [PE50]; Portex; Hythe, Kent, England) was inserted through the right external jugular vein into the superior caval vein. The ascending aorta was cannulated (PE50) through the right common carotid artery (PE50) to measure the heart rate and arterial blood pressure. Body temperature was maintained at 37°C with use of a temperature-controlled

heating pad. Systemic blood pressure and heart rate were monitored with a digital blood-pressure analyzer (Digimed; Micro-med, Louisville, Kentucky, U.S.A.).

Closed soft-tissue damage to the anterolateral compartment of the left hindlimb of the rat was induced with a modified controlled-impact device. This location was selected for its resemblance to the clinical situation of trauma to the lower extremities. The controlled-impact technique was initially developed as a model of experimental traumatic brain injury in rats, reproducing the pathophysiological and morphological responses of severe closed head injury as found in humans (10,28). The controlled-impact device consists of a compressed nitrogen gas source, an adjustable impactor, a displacement transducer, and a personal computer-assisted interface for data transmission and analysis of time/displacement parameters of the impact. Impact velocity was 7 m/sec, depth of deformation was 11 mm, impact duration was 100 milliseconds, and impact diameter was 11 mm. The left hindlimb was positioned in a plastic mold (Technovit; Kulzer, Wertheim, Germany) shaped like the hindlimb to ensure optimal energy transmission to the tissue by avoiding hindlimb movement during the impact.

At the end of each observation period, the rat extensor digitorum longus muscle preparation, as described by Tymi and Budaire (52), was modified for *in vivo* microscopy of the skeletal muscle tissue. The muscle was carefully exposed on its total length by retraction of the overlying muscles and fascia. To retract neighboring tissue and secure the hindlimb in a flat position, sutures were placed on the margin of the anterior tibialis and soleus muscles. Thus, *in vivo* microscopic analysis of the microcirculation in the entire extensor digitorum longus muscle was permitted, particularly in areas remote from the central impact site. Throughout the surgical procedure, the preparation was irrigated with physiological saline solution to prevent drying. To minimize tissue dehydration and interference with ambient oxygen during *in vivo* microscopy, the surface of the exposed muscle was covered with a glass coverslip.

### Experimental Groups and Protocol

Analysis of microcirculation did not begin until 20-30 minutes after preparation. The rats were assigned to four experimental groups that differed by the time of analysis, i.e., 1.5, 24, 72, or 120 hours after injury; sham-operated animals that were not injured served as controls ( $n = 7$  for all groups). Due to the short observation period, rats from the control group and from the group observed at 1.5 hours underwent a single anesthesia for implantation of catheters, induction of closed soft-tissue trauma, measurement of tissue pressure, and *in vivo* fluorescence microscopy. The rats from the other experimental groups were anesthetized for a brief time for production of closed soft-tissue injury and were returned to their cages and allowed to recover for 24, 72, or 120 hours. After the recovery period, the rats were anesthetized again for measurement of intramuscular pressure, surgical preparation, and subsequent microvascular observations. After production of closed soft-tissue injury and throughout the entire observation period, awake and traumatized animals had full weight-bearing of the injured extremity and no obvious signs of pain or immobilization. In particular, no changes in feeding or sleeping habits were observed.

Before the extensor digitorum longus muscle was surgically prepared, the intramuscular pressure in the anterior and posterior tibial compartments was measured with a microsensor catheter (0.7-mm outside diameter, Codman microsensors; Johnson and Johnson, Raynham, MA, U.S.A.) that was connected to a pressure transducer. Without significant local hemorrhage, the skin and fascia in the middle of the anterolateral and posterolateral tibial compartments were penetrated with a cannula (1.7-mm outside diameter; Ohmeda, Helsingborg, Sweden). After the metal needle was completely retracted, the microsensors were inserted through

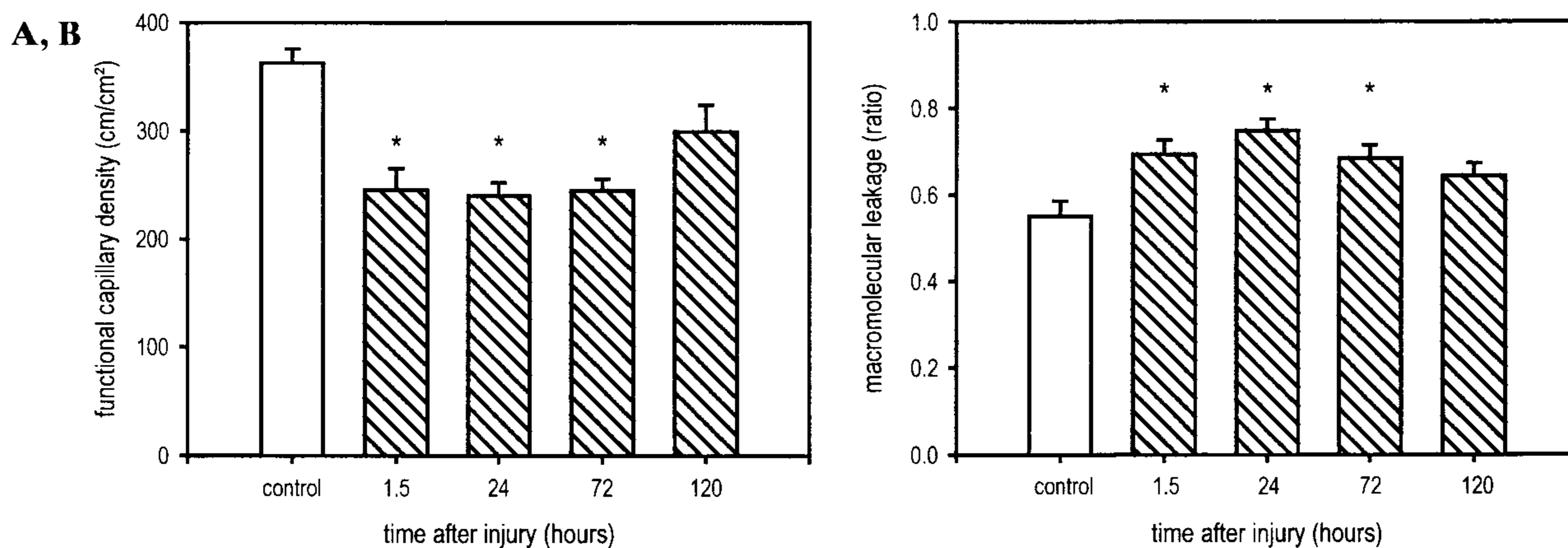


**FIG. 1. A:** Functional capillary density (length of perfused capillaries per observation area;  $\text{cm}^{-1}$ ) and **B:** microvascular permeability (leakage of fluorescein isothiocyanate-labeled dextran, assessed densitometrically by the ratio of extravascular to intravascular fluorescence intensity) 1.5, 24, 72, and 120 hours after trauma. Hatched bars: experimental groups,  $n = 7$  per time point; open bars: controls,  $n = 7$ . Values are mean  $\pm$  SEM. \* $P < 0.05$  compared with controls.

the outer plastic tube to the desired intramuscular position (8 mm underneath the skin). Thereafter, the outer plastic-shielding tube was withdrawn to guarantee that only tissue from the tibialis muscle surrounded the tip of the microsensors during measurement of tissue pressure.

For *in vivo* microscopy, the surface of the extensor digitorum longus muscle was sequentially scanned from the distal to the proximal part in approximately 2-mm steps with use of a computer-assisted microscope stage equipped with a stepping motor (MC 2000; Merzhäuser, München, Germany). To reliably assess microcirculation in the muscle, microscopic images from at least eight observation areas in each muscle were recorded. Values obtained for each of these areas were averaged per animal.

The rats were killed at the end of the microscopic procedures, and the left (injured) and right (not injured) extensor digitorum longus muscles were harvested for determination of edema formation by measurement of the ratio of wet to dry weight in the muscle. Edema weight gain was assessed by calculating the edema index (experimental/contralateral limb).

### In Vivo Microscopy

The microvasculature of the extensor digitorum longus muscle was investigated in epi-illumination (100-W mercury lamp) through an *in vivo* microscope (Optiphot; Nikon, Tokyo, Japan) equipped with a water-immersion objective ( $\times 20$ ) and fluorescence filters for visualization of fluorescein isothiocyanate-labeled dextran (450-490/ $>580$  nm) and rhodamine (530-560/ $>580$  nm). With a final magnification of  $\times 940$ , microcirculatory images were recorded for 60 seconds with use of a CCD video camera (FK 6990-IQ; Pieper, Schwerte, Germany) connected to an SVHS video recorder (HR-S4700EG/E; JVC, Friedberg, Germany) and stored on videotapes for off-line evaluation. Prior to microscopy, a single bolus of fluorescein-isothiocyanate-labeled dextran (5%, 150,000 MW, 15 mg/kg body weight; Sigma Chemical, Deisenhofen, Germany) and rhodamine 6G (0.1%, 0.15 mg/kg body weight; Sigma Chemical) was injected intravenously to enhance the contrast of the vascular network and to perform *in vivo* staining of leukocytes (6,33,49). To minimize the phototoxic effects of the high-energy light on the tissue, each observation period was limited to a maximum of 60 seconds (44,49).

### Analysis of Microcirculation

Microvessel diameters, functional capillary density (total length of perfused capillaries per observation area [ $\text{cm}/\text{cm}^2$ ]), and microvascular permeability were determined by a computerized microcirculation image-analysis system (Cap Image; Zeintl, Heidelberg,

Germany) (23,53). With use of a densitometric technique, macromolecular leakage was assessed in several fields per image and expressed as the ratio of fluorescence to density selected from the perivascular area to the corresponding intravascular area (plasma gaps in the microvessels between erythrocytes) (22,23). Leukocyte-endothelium interaction was quantified by counting the number of rolling and permanently adherent leukocytes as well as the total leukocyte flux along a 100- $\mu\text{m}$  venular segment. Rolling leukocytes were defined as those moving along the vessel wall at a velocity less than 40% that of leukocytes at the center line and were expressed as a percentage of the total leukocyte flux. Leukocyte adherence was given as the number of leukocytes not moving or detaching from the endothelial lining of the postcapillary vessel wall during an observation period of 20 seconds; it was expressed as cells/ $\text{mm}^2$  of endothelial surface, calculated from the diameter and length (100  $\mu\text{m}$ ) of the microvessel segment and assuming cylindrical geometry.

### Statistics

Results are given as mean  $\pm$  SEM. One-way analysis of variance for independent samples and a Tukey-B test for multiple comparison procedures with Bonferroni correction for multiple measurements were used to compare differences in microvascular diameters, permeability, leukocyte rolling and sticking, intramuscular pressure, water content, and edema index between the groups. Differences were significant at  $p < 0.05$ .

## RESULTS

### Macrohemodynamics

Mean arterial blood pressure generally ranged from 80 to 115 mm Hg and did not change significantly during the course of the experiments in the different experimental groups compared with that in the controls. Heart rate was in the range of 248-332 beats/min and did not differ between groups. Although administration of fluorescein isothiocyanate-labeled dextran has been reported to cause anaphylactic-like responses in Sprague-Dawley rats, we did not observe any of these changes. In particular, no cardiorespiratory distress, hypotension, or inflammatory erythema or edema of snout, ears, or paws was observed at any time point during the study.

**TABLE 1.** Leukocyte-endothelial cell interaction in the extensor digitorum longus muscle of controls and experimental rats at different time points (hours) after closed soft-tissue injury

	Leukocyte rolling <sup>a</sup>	Leukocyte adherence <sup>b</sup>
Control	21.3 ± 2.6	157.9 ± 25.1
1.5	38.9 ± 3.1 <sup>c</sup>	915.9 ± 165.4 <sup>c</sup>
24	32.9 ± 4.1 <sup>c</sup>	994.7 ± 125.3 <sup>c</sup>
72	45.6 ± 1.0 <sup>c</sup>	623.9 ± 64.0
120	36.7 ± 1.7 <sup>c</sup>	1,096.7 ± 136.9 <sup>c,d</sup>

<sup>a</sup> Percentage of total leukocyte flux.

<sup>b</sup> 1/mm<sup>2</sup> endothelial surface.

<sup>c</sup> P < 0.05 compared with controls.

<sup>d</sup> P < 0.01 compared with controls.

### Nutritive Capillary Perfusion

Closed soft-tissue injury resulted in a significant reduction in functional capillary density throughout the 120-hour observation period (Fig. 1A); it was maximally decreased 1.5-72 hours after the trauma. At the core of the tissue damage, the reduction in functional capillary density was predominantly related to a decline in the number of perfused capillaries; in areas of the extensor digitorum longus muscle remote from the central impact site, however, the reduction was mainly caused by an increase in intercapillary distance. Also, the marked decrease in functional capillary density was associated with an increase in capillary diameter. The capillary diameters measured at 1.5 ( $5.2 \pm 0.1 \mu\text{m}$ ) and 24 ( $5.7 \pm 0.7 \mu\text{m}$ ) hours were comparable with control values ( $5.1 \pm 0.2 \mu\text{m}$ ). At 72 hours, the capillary diameter ( $6.3 \pm 0.4 \mu\text{m}$ ) was significantly ( $p < 0.05$ ) increased and remained dilated to 120 hours after the trauma ( $5.7 \pm 0.3 \mu\text{m}$ ). Furthermore, these

effects were accompanied by a substantial loss of endothelial integrity as assessed by macromolecular leakage into the perivascular space (Fig. 1B). Microvascular permeability was significantly increased at 1.5, 24, and 72 hours following trauma and was most pronounced in the vicinity of postcapillary venules (Fig. 2A).

Finally, closed soft-tissue injury characteristically induced the occurrence of a transitional region surrounding the core of the damaged zone. Besides directly destroyed microvessels, total microvascular perfusion failure with development of thrombosis, narrowing and collapse of nutritive capillaries with maximum microvessel leakage were found in the core of the damage. The transitional zone, however, had a heterogeneous perfusion pattern, consisting of a patchwork of microvascular thrombosis and perfusion failure in collapsed capillaries. Simultaneously, a widening of perfused microvessels accompanied by a significant increase in macromolecular leakage (Fig. 2A) and microvascular adherence of leukocytes (Fig. 2B) was observed.

### Leukocyte-Endothelial Cell Interaction

Trauma-induced inflammatory responses were characterized by a statistically significant microvascular leukocyte-endothelial cell interaction. Leukocyte rolling was significantly increased at all time points of analysis after closed soft-tissue injury when compared with control values (Table 1). Microscopic analysis revealed a significant increase in firm leukocyte adherence 1.5, 24, and 120 hours after injury (Table 1). Increased microvascular rolling and adherence of leukocytes seemed primarily restricted to the endothelium of postcapillary venules. In particular, venules

A, B

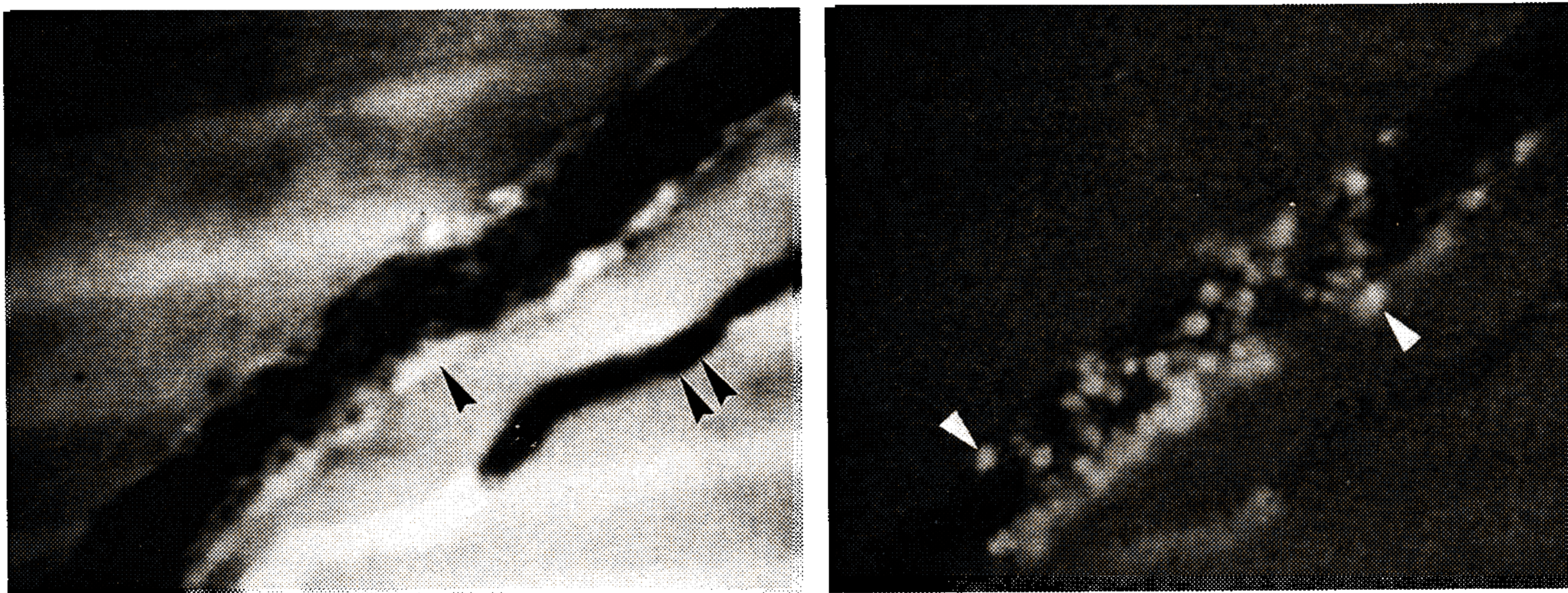


**FIG. 2.** Simultaneous *in vivo* microscopic visualization of perfused (arrow) and thrombotic (double arrow) postcapillary venules at the interface adjacent to the site of maximum damage 24 hours after closed soft-tissue injury was induced in the extensor digitorum longus muscle. **A:** Fluorescein isothiocyanate-labeled dextran was used as an intravascular marker, and **B:** rhodamine 6G was used for *in vivo* staining of leukocytes ( $\times 940$ ). **A:** Leakage of fluorescently labeled macromolecules (fluorescein isothiocyanate-labeled-dextran, 150,000 MW) into the extravascular space was increased, indicative of a loss of endothelial integrity. **B:** Simultaneously, the posttraumatic interaction of fluorescently (rhodamine 6G) stained leukocytes with the endothelium of identical microvessel segments was enhanced, as visualized by the increased number of leukocytes (arrow) rolling along and adhering to the postcapillary endothelial lining.

**TABLE 2.** Intramuscular pressure and edema formation in controls and experimental rats at different time points (hours)

	Intramuscular pressure (mm Hg)		EDL water content (%)		Edema index <sup>a</sup>
	Anterior	Posterior	Left	Right	
Control	7.2 ± 0.4	5.5 ± 0.7	77.3 ± 0.3	76.9 ± 0.5	1.01 ± 0.03
1.5	20.4 ± 15 <sup>b,c,d</sup>	7.9 ± 1.0 <sup>c</sup>	79.2 ± 0.5 <sup>e</sup>	76.2 ± 0.5	1.16 ± 0.02 <sup>b</sup>
24	25.4 ± 1.3 <sup>b,d</sup>	16.1 ± 2.1 <sup>b</sup>	78.7 ± 0.4 <sup>e</sup>	76.3 ± 0.5	1.13 ± 0.03 <sup>b</sup>
72	19.9 ± 0.6 <sup>b,c,d</sup>	11.4 ± 1.7 <sup>b</sup>	79.7 ± 0.4 <sup>e</sup>	76.4 ± 0.2	1.17 ± 0.03 <sup>b</sup>
120	13.6 ± 0.8 <sup>b,c</sup>	8.8 ± 0.8 <sup>c</sup>	79.5 ± 0.3 <sup>e</sup>	76.8 ± 0.3	1.16 ± 0.01 <sup>b</sup>

Intramuscular pressure was measured in the anterior and posterior compartments of the hindlimbs; edema formation was calculated in the left and right (experimental and contralateral) hindlimbs. Values are mean ± SEM. EDL = extensor digitorum longus muscle.

<sup>a</sup> Calculated by the ratio of wet to dry weight in the experimental compared with contralateral limb.

<sup>b</sup> P < 0.05 compared with controls.

<sup>c</sup> P < 0.05 compared with hindlimbs analyzed at 24 hours.

<sup>d</sup> P < 0.05 compared with hindlimbs analyzed at 120 hours.

<sup>e</sup> P < 0.01 compared with the contralateral (not injured, right hindlimb) muscle.

surrounding the core of the central damaged zone (original impact site) had impressive leukocyte accumulation due to enhancement of leukocyte rolling and adhesion (Fig. 2B). Leukocyte plugging of the capillary network was not observed in this transitional zone or in nonperfused microvessels at the core of the damage.

### Intramuscular Pressure

Tissue pressure after closed soft-tissue injury in the anterior tibial compartment was significantly increased at all time points when compared with control values (Table 2). Tissue pressure never exceeded 30 mm Hg, despite a distinct variability within the compartment. Remote from the anterior impact site, intramuscular pressure in the posterior compartment was less pronounced but reached its maximum at the same time as in the anterior compartment (Table 2). Even 5 days after closed soft-tissue injury, intramuscular pressure in the anterior and posterior compartments increased by approximately 2-fold in comparison with baseline values in the controls.

### Edema Formation

Edema formation increased significantly in all experimental groups compared with control values. In contrast to the time course of tissue pressure, the edema index exhibited peak levels 1.5 and 72 hours after the trauma (Table 2). The water content of the sham-operated extensor digitorum longus muscle in the control rats did not differ significantly ( $p = 0.6$ ;  $t$  test) from that of the contralateral muscle in the injured animals. These findings indicate that closed soft-tissue injury did not influence edema formation in the contralateral extensor digitorum longus muscle.

## DISCUSSION

Most recent microcirculatory investigations in striated muscle have focused on characterizing the micro-

vascular response after focal ischemia and reperfusion (1,5,13,31-33,35,41). The precise role of inflammation and microvascular dysfunction induced by severe trauma in a skeletal muscle of the locomotor system remains to be assessed, probably due to the lack of an appropriate and valid model. A new animal model of standardized closed soft-tissue injury was developed to directly address the clinically important issue of whether microcirculatory changes combined with increased leukocyte recruitment are responsible for the progressive course of closed soft-tissue damage. By means of *in vivo* fluorescence microscopy, posttraumatic microcirculation in skeletal muscle was shown to be characterized by a drastic and long-lasting decrease in capillary perfusion, which is accompanied by a marked increase in leukocyte-endothelium interaction and microvascular leakage.

### Model

By use of a computer-assisted modified controlled-impact technique with known and measurable mechanical variables and loading parameters, this animal model can be used to accurately induce standardized closed soft-tissue injury in a skeletal muscle of the locomotor system. We assumed that the response to injury in the extensor digitorum longus muscle of the rat resembles and reproduces clinical features of severe closed soft-tissue injury in humans as found in high-energy/velocity trauma.

Numerous reports describing animal models for the study of muscle contusion have been published (8,12,18,30,51). These studies demonstrated impairment of contractile function and changes in functional recovery and histology following muscle contusion (8) and tested the efficacy of immobilization (18) and anti-inflammatory medication (12). Soft-tissue trauma was induced in these models by insertion of forceps through a skin incision (crush injury), employment of a spring hammer (18), or use of the drop-mass tech-

nique (8, 51). These studies, using different models and energy levels, were restricted to mild and moderate muscle contusion. Therefore, modification of the controlled-impact technique (10) provides a complementary and clinically relevant experimental model of standardized closed soft-tissue injury caused by high-velocity trauma. The technique allows simulation of the clinical situation of high-energy/velocity injury to the extremities. Furthermore, the observed microcirculatory changes can be related to clinical features following severe blunt trauma to skeletal muscles of the locomotor system. As a restrictive condition, however, application of the model involves anesthetized animals. Possible microcirculatory changes caused by anesthetic drugs should therefore be considered: halothane and sevoflurane induce leukocyte rolling and adherence (39), fentanyl increases leukocyte rolling (17), midazolam and thiopental depress neutrophil functions (40), and ketamine can cause slight venular vasospasm (51).

Because of the total breakdown and occlusion of the intracompartmental microvasculature associated with compartment syndrome (3,7,15,21,46,50), dynamic and repetitive analysis of microcirculation is impossible. Therefore, impact parameters were selected to reliably exclude development of compartment syndrome. Nevertheless, the present model of severe closed soft-tissue injury should lead to conditions that precede compartment syndrome. This, in turn, facilitates *in vivo* analysis of posttraumatic microcirculatory changes and cellular interactions to a degree that lies just at the threshold of critical tissue pressure. If microvascular pathways preceding the transition to compartment syndrome can be identified and subsequently blocked (e.g., pharmacologically), tissue damaged by reactions secondary to trauma/ischemia can perhaps be rescued. Consequently, this model appears to provide essential insight into the microcirculatory mechanisms regulating these pathways and into testing promising new therapeutic interventions.

### ***In Vivo* Microscopy**

*In vivo* microscopy demonstrated for the first time that the damaging effects of closed soft-tissue injury resulted in a substantial and sustained (as long as 5 days) impairment of nutritive perfusion, as indicated by a significant reduction in functional capillary density. This prolonged reduction of functional capillary density, together with a delayed peak level of microvascular permeability in the entire extensor digitorum longus muscle, suggests the involvement of mechanisms other than the direct tissue destruction caused instantaneously by the impact itself. The changes in microvascular function as early as 1.5 hours after the trauma probably occurred in response to a wide range

of stimuli, including traumatically induced inflammatory reactions. Among the many factors leading to ultimate posttraumatic tissue damage, ischemia due to the microvessel trauma represents the most likely and decisive trigger.

The core of the damaged tissue was characterized by total microvascular perfusion failure combined with maximum microvascular leakage. These initial alterations, traditionally considered indicative of endothelial dysfunction (9,43), suggest an active participation of damaged endothelium. Therefore, endothelial cell injury leading to exposure of sub-endothelial collagen and disturbance of transcapillary fluid balance may form the cellular basis for these early posttraumatic microvascular changes.

Trauma-induced microcirculatory deterioration requires time to develop, as indicated by the maximally decreased functional capillary density and maximally increased microvascular leakage found at 24 hours. In addition, the persistence of these microcirculatory disorders (as long as 5 days after trauma) indicates that traumatically induced changes of the microcirculation are long-lasting, implying that some factors act to maintain microcirculatory impairment. The prolongation of impaired microcirculation probably reflects trauma-induced nonspecific inflammatory reactions, particularly within the tissue surrounding the original impact site. Local tissue destruction after closed soft-tissue injury ultimately leads to local bleeding due to vessel trauma. Hemorrhage into the tissue exposes the surrounding microenvironment to many blood-derived growth factors and pro-inflammatory cytokines, which can induce rapid expression of various adhesion molecules (6,29,34) as well as attract leukocytes (16,24,47). In this way, a neutrophilic chemotactic gradient may be established immediately after trauma. This pathway of excessive neutrophil sequestration secondary to closed soft-tissue injury is strongly supported by the observation that the closed soft-tissue injury induced a striking inflammatory response as early as 1.5 hours after the trauma, which was primarily restricted to the endothelial lining of postcapillary venules. The fact that enhanced leukocyte-endothelial cell interactions, coupled with increased microvascular permeability of identical vessel segments, were most pronounced within the immediate vicinity of the core of the damaged zone suggests the central role of leukocyte activity in the development of progressive tissue damage following closed soft-tissue injury. The consistent finding of increased and sustained posttraumatic leukocyte rolling and sticking, which closely paralleled the increased microvascular leakage and tissue damage, raises the question of whether tissue destruction by leukocytes is the effect, or rather the cause, of aggressive tissue death following severe closed soft-tissue injury. Under the



chosen study design, however, cause and effect cannot be differentiated. Rather, it seems likely that direct response to the trauma and posttraumatic inflammatory reactions are closely linked, and probably overlapping, changes.

The present data on capillary diameters following closed soft-tissue injury are in agreement with the findings of Rubinstein et al., who showed that crushed skeletal muscle was characterized by extreme capillary vasodilation 4 days after injury, as demonstrated by histology and capillary morphometry (48). This phenomenon has been attributed to increased levels of nitric oxide (38) due to a selective induction of nitric oxide synthase.

Finally, a clinically relevant finding was that the closed soft-tissue injury characteristically resulted in the formation of a heterogeneously perfused transitional zone surrounding a nonperfused center of maximally damaged skeletal muscle. Posttraumatic microcirculatory alterations in this transitional zone displayed some features reminiscent of microvascular changes classically viewed as hallmarks of ischemia-reperfusion injury (1,2,19,32,33,35). This similarity suggests that damage secondary to closed soft-tissue injury and development of ischemia-reperfusion injury may, in part, share identical pathways in the progression of microvascular injury, which in turn causes ultimate tissue death. However, in contrast to ischemia-reperfusion injury, in which microvascular injury precedes parenchymal damage, destruction of vascular and parenchymal cells is induced simultaneously in closed soft-tissue injury.

### Intramuscular Pressure

To rule out the possibility that closed soft-tissue injury resulted in a compartment syndrome that is a different entity, intramuscular pressure was measured in the anterior and posterior tibial compartments of the rat hindlimb. In addition, measuring tissue pressure indirectly verified that the extent and severity of closed soft-tissue injury were equally induced in all rats. Intramuscular pressure varied little between the different groups (Table 2), indicating the necessity for standardization of the closed soft-tissue injury by means of the controlled-impact technique. The elevated intracompartmental pressure was probably initiated by increased vascular leakage caused by the trauma. This is substantiated by the fact that peak levels of intracompartmental pressure coincided with the maximally increased microvascular permeability 24 and 72 hours following closed soft-tissue injury. Delayed increase in posterior intramuscular pressure following anterior impact reflects the clinical experience: in skeletal muscles enclosed by a tight fascial sheath, trauma-induced increase in intracompartmental pressure affects tissue pressure and consequently

tissue viability in neighboring compartments (15,46).

### Edema Formation

As an additional marker of muscle injury, edema weight gain of the damaged muscle was determined. In contrast to the peak level of microvascular permeability and tissue pressure, the edema index was maximally increased at 72 hours. By increasing the intercapillary distance, the interstitial edema appears to partially underlie the decline of functional capillary density, which was persistently pronounced at the same time. Therefore, the edema weight gain further supports the finding that microvascular response to closed soft-tissue injury is substantially prolonged.

### Conclusion

The approach of the present study offers three new aspects. First, a standardized model for induction of closed soft-tissue damage was developed, which closely reproduces characteristics observed clinically in patients suffering from a high-energy trauma. Second, this model permits direct visualization and quantification of posttraumatic microvascular perfusion and allows assessment of local and temporal relationships between microvascular parameters. Third, the model enables the testing of various potentially beneficial therapeutic regimens. On the basis of our findings, prolonged propagation of tissue damage following closed soft-tissue injury may be caused by progressive microvascular perfusion failure in combination with a delayed increase in microvascular leakage and persistently enhanced leukocyte-endothelial cell interaction. Thus, our observations offer a clue to delineate the microvascular trigger mechanisms that precede the escalation and end stage of closed soft-tissue injury. Clinical management of closed soft-tissue injury aimed at preservation of the tissue should consider improvement of microvascular perfusion and inhibition of leukocyte-mediated tissue injury. Our current efforts are directed toward testing this concept.

**Acknowledgment:** We wish to thank J. Hoffmann, G. Hardung, and M. Princ for expert technical assistance. We are grateful to Dr. G. Duda and Dr. J. Stover for advice and helpful discussion. The work has been supported by a grant from the AO-ASIF Foundation, Switzerland. B. Vollmar is supported by the Heisenberg Stipendium of the Deutsche Forschungsgemeinschaft (Vo 450/6-1).

### REFERENCES

1. Allen DM, Chen L-E, Seaber AV, Urbaniak JR: Pathophysiology and related studies of the no reflow phenomenon in skeletal muscle. *Clin Orthop* 314:122-133, 1995
2. Ames A 3rd, Wright RL, Kowada M, Thurston JM, Majno G: Cerebral ischemia. II. The no-reflow phenomenon. *Am J Pathol* 52:437-453, 1968
3. Ashton H: The effect of increased tissue pressure on blood flow. *Clin Orthop* 113:15-26, 1975
4. Barlow Y, Willoughby J: Pathophysiology of soft tissue repair. *Br Med Bull* 48:698-711, 1992
5. Carden DL, Smith KJ, Korthuis RJ: Neutrophil-mediated micro-

- vascular dysfunction in postischemic canine skeletal muscle: role of granulocyte adherence. *Circ Res* 66:1436-1444, 1990
6. Carlos TM, Harlan JM: Leukocyte-endothelial adhesion molecules. *Blood* 84:2068-2101, 1994
  7. Clayton JM, Hayes AC, Barnes RW: Tissue pressure and perfusion in the compartment syndrome. *J Surg Res* 22:333-339, 1977
  8. Crisco JJ, Jokl P, Heinen GT, Connell MD, Panjabi MM: A muscle contusion injury model: biomechanics, physiology, and histology. *Am J Sports Med* 22:702-710, 1994
  9. Davies MG, Hagen PO: The vascular endothelium: a new horizon. *Ann Surg* 218:593-609, 1993
  10. Dixon CE, Clifton GL, Lighthall JW, Yaghami AA, Hayes RL: A controlled cortical impact model of traumatic brain injury in the rat. *J Neurosci Methods* 39:253-262, 1991
  11. Esterhai JL Jr, Queenan J: Management of soft tissue wounds associated with type III open fractures. *Orthop Clin North Am* 22:427-432, 1991
  12. Fisher BD, Baracos VE, Reid DC: Effect of systemic inhibition of prostaglandin synthesis on muscle protein balance after trauma in the rat. *Can J Physiol Pharmacol* 69:831-836, 1991
  13. Forbes TL, Harris KA, Jamieson WG, DeRose G, Carson M, Potter RF: Leukocyte activity and tissue injury following ischemia-reperfusion in skeletal muscle. *Microvasc Res* 51:275-287, 1996
  14. Gustafsson U, Sjöberg F, Lewis DH, Thorborg P: Influence of pentobarbital, propofol and ketamine on skeletal muscle capillary perfusion during hemorrhage: a comparative study in the rabbit. *Int J Microcirc Clin Exp* 15:163-169, 1995
  15. Heppenstall RB: Compartment syndrome: pathophysiology, diagnosis, and treatment. *Tech Orthop* 12:92-108, 1997
  16. Huber AR, Kunkel SL, Todd RF 3rd, Weiss SJ: Regulation of transendothelial neutrophil migration by endogenous interleukin-8 [published errata appear in *Science* 254:631 and 1435, 1991]. *Science* 254:99-102, 1991
  17. Janssen GH, Tangelder GJ, oude Egbrink MG, Reneman RS: Different effects of anesthetics on spontaneous leukocyte rolling in rat skin. *Int J Microcirc Clin Exp* 17:305-313, 1997
  18. Jarvinen M, Sorvari T: Healing of a crush injury in rat striated muscle. I. Description and testing of a new method of inducing a standard injury to the calf muscles. *Acta Pathol Microbiol Scand A* 83:259-265, 1975
  19. Jerome SN, Akimitsu T, Korhuis RJ: Leukocyte adhesion, edema, and development of postischemic capillary no-reflow. *Am J Physiol* 267:H1329-H1336, 1994
  20. Kellett J: Acute soft tissue injuries: a review of the literature. *Med Sci Sports Exerc* 18:489-500, 1986
  21. Kiaer T, Kristensen KD: Intracompartmental pressure, PO<sub>2</sub>, PCO<sub>2</sub> and blood flow in the human skeletal muscle. *Arch Orthop Trauma Surg* 107:114-116, 1988
  22. Kim D, Armenante PM, Duran WN: Transient analysis of macromolecular transport across microvascular wall and into interstitium. *Am J Physiol* 265:H993-H999, 1993
  23. Klyszcz T, Junger M, Jung F, Zeintl H: [Cap image: a new kind of computer-assisted video image analysis system for dynamic capillary microscopy.] *Biomed Tech (Berlin)* 42:168-175, 1997
  24. Lefer AM, Ma XL: Cytokines and growth factors in endothelial dysfunction. *Crit Care Med* 21:S9-S14, 1993
  25. Levin LS, Condit DP: Combined injuries: soft tissue management. *Clin Orthop* 327:172-181, 1996
  26. Levin SL: Personality of soft tissue injury. *Tech Orthop* 10:65-73, 1995
  27. Levin SL: The reconstructive ladder. *Tech Orthop* 10:88-94, 1995
  28. Lighthall JW, Dixon CE, Anderson TE: Experimental models of brain injury. *J Neurotrauma* 6:83-97, 1989
  29. Lusinskas FW, Cybulsky MI, Kiely JM, Peckins CS, Davis VM, Gimbrone MA Jr: Cytokine-activated human endothelial monolayers support enhanced neutrophil transmigration via a mechanism involving both endothelial-leukocyte adhesion molecule-1 and intercellular adhesion molecule-1. *J Immunol* 146:1617-1625, 1991
  30. McGeachie JK, Grounds MD: Initiation and duration of muscle precursor replication after mild and severe injury to skeletal muscle of mice: an autoradiographic study. *Cell Tissue Res* 248:125-130, 1987
  31. Menger MD, Feifel G, Messmer K: Distribution pattern of capillary and venular red blood cell velocity following ischemia-reperfusion in striated muscle. *Adv Exp Med Biol* 317:765-769, 1992
  32. Menger MD, Steiner D, Messmer K: Microvascular ischemia-reperfusion injury in striated muscle: significance of "no reflow." *Am J Physiol* 263:H1892-H1900, 1992
  33. Menger MD, Kerger H, Geisweid A, Leu AJ, Hecht R, Nolte D, Messmer K: Leukocyte-endothelium interaction in the microvasculature of postischemic striated muscle. *Adv Exp Med Biol* 361:541-545, 1994
  34. Menger MD, Vollmar B: Adhesion molecules as determinants of disease: from molecular biology to surgical research. *Br J Surg* 83:588-601, 1996
  35. Menger MD, Rucker M, Vollmar B: Capillary dysfunction in striated muscle ischemia/reperfusion: on the mechanisms of capillary "no-reflow." *Shock* 8:2-7, 1997
  36. Mercer NS, Moss AL: Soft tissue management of compound leg fractures: a 5-year experience. *J R Coll Surg Edinb* 33:263-266, 1988
  37. Miles W: Soft tissue trauma. *Hand Clin* 2:33-43, 1986
  38. Moncada S, Higgs A: The L-arginine-nitric oxide pathway. *N Engl J Med* 329:2002-2012, 1993
  39. Morisaki H, Suematsu M, Wakabayashi Y, Moro-oka S, Fukushima K, Ishimura Y, Takeda J: Leukocyte-endothelium interaction in the rat mesenteric microcirculation during halothane or sevoflurane anesthesia [published erratum appears in *Anesthesiology* 88:560, 1998]. *Anesthesiology* 87:591-598, 1997
  40. Nishina K, Akamatsu H, Mikawa K, Shiga M, Maekawa N, Obara H, Niwa Y: The inhibitory effects of thiopental, midazolam, and ketamine on human neutrophil functions. *Anesth Analg* 86:159-165, 1998
  41. Nolte D, Hecht R, Schmid P, Botzlar A, Menger MD, Neumueller C, Sinowatz F, Vestweber D, Messmer K: Role of Mac-1 and ICAM-1 in ischemia-reperfusion injury in a microcirculation model of BALB/C mice. *Am J Physiol* 267:H1320-H1328, 1994
  42. Oestern HJ, Tschernhe H: [Pathophysiology and classification of soft tissue damage in fractures.] *Orthopade* 12:2-8, 1983
  43. Pober JS, Cotran RS: The role of endothelial cells in inflammation. *Transplantation* 50:537-544, 1990
  44. Reed MW, Miller FN: Importance of light dose in fluorescent microscopy. *Microvasc Res* 36:104-107, 1988
  45. Rodgers CM, Ketch LL: Management of associated soft-tissue injury. *Surg Clin North Am* 68:823-835, 1988
  46. Rorabeck CH: The treatment of compartment syndromes of the leg. *J Bone Joint Surg [Br]* 66:93-97, 1984
  47. Rot A, Hub E, Middleton J, Pons F, Rabeck C, Thierer K, Wintle J, Wolff B, Zsak M, Dukor P: Some aspects of IL-8 pathophysiology. III. Chemokine interaction with endothelial cells. *J Leukoc Biol* 59:39-44, 1996
  48. Rubinstein I, Abassi Z, Coleman R, Milman F, Winaver J, Better OS: Involvement of nitric oxide system in experimental muscle crush injury. *J Clin Invest* 101:1325-1333, 1998
  49. Saetzler RK, Jallo J, Lehr HA, Philips CM, Vasthare U, Arfors KE, Tuma RF: Intravital fluorescence microscopy: impact of light-induced phototoxicity on adhesion of fluorescently labeled leukocytes. *J Histochem Cytochem* 45:505-513, 1997
  50. Shrier I, Magder S: Pressure-flow relationships in in vitro model of compartment syndrome. *J Appl Physiol* 79:214-221, 1995
  51. Smith TL, Curl WW, Smith BP, Holden MB, Wise T, Marr A, Koman LA: New skeletal muscle model for the longitudinal study of alterations in microcirculation following contusion and cryotherapy. *Microsurgery* 14:487-493, 1993
  52. Tyml K, Budreau CH: A new preparation of rat extensor digitorum longus muscle for intravital investigation of the microcirculation. *Int J Microcirc Clin Exp* 10:335-343, 1991
  53. Zeintl H, Sack FU, Intaglietta M, Messmer K: Computer assisted leukocyte adhesion measurement in intravital microscopy. *Int J Microcirc Clin Exp* 8:293-302, 1989

### **3.1.2 Der Einfluss des isolierten Weichteilschadens auf die periostale Mikrozirkulation**

Obgleich zahlreiche Untersuchungen in verschiedenen Spezies die Mikrozirkulation des kortikalen Knochens nach Verletzung in vivo untersuchten und zum Teil auch quantifizierten (78) und direkt visualisierten (94, 197), fehlen ähnliche Untersuchungen für das Periost. So ist es im Einzelnen unbekannt, wie und in welchem Ausmaß und Zeitraum ein isolierter Weichteilschaden zu einer mikrovaskulären Dysfunktion des Periostes führt. Nachfolgende tierexperimentelle Studien wurden daher geplant mit dem Ziel, eine genaue quantitative Analyse der periostalen Mikrozirkulationsstörungen nach geschlossener Weichteilschädigung durchzuführen, um deren kausale Bedeutung für eine reduzierte ossäre-kortikale Durchblutung und damit potentiell verzögerte Frakturheilung herauszustellen.

Ferner sollten diese mikrovaskulären Veränderungen auf Ebene des Periostes auch in ihrer zeitlichen Dynamik sowohl zu den frühen (2h, 24h, und 48h) als auch zu den späteren Zeitpunkten (1, 3 und 6 Wochen) nach geschlossenem Weichteiltrauma analysiert und mit der Schwere der traumatischen Weichteilschädigung (Kompartimentdruck) und Entzündungsreaktion (Leukozytenadhärenz) korreliert werden.

Diese Studien zeigten, dass bereits ein isolierter schwerer geschlossener Weichteilschaden ohne gleichzeitige Fraktur mit einer lang anhaltenden Dysfunktion der periostalen Mikrozirkulation und damit ossären Durchblutung vergesellschaftet ist (152). Darüber hinaus zeigten sich funktionelle Zusammenhänge zwischen der Höhe des posttraumatisch gesteigerten Kompartimentdruckes und dem Ausmaß der assoziierten periostalen Entzündungsreaktion (endotheliale Leukozytenadhärenz) (152).

K. D. Schaser  
L. Zhang  
N. P. Haas  
T. Mittlmeier  
G. Duda  
H. J. Bail

## Temporal profile of microvascular disturbances in rat tibial periosteum following closed soft tissue trauma

Received: 25 May 2003  
Accepted: 8 July 2003  
Published online: 8 October 2003  
© Springer-Verlag 2003

The paper was presented at the 2nd Musculoskeletal Symposium “Significance of Musculo-Skeletal Soft Tissue on Pre-Operative Planning, Surgery and Healing”, 13–14 February 2003, Berlin, Germany

K. D. Schaser (✉) · L. Zhang · N. P. Haas · G. Duda · H. J. Bail  
Department of Trauma and Reconstructive Surgery, Charité, Campus Virchow, Humboldt University, Augustenburger Platz 1, 13353 Berlin, Germany  
e-mail: klaus-dieter.schaser@charite.de  
Tel.: +49-30-450552098  
Fax: +49-30-450552958

T. Mittlmeier  
Department of Trauma and Reconstructive Surgery, University of Rostock, Rostock, Germany

**Abstract** *Background and aims:* Bone devascularization due to impaired periosteal perfusion following fracture with severe soft tissue trauma has been proposed to precede and underlie perturbed bone healing. The extent and temporal relationship of periosteal microcirculatory deteriorations after severe closed soft tissue injury (CSTI) are not known. We hypothesized that periosteal microcirculation is adversely affected and the manifestation of trauma-initiated microvascular impairment in periosteum is substantially prolonged following CSTI. *Material and methods:* Using the controlled-impact injury device, we induced standardized CSTI in the tibial compartment of 35 isoflurane-anesthetized rats. Following the trauma the rats were assigned to five groups, differing in time of analysis (2 h, 24 h, 48 h, 1 and 6 weeks). Non-injured rats served as controls. Before the metaphyseal/diaphyseal periosteum was surgically exposed, intramuscular pressure within tibial compartment was measured. Using intravital fluorescence microscopy (IVM) we studied the microcirculation of the tibial periosteum. We calculated the edema index (EI) by measuring the skeletal muscle wet-to-dry weight ratio (EI = injured limb/contralateral limb). *Results:* Microvascular deteriorations of peri-

osteal microhemodynamics caused by isolated CSTI were reflected by persistent decrease in nutritive perfusion, markedly prolonged increase in microvascular permeability associated with increasingly sustained leukocyte rolling and adherence throughout the entire study period, mostly pronounced 48 h after the trauma. Peak level in capillary leakage coincided with the maximum leukocyte adherence, tissue pressure, and edema. Microcirculation of tibial periosteum in control rats demonstrated a homogeneous perfusion with no capillary or endothelial dysfunction.

*Conclusion:* Isolated CSTI in absence of a fracture exerts long-lasting disturbances in periosteal microcirculation, suggesting a delayed temporal profile in manifestation of CSTI-induced periosteal microvascular dysfunction and inflammation. These observations may have therapeutic implications in terms of preserving periosteal integrity and considering the interaction of skeletal muscle damage and periosteal microvascular injury during management of musculoskeletal trauma.

**Keywords** Periosteum · Closed soft tissue trauma · Intravital fluorescence microscopy · Microcirculation · Leukocyte–endothelial cell interaction

## Introduction

Apart from its biological relevance, such as containing precursor cells of osteoblasts [1], another principal function of the periosteum and its microvasculature is to supply oxygenated blood and nutrients to the cortical bone [2, 3, 4]. In addition, extensive characterization of initial stages in fracture healing has identified the periosteum as the key structure for initiating and mediating the very first steps of fracture healing. Among others, these may include hemostasis, generation and resorption of the fracture hematoma, migration of osteoblast and chondroblast precursor cells, formation of periosteal callus and remodeling, and revascularization of the injured bone [1, 5]. The trigger event of this healing cascade is the *periosteal microvascular trauma*, which subsequently causes ischemia, inflammation, and nutritive dysfunction. The pathogenetic influence of trauma-induced cellular and microvascular changes in the periosteum is underlined by the clinical observation that extensive soft tissue injury and periosteal stripping typically precedes delayed fracture repair and frequently results in a non-union or manifest pseudarthrosis [6, 7, 8, 9, 10]. Despite this critical decrease in extra-osseous nutritional blood flow to the bone, which appears to be a causative factor, the precise extent and temporal relationship of microcirculatory deteriorations and post-traumatic inflammation in periosteum caused by isolated and severe closed soft tissue injury (CSTI) is not known. Therefore, we hypothesized that in the absence of a fracture the periosteal microcirculation is adversely affected by a severe CSTI. We further hypothesized that, consistent with the delayed healing response of fractures with severe soft tissue damage, the manifestation of trauma-initiated microvascular impairment is substantially prolonged, and is caused by persistently enhanced capillary and endothelial dysfunction, and increased microvascular permeability and leukocyte activity in the periosteum.

## Material and methods

### Animal preparation and closed soft tissue injury

Following approval of the experimental protocol by the local committee of animal research, 35 spontaneously breathing male SD rats were anesthetized with isoflurane (1.6 vol%) in a 2:1 mixture of N<sub>2</sub>O/O<sub>2</sub> (0.4 and 0.2 l/min). Body temperature was measured with a rectal probe and maintained between 37° and 38°C by the animals' being placed on a homoeothermic-heating pad. The right carotid artery and jugular vein were cannulated with PE catheters (PE50, 0.58 mm inner diameter, Portex, Hythe, Kent, UK) for the monitoring of mean arterial blood pressure (MABP) and heart rate (HR) and intravenous administration of fluorescence dyes.

With the animal's left hind limb fixed in a specifically shaped mold we induced the standardized CSTI in the antero-lateral tibial compartment, using the computer-assisted controlled-impact injury (CII) device (penetration depth 11 mm; velocity 7 m/s; contact time 0.1 s) and keeping the skin intact [11]. For intravital fluorescence

microscopic observations the metaphyseal and diaphyseal periosteum was surgically prepared, modified to a technique previously described [12].

### Experiment protocol

Following the trauma the rats were assigned to five groups ( $n=7$ ) differing in time of analysis (2 h, 24 h, 48 h, 1 and 6 weeks after the trauma). Non-injured, sham-operated rats served as controls ( $n=7$ ). Before the tibial periosteum was surgically exposed, the intramuscular pressure within the antero-lateral and posterolateral tibial compartment (8 mm beneath the skin surface) was measured percutaneously (45 min post-trauma) during the first week after CSTI with a microsensors catheter (0.7 mm outside diameter, CODMAN microsensors, Johnson & Johnson Professional, Raynham, Mass., USA). After a stabilization period of 15 min, values for macrohemodynamics were collected and the tibial periosteum was then sequentially scanned from proximal (metaphyseal) to distal (mid-diaphyseal) part in 1.5-mm increments by intravital fluorescence microscopy to allow microcirculatory images for nutritive capillaries and post-capillary venules to be recorded. Microcirculatory recordings for nutritive capillaries and post-capillary venules of at least six video-frames of each tibial periosteum were taken, and values were averaged per animal.

At completion of each experiment the animals were killed and the extensor digitorum longus muscle muscles of both hind limbs were removed for gravimetric determination of edema weight gain.

### Intravital fluorescence microscopy

For visualization of the periosteal microcirculation an intravital fluorescence microscope (Axiovert Vario, Carl Zeiss, Goettingen, Germany) equipped with a water-immersion objective (Achromat,  $\times 20$ , Carl Zeiss) was used. The tibial periosteum surface was epilluminated by a high-pressure mercury lamp (100 W), and fluorescence emission of fluorescein-isothiocyanate (FITC)-dextran (450–490 nm/ $>580$  nm) and rhodamine (530–560 nm/ $>580$  nm) was detected by means of an appropriate filter system. Microcirculatory images were recorded by a CCD-video-camera (FK 6990-IQ, Pieper, Schwerte, Germany) and transferred to an SVHS-video-recorder (HR-S4700EG/E, JVC, Friedberg, Germany) for off-line analysis. The final magnification on the video-screen was 405-fold.

For contrast enhancement of the microvascular network and for in vivo staining of leukocytes a single bolus of FITC-labeled dextran (5%, 150,000 mol. wt; 15 mg/kg body wt; Sigma Chemical, Deisenhofen, Germany) and rhodamine 6G (0.1%, 0.15 mg/kg body wt.; Sigma Chemical) were injected intravenously [13, 14]. For prevention of phototoxic effects the duration of continuous light exposure per observation area was limited to 60 s at maximum [15, 16].

### Microcirculatory analysis

The video-taped microcirculatory images were analyzed off-line for microvessel diameters, functional capillary density (FCD), microvascular permeability (macromolecular leakage), and red blood cell velocity ( $V_{RBC}$ ) by a computerized microcirculation image-analysis system [17, 18]. FCD was quantified by the length of FITC-dextran-perfused capillaries per observation area (per centimeter). Microvascular permeability (macromolecular leakage) is expressed as the ratio of fluorescence intensity, selected from perivascular area, to the corresponding intravascular area (plasma gaps between erythrocytes). The centerline red blood cell velocity ( $V_{RBC-centerline}$ ) in capillaries and venules of skeletal muscle was determined by

means of a PC-associated image-analysis system [17, 18]. The number of rolling and adherent leukocytes and the total leukocyte flux was counted for 30 s along a 100- $\mu\text{m}$  vessel segment. Leukocyte rolling was defined as slow passage of leukocytes rolling along the vessel wall with a velocity less than 40% of centerline velocity [19] and expressed in percent of rolling cells to total leukocyte flux [20]. Adherence of leukocytes was defined by non-moving leukocytes firmly contacting the endothelium of post-capillary venules for at least 20 s. With the assumption of cylindrical microvessel geometry, leukocyte adherence was expressed as the number of permanently adherent leukocytes per endothelial surface (cells per square millimeter), calculated from the diameter and length (100  $\mu\text{m}$ ) of the venular segment being analyzed.

#### Quantification of edema formation (edema weight gain)

During the first week following the trauma, the formation of skeletal muscle edema was assessed gravimetrically by measurement of the wet-to-dry-weight ratio of the left (traumatized) and contralateral (non-injured) extensor digitorum longus (EDL) muscle [edema index (EI) = left EDL/contralateral EDL]. After determination of wet weight, EDL muscles were dried for 24 h in a laboratory oven (80°C) and weighed again so that the dry weight could be assessed.

#### Statistics

Data were analyzed by a repeated-measures analysis for six groups as previously described [21]. After passing the normality test (Kolmogorov–Smirnov) differences between groups were tested by ANOVA for independent samples followed by post-hoc analysis using Bonferroni-correction for multiple comparisons. To assess the correlation between leukocyte adherence and microvascular permeability and intramuscular pressure we used linear regression analysis. Statistical significance was set at  $P < 0.05$ .

## Results

### Systemic hemodynamics and intramuscular pressure

In all investigated groups, HR and MABP remained unchanged and within normal limits (Table 1). Anaphylactic-like responses to FITC-labeled dextran were not observed in any of the rats. CSTI significantly increased intramuscular pressure ( $P_{\text{im}}$ ) within the anterior and posterior compartment, which persisted to 1 week when compared with that of non-injured controls (Table 2). Due to the antero-lateral impact this increase in  $P_{\text{im}}$  was more pronounced in the anterior compartment. Throughout the entire study period the  $P_{\text{im}}$  did not exceed a critical threshold of 30 mmHg, which would be indicative of manifest compartment syndrome under normal MABP.

### Periosteal microcirculation

Microcirculation of metaphyseal and diaphyseal tibial periosteum in non-injured rats demonstrated homogeneous perfusion with no significant capillary or endothelial dysfunction. Microvascular deterioration of periosteal microhemodynamics caused by isolated CSTI was reflected by a persistent decrease in nutritive perfusion. Over time, FCD determined by intravital microscopy was significantly decreased throughout the entire study period (Fig. 1a). This decrease was most pronounced during the first 2 days after the trauma, followed by a reversible increase at 1 week after CSTI, which, however, remained significantly decreased when compared with control values. Parallel to markedly reduced FCD, CSTI significantly reduced capillary red blood cell velocity (RBCV) at 2, 24 and 48 h after injury, whereas RBCV in post-

**Table 1** MABP, microvascular diameters, volumetric blood flow (VBF) and RBCV in capillaries and venules of tibial periosteum at 2 h, 24 h, 48 h, and 1 and 6 weeks following closed soft tissue injury (mean  $\pm$  SD)

Group	MABP (mmHg)	Diameter ( $\mu\text{m}$ )		VBF (pl/s)		RBCV ( $\mu\text{m/s}$ )	
		Capillary	Venule	Capillary	Venule	Capillary	Venule
Control/sham	82 $\pm$ 4	10 $\pm$ 1	30 $\pm$ 3	16 $\pm$ 4	97 $\pm$ 29	219 $\pm$ 10	166 $\pm$ 32
2 h	92 $\pm$ 5	12 $\pm$ 3	32 $\pm$ 1	13 $\pm$ 3	188 $\pm$ 83	127 $\pm$ 2 <sup>a</sup>	140 $\pm$ 19 <sup>a</sup>
24 h	84 $\pm$ 5	11 $\pm$ 3	33 $\pm$ 7	17 $\pm$ 7	91 $\pm$ 34	160 $\pm$ 17 <sup>a</sup>	158 $\pm$ 18
48 h	88 $\pm$ 5	10 $\pm$ 4	37 $\pm$ 5	14 $\pm$ 4	129 $\pm$ 52	136 $\pm$ 25 <sup>a</sup>	150 $\pm$ 63
1 week	87 $\pm$ 4	10 $\pm$ 2	37 $\pm$ 4	14 $\pm$ 5	116 $\pm$ 58	186 $\pm$ 35	167 $\pm$ 10
6 weeks	91 $\pm$ 7	10 $\pm$ 2	36 $\pm$ 5	16 $\pm$ 3	178 $\pm$ 50	202 $\pm$ 17	180 $\pm$ 9

<sup>a</sup>ANOVA and post-hoc Bonferroni analysis:  $P < 0.05$  vs control

**Table 2** Time course of  $P_{\text{im}}$ , EDL muscle–water content and edema formation (EI) following closed soft tissue injury (mean  $\pm$  SD)

Group	Control	2 h	24 h	48 h	1 week
$P_{\text{im}}$ ant (mmHg)	7.4 $\pm$ 0.4 <sup>b</sup>	24.3 $\pm$ 2.2 <sup>a,b</sup>	24.5 $\pm$ 1.8 <sup>a,b</sup>	22.1 $\pm$ 1.9 <sup>a,b</sup>	13.4 $\pm$ 2.3 <sup>a</sup>
$P_{\text{im}}$ post (mmHg)	5.3 $\pm$ 0.7	15.8 $\pm$ 3.5	17.4 $\pm$ 1.7	15.1 $\pm$ 1.4	7.9 $\pm$ 1.9
H <sub>2</sub> O content of EDL (%)	74.8 $\pm$ 0.03	79.1 $\pm$ 2.3 <sup>a</sup>	80.4 $\pm$ 3.6 <sup>a</sup>	79.2 $\pm$ 3.6 <sup>a</sup>	78.9 $\pm$ 2.0
EI (ratio)	1.03 $\pm$ 0.03	1.11 $\pm$ 0.13	1.20 $\pm$ 0.13 <sup>a</sup>	1.20 $\pm$ 0.21 <sup>a</sup>	1.06 $\pm$ 0.17

<sup>a</sup>ANOVA and post-hoc Bonferroni analysis:  $P < 0.05$  vs control

<sup>b</sup>ANOVA and post-hoc Bonferroni analysis:  $P < 0.05$  vs  $P_{\text{im}}$  post

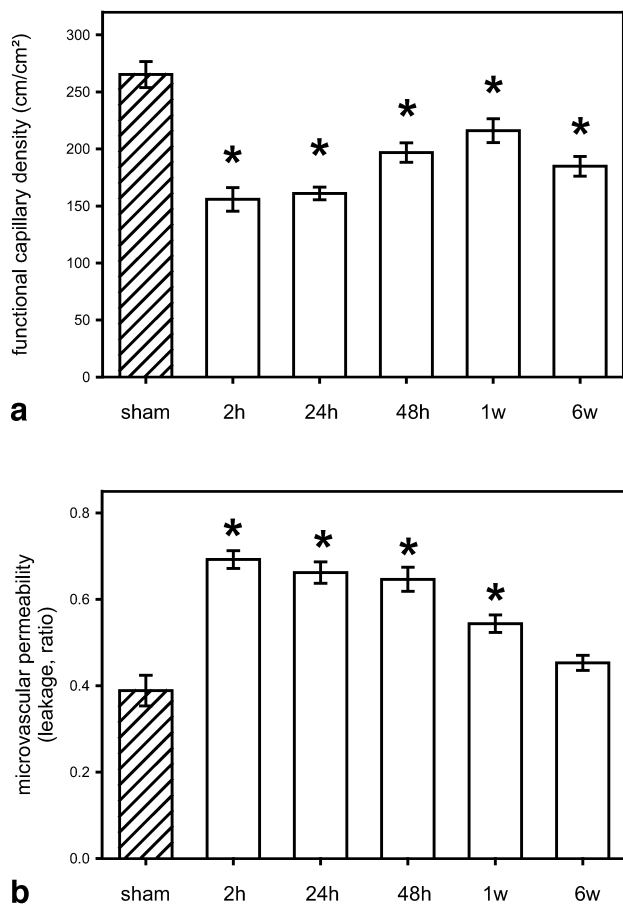


**Fig. 1a, b** Changes in capillary perfusion and trans-endothelial leakage in response to closed soft tissue trauma. **a** FCD [length of erythrocyte-perfused capillaries per observation area (per centimeter)]; **b** microvascular permeability (capillary macromolecular leakage of FITC-dextran, analyzed densitometrically by the ratio of extravascular to intravascular fluorescence intensity) in the tibial periosteum in control (non-injured) animals ( $n=7$ , hatched bar) and at 2, 24, and 48 h, and 1 and 6 weeks ( $w$ ) following the trauma ( $n=7$  per time point, open bars). Values are means  $\pm$  SD, ANOVA for independent samples followed by post-hoc analysis and Bonferroni correction for multiple comparison procedures. \* $P<0.05$  vs control (sham)

capillary venules was significantly decreased only at 2 h following CSTI (Table 1). These disturbances in nutritional capillary blood flow were accompanied by a reversible and markedly prolonged increase in trans-endothelial leakage (microvascular permeability) during the first week following CSTI, nearly reaching pre-injury values at 6 weeks following CSTI (Fig. 1b). The volumetric blood flow in capillaries showed a considerable variation (see standard deviations in Table 1). In particular, at 2 h post-trauma the capillary and venular blood flow volume displayed a diametric behavior with decreased values in capillaries, while the venular blood flow increased. Over time, however, neither the capillary

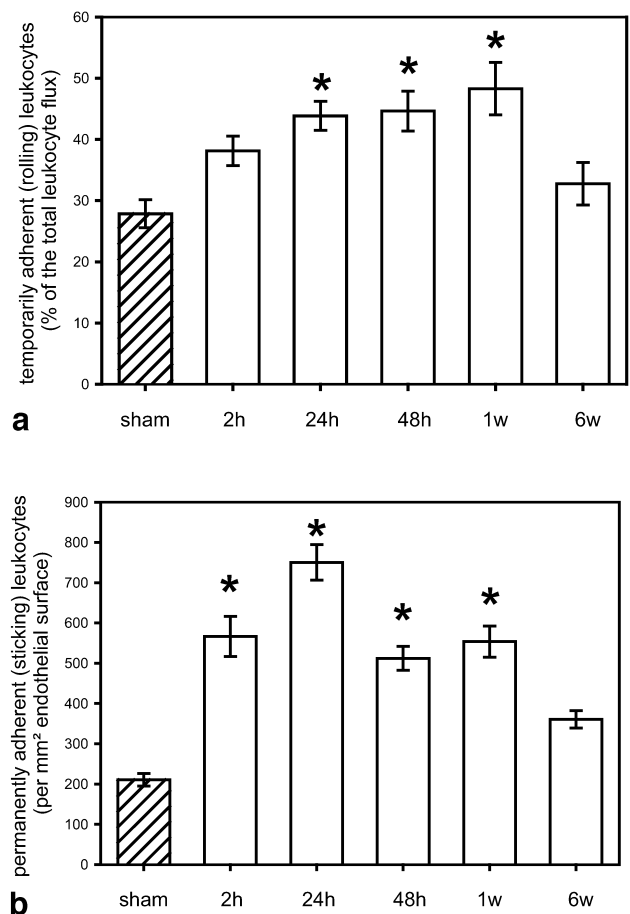


**Fig. 2a, b** Leukocyte-endothelial cell interaction in post-capillary venules of tibial periosteum in control (non-injured, sham-operated) animals ( $n=7$ , hatched bar) and at 2, 24, and 48 h, and 1 and 6 weeks ( $w$ ) following closed soft tissue trauma ( $n=7$  per time point, open bars). **a** Number of rolling leukocytes in percent of total leukocyte flux. **b** Number of adherent leukocytes per square millimeter of endothelial surface. Values are means  $\pm$  SD, ANOVA for independent samples followed by post hoc analysis and Bonferroni correction for multiple comparison procedures. \* $P<0.05$  vs control (sham)

nor the venular volumetric blood flow demonstrated significant changes.

#### Leukocyte-endothelial cell interaction

The changes in trans-endothelial fluid balance were furthermore associated with an increased leukocyte-endothelial cell interaction, mostly pronounced during the first 48 h following CSTI (Fig. 2). The percentage of leukocytes displaying loose contact by rolling along the microvascular endothelium of post-capillary venules was steadily increased up to 1 week, followed by a decrease at 6 weeks, nearly reaching baseline values in non-injured control animals (Fig. 2a). Permanent leukocyte adher-

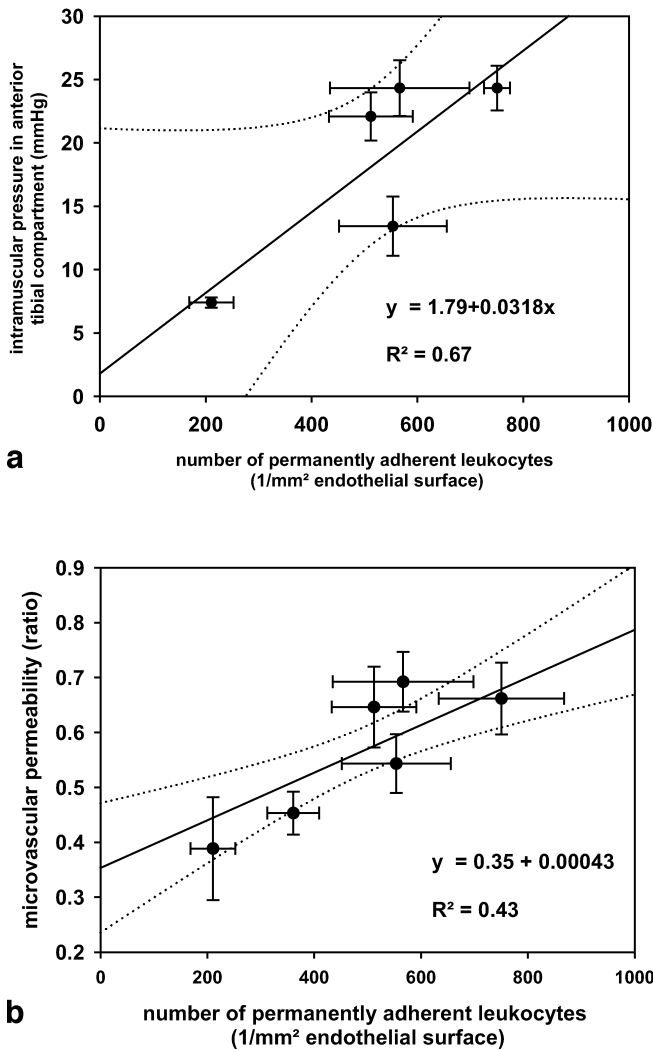


**Fig. 3a, b** Regression analysis between number of permanently adherent leukocytes and values of (a)  $P_{im}$  within the anterior tibial compartment and (b) microvascular permeability. Values are given as mean  $\pm$  SD, obtained at baseline (non-injured sham-operated rats) and at 2, 24, and 48 h, and 1 and 6 weeks (not for  $P_{im}$ ) post-injury. Dotted lines represent 95% confidence intervals.  $R^2$  coefficient of determination

ence, i.e., the number of leukocytes that exhibited firm endothelial contact in post-capillary venules, was increasingly sustained at 2 h and 24 h after CSTI, by 3-times when compared to that in the non-injured control animals. After 48 h permanent leukocyte adherence was reduced but remained significantly elevated up to 1 week after CSTI (Fig. 2b).

### Skeletal muscle edema formation and water content

CSTI significantly increased the formation of skeletal muscle edema at 24 and 48 h, when compared with that of the control animals, as reflected by gravimetric analysis of the post-traumatic EDL muscle-water content and calculation of the EI. After 1 week the EI decreased significantly, nearly reaching the level of controls at 6 weeks after injury.

### Regression of leukocyte adherence on microvascular permeability and tissue pressure

Regression analysis between the number of permanently adherent leukocytes and microvascular permeability as well as  $P_{im}$  in the antero-lateral tibial compartment revealed a positive functional relationship, with an  $R^2$  of 0.43 and 0.67, respectively (Fig. 3).

### Discussion

These results show that isolated closed soft tissue trauma causes a persistent decrease in periosteal and consecutive osseous nutritive perfusion in the absence of additional injury to the bone. These capillary derangements were accompanied by a significant increase in periosteal microvascular permeability, leukocyte adherence, tissue pressure, and edema formation. The time course of developing deterioration in periosteal microhemodynamics following CSTI suggests a prolonged and delayed temporal profile in manifestation of periosteal capillary dysfunction, endothelial disintegration, and inflammation.

Several studies have investigated the effect of soft tissue trauma on cellular periosteal response [22], skeletal muscle perfusion [11], and fracture healing [10]. To date, however, direct studies aiming to visualize and quantitatively analyze periosteal microcirculation following CSTI are missing. In previous studies the extent of periosteal contribution to diaphyseal/metaphyseal bone circulation is controversially discussed [3, 23, 24]. However, there is clear consensus in view of the periosteal microvasculature as the source for supply and exchange of oxygenated blood, nutrients, and metabolites to the osteogenic cells of the periosteal cambium layer and the cortical bone [3, 4]. Therefore, periosteal microvascular injury in terms of *microvascular disruption*, post-ischemic capillary “no reflow” phenomenon, and trauma-induced inflammation seems to be one initial key event in the pathophysiology of injury to the bone, i.e., fracture [25]. The present data suggest that similar microvascular deterioration in the periosteum also occurs in response to isolated CSTI without a concomitant fracture, as profound capillary and endothelial dysfunction in conjunction with progressive leukocyte activation have typically been observed. Clin-



ical [26] and experimental studies [24] have started to relate skeletal muscle perfusion to periosteal blood supply and fracture healing and revealed that skeletal muscle provides an important collateral source of blood to cortical bone. Furthermore, it has been demonstrated that the periosteum and overlying muscles share circulatory channels and have collateral circulation [24, 26]. Thus, soft tissue trauma-induced decrease in nutritional blood flow to the surrounding skeletal muscle may subsequently cause a decline in periosteal microvascular perfusion. This notion is also supported by the finding of decreased capillary blood flow volume at 2 h post-injury, while the venular volumetric blood flow simultaneously tends to increase. These observations may indicate that part of the blood flow volume usually passing the periosteal capillary bed is temporarily bypassed or otherwise shunted, possibly caused by the observed capillary dysfunction. The considerable increase in venular blood flow volume at 6 weeks post-trauma again has a marked variation and may be associated with structural changes of the periosteum and periosteal remodeling processes, known to evolve secondary to soft tissue trauma [22].

Therefore, the involvement of periosteal microvascular derangements in severe CSTI and skeletal muscle microcirculatory dysfunction provide an attractive mechanism by which fractures with severe soft tissue trauma may take longer to heal or even develop a non-union. However, the response of periosteum to additional soft tissue trauma does not appear to be uniform, as varying injury severities may obviously induce a different periosteal cellular response. Using a rat model of soft tissue injury without associated fracture Landry and co-workers have found a significant periosteal cell proliferation, osteoblast accumulation leading to significant callus formation in response to moderate soft tissue trauma [22]. In line with this view it has been reported that transient ischemia of the limb without any injury to the bone may induce a marked periosteal cell proliferation and osteogenic differentiation [27]. In addition, Brighton and Krebs have demonstrated that healing in terms of cartilage and bone formation occurs in periosteal areas of low oxygen tension [28]. This finding has been confirmed by Deren et al, as optimum alkaline phosphatase expression of cultured periosteal cells was found at lower oxygen tensions [29]. In this context limited periosteal microvascular injury with impaired nutritive blood flow may be seen as an ischemia trigger mechanism for subsequent stimulation and modulation of periosteal cells that allows them to promote initial steps of bone healing. To what extent, however, the decrease in periosteal blood flow and oxygen supply results in osteogenic differentiation and callus formation, beyond which injury-threshold trauma-induced ischemia turns into irreversible ischemic injury and adversely affects fracture healing, merits further study. Whether the presently used injury severity for CSTI and the evolving periosteal microcirculatory

disturbances might cause delayed fracture repair cannot be concluded from the present data. Future studies are warranted to determine the periosteal callus formation and biomechanical outcome following fractures with associated severe CSTI. Answers to these questions may result in a better understanding of mechanisms of periosteal microvascular injury and its effects on bone healing. Their appreciation will likely have a substantial impact on the therapeutic management of fractures with severe, associated soft tissue injury, involving increased risk of delayed or incomplete fracture healing.

Furthermore, the adverse effects on periosteum and bone perfusion are expected to be pronounced by the prolonged manifestation of CSTI-induced microvascular derangements. The delayed course, combined with the continued existence of microcirculatory dysfunction, implicates some factors other than the trauma itself for perpetuation of the sustained microvascular disturbances and *inflammation* evolving secondary to CSTI. How this secondary tissue damage following severe CSTI occurs is unclear, but may be attributed to a multitude of different changes that develop in parallel and sequentially showing a mutual dependency.

Among others, these secondary alterations may include metabolic dysfunction of skeletal muscle [30], ongoing degradation of membrane phospholipids [31], progressive accumulation of free radicals [32], and inflammation-induced oxidative stress [33, 34]. In addition, a sustained imbalance between vasodilation mediators (e.g., nitric oxide) [35] and vasoconstriction mediators (e.g., endothelins) [36] was demonstrated, which is thought to result in endothelial cell damage, platelet and leukocyte aggregation, and edema formation. Interstitial edema, in turn, contributes to pressure-induced collapse of capillaries. Although only a tendency towards lower diameters in periosteal capillaries has been observed at 2 h, 24 h and 48 h following CSTI, it was shown by Wolfard and co-workers that periosteal ischemia typically results in endothelin-dependent capillary constriction [36]. They further demonstrated that the decrease in capillary diameter is effectively reversed by the administration of endothelin antagonists. Along with these changes endothelin receptor antagonist treatment was also associated with improved nutritive perfusion and impaired inflammatory reaction, as a significantly increased FCD and decreased leukocyte adherence were observed. These *beneficial* effects make it tempting for one to conclude that endothelin is likely to play a causative role in periosteal ischemic tissue injury and that its receptor system may serve as a target for improving periosteal and osseous perfusion.

Furthermore, the fact that the antero-lateral surface of the tibial periosteum being investigated by intravital microscopy is located within the injured antero-lateral tibial skeletal muscle compartment points to a direct transmission of increased tissue pressure within the closed

osteofascial space to the adjacent periosteal microvasculature. Elevated tissue pressure, in turn, may result in reduced capillary perfusion pressure and increased hydraulic capillary flow resistance [37, 38], which cause secondary microcirculatory impairment in the periosteum. The notion of this pathway is substantiated by the fact that peak level in capillary extravasation of macromolecules (microvascular permeability) coincided with the maximum periosteal leukocyte adherence, tissue pressure, and edema, supporting the concept of leukocyte-mediated endothelial dysfunction and subsequent periosteal tissue injury. Further evidence for this pathway is provided by the observed positive correlation between leukocyte adherence and microvascular permeability as well as  $P_{im}$ .

At the 1-week and 6-week time points of analysis, periosteal involvement in fracture healing-associated alterations in the structure and function of periosteal microvasculature, i.e., regeneration, angiogenesis, and neovascularization [4, 39] may also interfere with the prolonged propagation of trauma-induced microvascular changes. However, as initial microvessel disruption, hemorrhage, hemostasis, and inflammation typically

precede every adequate post-traumatic healing response, these different pathophysiological changes do not seem to be mutually exclusive. Rather, they appear to be interdependent, closely linked, and probably overlapping processes.

In conclusion, the data provided here offer detailed information on periosteal microvascular response to closed soft tissue trauma. The findings could allow a temporal interrelation of the CSTI-induced individual microvascular derangements in periosteum to the healing response of fractures with associated soft tissue damage. Thus, these results may have therapeutic implications for the preservation of periosteal integrity and consideration of the interaction of soft tissue damage and periosteal microvascular injury during the management of musculoskeletal trauma.

**Acknowledgement** This work was supported by grants from Deutsche Forschungsgemeinschaft (DFG Scha 930/1-1) and the AO-ASIF Foundation, Switzerland.

## References

1. Einhorn TA (1998) The cell and molecular biology of fracture healing. *Clin Orthop* 355 [Suppl]:S7–21
2. Rhinelander FW (1965) Some aspects of the microcirculation of healing bone. *Clin Orthop* 400:12–16
3. Rhinelander FW (1974) Tibial blood supply in relation to fracture healing. *Clin Orthop* 105:34–81
4. Winet H (1996) The role of microvasculature in normal and perturbed bone healing as revealed by intravital microscopy. *Bone* 19:39S–57S
5. Einhorn TA, Simon G, Devli VVJ, Warman J, Sidhu SP, Vigorita VJ (1990) The osteogenic response to distant skeletal injury. *J Bone Joint Surg Am* 72:1374–1378
6. Gustilo RB, Mendoza RM, Williams DN (1984) Problems in the management of type III (severe) open fractures. *J Trauma* 24:742–746
7. Gustilo RB, Merkow RL, Templeman D (1990) The management of open fractures. *J Bone Joint Surg Am* 72:299–304
8. Esterhai JL, Queenan J (1991) Management of soft tissue wounds associated with type III open fractures. *Orthop Clin North Am* 22:427–432
9. Kowalski MJ, Schemitsch EH, Kregor PJ, Senft D, Swiontkowski MF (1996) Effect of periosteal stripping on cortical bone perfusion: a laser-Doppler study in sheep. *Calcif Tissue Int* 59:24–26
10. Utvag SE, Grundnes O, Reikeras O (1998) Effects of lesion between bone, periosteum and muscle on fracture healing in rats. *Acta Orthop Scand* 69:177–180
11. Schaser K, Vollmar B, Kroppenstedt S, Schewior L, Raschke M, Menger MD, Lübke A, Haas N, Mittlmeier T (1999) In vivo analysis of microcirculation following closed soft tissue injury. *J Orthop Res* 17:678–685
12. Rucker M, Roesken F, Vollmar B, Menger MD (1998) A novel approach for the comparative study of periosteum, muscle, subcutis, and skin microcirculation by intravital microscopy. *Microvasc Res* 56:30–42
13. Menger MD, Steiner D, Messmer K (1992) Microvascular ischemia–reperfusion injury in striated muscle: significance of “no reflow” *Am J Physiol* 263:H1892–1900
14. Villringer A, Dirnagel U, Them A, Shurer L, Krombach F, Einhüpl KM (1991) Imaging of leukocytes within the rat brain cortex in vivo. *Microvasc Res* 42:305–315
15. Reed MWR, Miller FN (1988) Importance of light dose in fluorescent microscopy. *Microvasc Res* 36:104–107
16. Saetzler RK, Jallo J, Lehr HA (1988) Intravital fluorescence microscopy: impact of light-induced phototoxicity on adhesion of fluorescently labeled leukocytes. *J Histochem Cytochem* 45:505–513
17. Klyszcz T, Junger M, Jung F, Zeintl H (1989) Cap image—a new kind of computer-assisted video image analysis system for dynamic capillary microscopy. *Biomed Tech* 42:168–175
18. Zeintl H, Sack FU, Intaglietta M, Messmer K (1989) Computer assisted leukocyte adhesion measurement in intravital microscopy. *Int J Microcirc Clin Exp* 8:293–302
19. Atheron A, Born GVR (1972) Quantitative investigation of the adhesiveness of circulating polymorphonuclear leukocytes to blood vessel walls. *J Physiol* 222:447–474
20. Menger MD, Pelikan S, Steiner D, Messmer K (1992) Microvascular ischemia–reperfusion injury in striated muscle: significance of “reflow paradox”. *Am J Physiol* 263:H1901–1906
21. Looney SW, Stanley, WB (1989) Exploratory repeated measures analysis for two or more groups. *Am Stat* 43:220–225
22. Landry PS, Marino AA, Sadasivan KK, Albright JA (2000) Effect of soft-tissue trauma on the early periosteal response of bone to injury. *J Trauma* 48:479–483
23. Brookes M, Elkin AC, Harrison RG (1961) A new concept of capillary circulation in bone cortex. *Lancet* 1:1078

24. Whiteside LA, Lesker PA (1978) The effects of extraperiosteal and subperiosteal dissection. I. On blood flow in muscle. II. On fracture healing. *J Bone Joint Surg Am* 60:23–30
25. Zhang L, Bail H, Mittlmeier T, Haas NP, Schaser KD (2003) Immediate microcirculatory derangements in skeletal muscle and periosteum following closed tibial fracture. *J Trauma* (in press)
26. Byrd HS, Cierny G, Tebbetts JB (1981) The management of open tibial fractures with associated soft tissue loss: external pin fixation with early flap coverage. *Plast Reconstr Surg* 68:73–79
27. Svindland AD, Nordsletten L, Reikeras O, Skjeldal S (1995) Periosteal response to transient ischemia. *Acta Orthop Scand* 66:468–472
28. Brighton CT, Krebs AG (1972) Oxygen tension of healing fractures in the rabbit. *J Bone Joint Surg Am* 54:323–332
29. Deren JA, Kaplan FS, Brighton CT (1990) Alkaline phosphatase production by periosteal cells at various oxygen tensions in vitro. *Clin Orthop* 252:307–312
30. Hill AG, Hill GL (1998) Metabolic response to severe injury. *Br J Surg* 85:884–890
31. van der Vusse GJ, van Bilsen M, Reneman RS (1994) Ischemia and reperfusion induced alterations in membrane phospholipids: an overview. *Ann N Y Acad Sci* 723:1–14
32. van der Laan L, Oyen WJ, Verhofstad AA (1997) Soft tissue repair capacity after oxygen-derived free radical-induced damage in one hindlimb of the rat. *J Surg Res* 72:60–69
33. Weiss SJ (1989) Tissue destruction by neutrophils. *N Engl J Med* 320:365–376
34. Giannoudis PV, Smith RM, Banks RE, Windsor ACJ, Dickson RA, Guillou PJ (1998) Stimulation of inflammatory markers after blunt trauma. *Br J Surg* 85:986–990
35. Lefer AM, Lefer DJ (1996) The role of nitric oxide and cell adhesion molecules on the microcirculation in ischemia–reperfusion. *Cardiovasc Res* 32:743–751
36. Wolfard A, Csaszar J, Gera L, Petri A, Simonka JA, Balogh A, Boros M (2002) Endothelin-a receptor antagonist treatment improves the periosteal microcirculation after hindlimb ischemia and reperfusion in the rat. *Microcirculation* 9:471–476
37. Vollmar B, Westermann S, Menger MD (1999) Microvascular response to compartment syndrome-like external pressure elevation: an in vivo fluorescence microscopic study in the hamster striated muscle. *J Trauma* 46:91–96
38. Shrier I, Magder S (1995) Pressure–flow relationships in in vitro model of compartment syndrome. *J Appl Physiol* 79:214–221
39. Brighton CT, Hunt RM (1997) Early histologic and ultrastructural changes in microvessels of periosteal callus. *J Orthop Trauma* 11:244–253

### **3.1.3 Der Einfluss einer geschlossenen Tibiaschaftfraktur auf die mikrovaskuläre Perfusion des Periostes und Skelettmuskels**

Initiale Untersuchungen konnten zeigen, dass bereits ein isolierter, schwerer geschlossener Weichteilschaden ohne gleichzeitige Fraktur mit sofortigen und protrahiert ablaufenden mikrovaskulären Perfusionsstörungen des umliegenden verletzten Skelettmuskels und Periostes vergesellschaftet ist (150, 152). Da aus klinischer Sicht jedoch komplexe Extremitätenverletzungen zumeist durch das kombinierte Auftreten von schweren Weichteiltraumen und offenen oder geschlossenen Frakturen gekennzeichnet sind, sollen nachfolgende Studien die frakturinduzierten Veränderungen in Skelettmuskel und Periost quantitativ analysieren.

Die standardisierte Frakturherstellung am Unterschenkelschaft der Ratte erfolgte dabei unter Zuhilfenahme eines in unserer Forschungsabteilung etablierten und standardisierten Frakturmodells der Ratte (63), welches eine Modifikation der von Bonnarens und Einhorn beschriebenen Technik darstellt (9). Dabei wird am Rattenhinterlauf ein Metallstempel auf die gewünschte Frakturstelle der antero-medialen Tibia justiert. Ein Guillotine-artig herabfallendes Gewicht induziert dann auf der Basis einer modifizierten Dreipunktbiegung im mittleren Schaftdrittel eine geschlossene kurze Schrägfraktur mit geringem Weichteilschaden.

Nach Frakturherstellung erfolgt die perkutane Stabilisierung der Fraktur mittels intramedullärer Spickdraht (SD)-Osteosynthese. Dabei entsteht eine belastungsstabile Osteosynthese, die eine Ruhigstellung ermöglicht und eine sekundäre Fragmentdislokation verhindert.

Die vorliegenden Arbeiten demonstrieren, dass eine einfache Tibiaschaftfraktur zu tiefgreifenden Mikrozirkulationsstörungen sowohl auf Ebene des Periostes als auch im umliegenden Skelettmuskel führt (199). Während die fraktur-induzierten Veränderungen der periostalen Kapillarperfusion und endothelialen Leukozytenadhärenz ein ähnliches Ausmaß zeigten wie nach isoliertem Weichteiltrauma, waren diese Störungen im Skelettmuskel vergleichsweise geringer ausgeprägt.

Die gleichzeitige Bestimmung der mikrovaskulären Dysfunktion und der zellulären inflammatorischen Reaktion in Periost und umliegenden Skelettmuskel nach einer Fraktur erlaubte somit die detaillierte Analyse der Interaktion von periostaler-ossärer und angrenzender Skelettmuskelperfusion. Außerdem erlaubte die genaue

quantitative Kenntnis der frakturbedingten Mikrozirkulationsstörungen im Periost und Skelettmuskel weitere Schlussfolgerungen über deren Auswirkung auf die zellulären Prozesse der Frakturheilung. Auf Grundlage dieser Daten (199) besteht die Möglichkeit, periostale Mikrozirkulationsstörungen mit biomechanischen und histomorphologischen Parametern der Frakturheilung zu korrelieren und kausale funktionelle Zusammenhänge zum Ausmaß der Frakturheilungsverzögerung aufzudecken.

# Immediate Microcirculatory Derangements in Skeletal Muscle and Periosteum after Closed Tibial Fracture

Li Zhang, MD, PhD, Hermann Bail, MD, Thomas Mittlmeier, MD, Norbert P. Haas, MD, and Klaus-D. Schaser, MD

**Background:** Severe musculoskeletal soft tissue injury sustained after a closed fracture to the extremities significantly influences bone healing and determines the patient's prognosis. The present study was aimed at quantitatively assessing immediate microcirculatory changes in skeletal muscle and periosteum after standardized closed fracture.

**Methods:** Standardized closed fracture of the left tibia in isoflurane-anesthetized Sprague-Dawley rats (n = 14) was induced using a modified weight-drop technique. The left extensor digitorum longus (EDL) muscle (n = 7) and tibial periosteum (n = 7) were surgically ex-

posed for *in vivo* fluorescence microscopy 15 minutes after fracture. Nonfractured rats (n = 14) served as controls. EDL muscle edema was determined by the ratio of wet to dry weight (EDL water content).

**Results:** Closed tibial fracture resulted in a significant reduction of functional capillary density, red blood cell velocity, and volumetric blood flow in both EDL muscle and periosteum. Microvascular diameter, leukocyte adherence, and macromolecular leakage were markedly increased, indicating trauma-induced inflammation and endothelial disintegration. EDL muscle edema was found increased significantly after fracture.

**Conclusion:** This model permits for the first time direct *in vivo* visualization and quantification of fracture-induced microhemodynamic changes and cellular interactions within the surrounding soft tissue. It demonstrates that even simple fractures lead to profound microcirculatory disturbances in skeletal muscle and periosteum, and also at sites remote from the diaphyseal fracture site. It provides a useful approach for the development of therapeutic strategies to counteract fracture-induced microvascular dysfunction.

**Key Words:** Fracture, Microcirculation, Skeletal muscle, Periosteum, Leukocyte adherence, Intravital microscopy.

*J Trauma.* 2003;54:979–985.

Complex fractures of the extremities typically involve severe closed or open trauma to the musculoskeletal soft tissue and periosteum. Pathophysiologic pathways activated after severe trauma to skeletal muscle and periosteum are of essential clinical importance because they trigger bone healing and decisively determine the patient's prognosis.<sup>1</sup>

At present, quantitative assessment of posttraumatic soft tissue damage and consecutively developing perfusion disturbances is performed on the basis of evaluation of clinical gross findings and relies mainly on empiric evidence.<sup>1,2</sup> Although there is now clinical consensus concerning the integrity of musculoskeletal soft tissues and their influence on bone healing, the extent of microcirculatory deterioration of skeletal muscle and periosteum

caused by a simple fracture is not known. Therefore, several indirect microcirculatory studies of skeletal muscle and cortical bone including laser Doppler flowmetry have been performed.<sup>3–5</sup> However, these studies did not directly allow for simultaneous visualization and quantification of fracture-induced microcirculatory disturbances in skeletal muscle and periosteum.

The clinical observation that extensive soft tissue injury and widespread periosteal stripping frequently precede delayed fracture repair, possibly resulting in nonunion or pseudarthrosis, points to the pathogenetic influence of fracture-induced cellular and microvascular changes within the surrounding skeletal muscle and periosteum. Therefore, we hypothesized that closed tibial fracture adversely affects microcirculation in both skeletal muscle and periosteum. To test this hypothesis, we aimed to quantitatively assess immediate microcirculatory changes in skeletal muscle and periosteum after standardized closed fracture.

## MATERIALS AND METHODS

### Animals

The experiments were performed using 28 Sprague-Dawley rats (body weight, 250–300 g). Experiments were approved by the local animal care authorities and have been performed in accordance with the guidelines for laboratory animal use set forth by the National Institutes of Health (NIH Publication No. 80–23, revised 1985).

Submitted for publication January 7, 2002.

Accepted for publication May 27, 2002.

Copyright © 2003 by Lippincott Williams & Wilkins, Inc.

From the Department of Trauma and Reconstructive Surgery, Charité Campus Virchow, Humboldt-University (L.Z., H.B., N.P.H., K.-D.S.), Berlin, and Department of Trauma and Reconstructive Surgery, Universität Rostock (T.M.), Rostock, Germany.

Supported, in part, by Deutsche Forschungsgemeinschaft grants Scha 930/1-1 and 1-2.

Address for reprints: Klaus-D. Schaser, MD, Department of Trauma and Reconstructive Surgery, Charité, Campus Virchow-Klinikum, Humboldt-University, Augustenburger Platz 1, D-13353 Berlin, Germany; email: klaus-dieter.schaser@charite.de.

DOI: 10.1097/01.TA.0000025796.74054.5B

## Surgical Procedure

Closed tibial fracture of left hindlimb was induced in anesthetized (isoflurane 1.5 vol%, N<sub>2</sub>O 0.5 L/min and O<sub>2</sub> 0.3 L/min) Sprague-Dawley rats (n = 14) using a standardized fracture model for production of diaphyseal fractures using a modified weight-drop technique to the medial aspect of the rat tibia.<sup>6</sup> Using this technique, simple oblique or transversal fractures (AO types A<sub>2</sub> and A<sub>3</sub>) without a spiral component or a bending wedge are reliably produced. Furthermore, application of this model to the medial aspect of the subcutaneously located tibia does not induce significant soft tissue trauma. Subsequent to fracture, intramedullary stabilization of the tibia was achieved by manual insertion of a 1.0-mm Kirschner wire. Intramedullary stabilization was necessary to prevent secondary loss of reduction of the fragments and to provide a horizontal focus level during the microscopic procedure. The location and type of fracture were selected to simulate the clinical situation of lower extremity trauma involving a closed fracture of the tibial diaphysis. A venous catheter (0.58-mm inner diameter, polyethylene 50 [PE 50]; Portex, Hythe, Kent, UK) was inserted through the right external jugular vein into the superior caval vein for injection of fluid and fluorescence dyes. The ascending aorta was cannulated (PE 50) through the right common carotid artery for monitoring of the heart rate (HR) and mean arterial blood pressure. Systolic and diastolic blood pressure as well as HR were monitored with a digital blood pressure analyzer (Digimed, Micro-Med, Louisville, KY). Body temperature was maintained at 37°C with use of a temperature-controlled heating pad.

The extensor digitorum longus (EDL) muscle preparation was performed as described previously by Tysl and Budreau.<sup>7</sup> The EDL muscle was surgically exposed by dissecting the overlying muscles and fascia. To retract neighboring tissue and keep the hindlimb in a horizontal position, sutures were placed on the margin of the anterior tibialis and soleus muscles. Throughout the surgical procedure, the preparations were irrigated with physiologic saline solution and covered with a glass coverslip to prevent drying, tissue dehydration, and oxygen interference.

The tibial periosteum preparation was modified and performed in accordance with Rucker et al.<sup>8</sup> In brief, the gracilis anticus, gracilis posticus, and semitendinosus muscles were dissected medioproximally from the distal to the proximal part. To stabilize periosteum, preparation sutures were placed on the margin of the neighboring muscles. Irrigation of the preparation was the same as described for EDL muscle.

## Experimental Groups and Protocol

Depending on the tissue being investigated, the traumatized rats were assigned to group 1 (skeletal muscle, n = 7) or group 2 (periosteum, n = 7). Nonfractured (sham-operated) animals (n = 14) served as controls for the study of both skeletal muscle (n = 7) and periosteum (n = 7). In vivo

fluorescence microscopy of either EDL muscle or periosteum was performed 15 minutes after termination of surgical preparation (i.e., 1 hour after induction of the fracture). The rats were killed by exsanguination at the end of the microscopic procedures, and the EDL muscle of the left (fractured) and right (nonfractured) legs was harvested for determination of edema formation.

## Intravital Fluorescence Microscopy

The microvasculature of the EDL muscle and periosteum was investigated in epi-illumination (100-W mercury lamp) through an in vivo microscope (AxioTech Vario, Carl Zeiss, Goettingen, Germany) equipped with a water-immersion objective (Achromplan, ×20, Carl Zeiss, Germany) and fluorescence filters for visualization of fluorescein isothiocyanate-labeled dextran (450–490/>580 nm) and rhodamine (530–560/>580 nm). Microcirculatory images were recorded using a CCD-video camera (FK 6990-IQ, Pieper, Schwerte, Germany) connected to an SVHS video recorder (HR-S4700EG/E, JVC, Friedberg, Germany) and stored on videotapes for off-line evaluation. Before microscopy, a single bolus of fluorescein isothiocyanate-labeled dextran (5%, 150,000 MW, 15 mg/kg body weight; Sigma Chemical, Deisenhofen, Germany) and rhodamine 6G (0.1%, 0.15 mg/kg body weight; Sigma Chemical) was injected intravenously to enhance the contrast of the microvascular network and to perform in vivo staining of leukocytes.<sup>9–11</sup> For in vivo microscopy, the surface of the EDL muscle and periosteum was sequentially scanned from the distal to the proximal part in approximately 2-mm increments with use of a computer-assisted microscope stage equipped with a stepping motor (MC 2000, Merzhäuser, München, Germany). To reliably assess microcirculation of EDL muscle and periosteum, microscopic images from at least six observation areas in each type of tissue were recorded. Thus, in vivo microscopic analysis of the microcirculation in the entire EDL muscle or meta- and diaphyseal periosteum was permitted, particularly in areas remote from the fracture site. Values obtained for each of these areas were averaged per animal. To minimize phototoxic effects, each observation in vivo microscopic period (i.e., continuous exposure with fluorescence light) was limited to a maximum of 60 seconds.<sup>11,12</sup>

## Microcirculatory Analysis

Microcirculatory parameters were analyzed off-line using computer-assisted image analysis systems (Capimage, Zeintl, Heidelberg, Germany).<sup>13,14</sup> Microhemodynamic analysis included the determination of functional capillary density (FCD) (defined as the total length of red blood cell-perfused capillaries per observation area, cm<sup>-1</sup>), capillary and venular red blood cell velocity ( $V_{RBC}$ ) (determined by frame-to-frame analysis, mm/s) and capillary and venular diameters (D) (μm). Microvascular permeability (macromolecular leakage) was expressed as the ratio of fluorescence intensity, selected from perivascular area to the corresponding intravascular

**Table 1** Macrohemodynamic Parameters<sup>a</sup>

Group	EDL Muscle		Periosteum	
	Sham	Fracture	Sham	Fracture
MABP (mm Hg)	82.3 ± 3.9	86.3 ± 5.9	80.3 ± 6.9	86.4 ± 5.6
HR (beats/min)	321.4 ± 65.5	297.2 ± 54.1	327.1 ± 47.7	325.8 ± 22.1

MABP, mean arterial blood pressure.

<sup>a</sup> MABP and HR of sham-operated and fractured rats showed no significant differences between both groups and were stable throughout the study period. Values were expressed as mean ± SD.

region (plasma gaps between erythrocytes).<sup>13,14</sup> Volumetric capillary and venular blood flow (VBF) (pl/s) was calculated from  $V_{RBC}$  and  $D$  for each vessel as  $VBF = \pi/4 \times D^2 \times V_{RBC}$ .

In each animal, leukocyte-endothelial cell interaction was analyzed in at least six postcapillary venules of EDL muscle and periosteum, respectively. Leukocyte rolling was assessed by the ratio of leukocytes moving significantly slower than the mainstream velocity to the total leukocyte flux (percent).<sup>10</sup> Permanently adherent leukocytes were defined by leukocytes with stable endothelial contact, not moving or detaching from the endothelium line during an observation period of 30 seconds. Leukocyte adherence was expressed per square millimeter of endothelial surface, calculated from diameter and length of the vessel segment studied, assuming cylindrical geometry.<sup>10,15</sup>

### Determination of Skeletal Muscle Edema Formation

Edema weight gain was assessed by measuring the wet-to-dry weight ratio of EDL muscle. After determination of wet weight, the EDL muscle was dried for 24 hours in a laboratory oven (80°C) and weighed again (dry weight). Stable dry weight was found after 24 hours in all animals. Edema formation was determined by the water content of EDL muscle (percent) and finally expressed as edema index (EI) (i.e., the wet-to-dry weight ratio of left vs. right EDL muscle).

### Statistical Analysis

Results are expressed as mean ± SD. After passing Kolmogorov-Smirnov test for normality, the groups were compared using Student's *t* test. Differences were considered significant at  $p < 0.05$ .

## RESULTS

### Macrohemodynamics

Mean arterial blood pressure generally ranged from 78 to 92 mm Hg and HR was in the range of 243 to 387 beats/min and remained stable with no significant difference between groups throughout the study period (Table 1).

### EDL Muscle

In EDL muscle of the nonfractured group, capillaries were found arranged in parallel to each other, with only a few intercapillary anastomoses. They were straightened in the

longitudinal axis of the muscle fibers. No significant microvascular thrombosis and macromolecular leakage or leukocyte adherence were found (Fig. 1A).

EDL muscle microcirculation after closed tibial fracture displayed a heterogeneous perfusion pattern with severe microvascular dysfunction, including stasis and collapse of capillaries, increase in intercapillary distance, microvascular thrombosis, and direct disruption of microvessels with subsequent hemorrhage (Fig. 1B). FCD ( $197.8 \pm 32.8$ ) and  $V_{RBC}$  ( $134.6 \pm 27.7$ ) of EDL muscle after fracture were found to be significantly reduced compared with noninjured controls (FCD,  $261.7 \pm 23.8$ ;  $V_{RBC}$ ,  $233.8 \pm 18.6$ ) (Fig. 2A and Table 2). Immediate disturbances in nutritive perfusion were further characterized by a significant hypoperfusion as demonstrated by a marked (Table 2). Changes in microvascular diameters in response to fracture were characterized by a simultaneous vasodilation of capillaries ( $42.0 \pm 11.3$  vs.  $28.7 \pm 11.6$ ) and postcapillary ( $5.9 \pm 0.4$  vs.  $5.5 \pm 0.2$ ) venules (Table 2). In addition, a significant increase in microvascular permeability (transendothelial leakage) was found (Fig. 2B), indicating substantial loss of endothelial integrity in the skeletal muscle in response to fracture. Analysis of leukocyte-endothelial cell interaction revealed a substantial increase when compared with nonfractured animals. Leukocyte rolling and adherence were found to be increased by twofold, mostly restricted to the endothelium of postcapillary venules (Fig. 3).

### Periosteum

In the tibial periosteum of nonfractured rats, microvascular perfusion was characterized by two distinct types of capillary arrangements. Adjacent to the supplying and draining vessels, at the metaphysis, capillaries were arranged as densely meshed, reticular networks with numerous intercapillary connections. The arrangements of capillaries more distant to the supplying vessels were different, with a relatively parallel alignment to the axis of the tibial diaphysis. Perfusion in both tissue types was found to be homogeneous, with no significant capillary dysfunction (Fig. 1C) or leukocyte adhesion (Fig. 1E).

On the contrary, microvascular response of periosteum to fracture showed striking changes that were dependent on the region being analyzed. In the immediate vicinity of the fracture site, a total microvascular perfusion failure with hemorrhage and a significantly increased microvascular permeability (leakage,  $0.60 \pm 0.08$  vs.  $0.49 \pm 0.02$ ) were found (Figs.



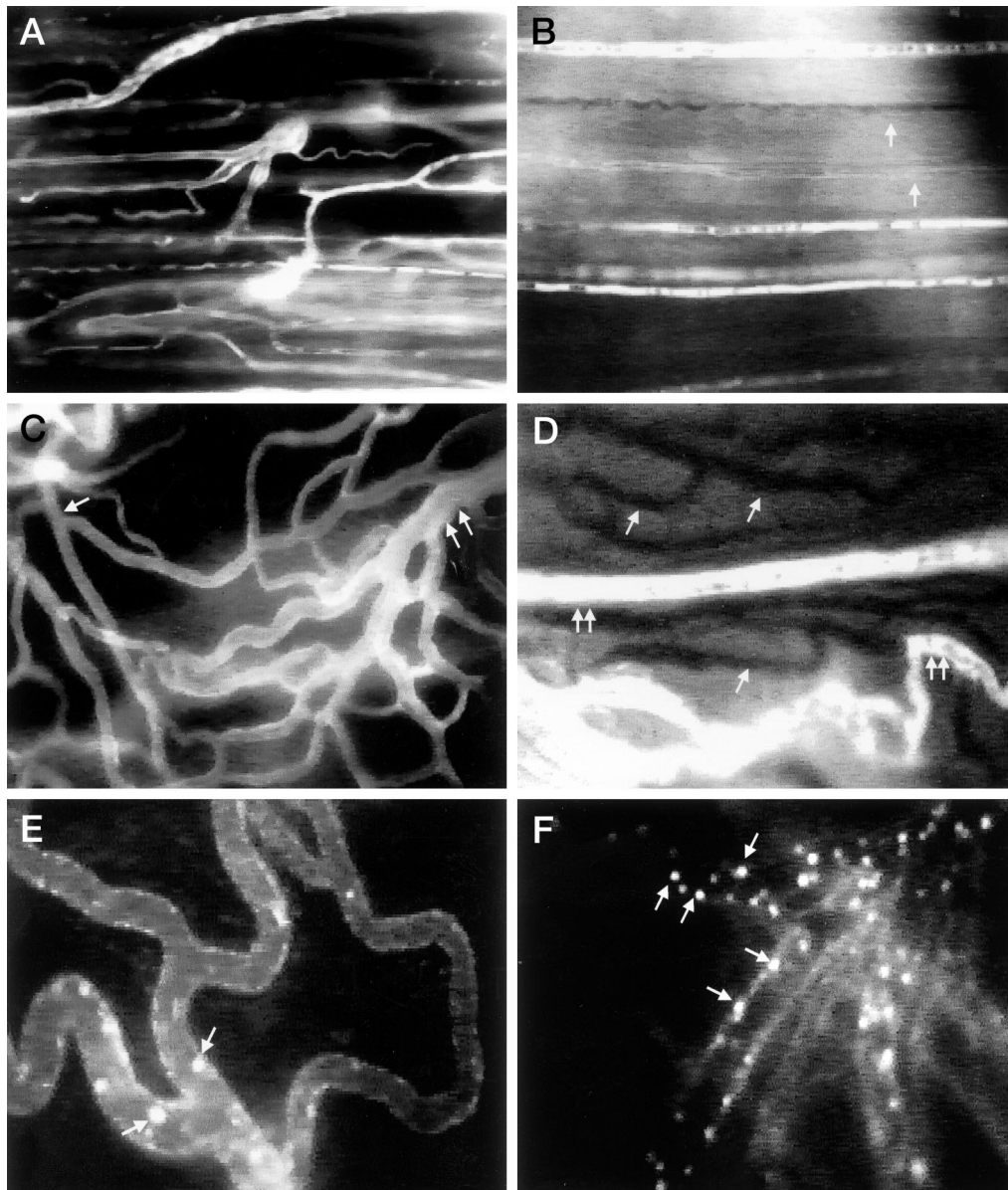


**Fig. 1.** (A) Intravital microscopy of EDL muscle in sham-operated animals typically demonstrated perfused capillaries draining into a postcapillary venule. Capillaries were arranged in parallel and along the longitudinal axis of the muscle fibers. Note the homogeneous perfusion and close intercapillary distance. (B) Intravital microscopy of rat EDL muscle after closed tibial fracture, demonstrating heterogeneous perfusion with significant capillary thrombosis (arrows), increase in intercapillary distance, and microvascular permeability (extravasation of fluorescently labeled macromolecules) indicating interstitial edema formation because of the posttraumatic loss of endothelial integrity. (C) Intravital microscopy of homogeneous periosteal microcirculation at the tibial metaphysis of sham-operated rats, displaying a meshed network of capillaries with supplying arteriole (arrow) and draining postcapillary venule (double arrow). (D) Intravital microscopy of heterogeneous periosteal microcirculation at the rat tibial metaphysis after closed tibial fracture, displaying a severe microvascular perfusion failure indicated by silhouettes of nonperfused and clotted capillaries (arrow). Only a few capillaries remained perfused (double arrow). (E) Leukocyte-endothelial cell interaction in periosteal postcapillary venules of sham-operated rats, demonstrating the rarity of temporarily and permanently adherent leukocytes (arrow). (F) Leukocyte-endothelial cell interaction in periosteal postcapillary venules after closed fracture of rat tibia. Note the marked increase in accumulation and adherence of leukocytes rolling along and sticking to the postcapillary endothelium (arrow), indicative of significant fracture-induced inflammatory reaction of rat periosteum. Original magnification,  $\times 405$ .

1D and 2B). However, metaphyseal areas remote from the fracture site displayed a heterogeneous perfusion with decreased  $V_{RBC}$  (Table 2) and scattered capillary thrombosis,

increased microvascular leakage, and drastically increased leukocyte-endothelium cell interaction (Fig. 1F). Again, rolling and adherence of leukocytes were increased by twofold when

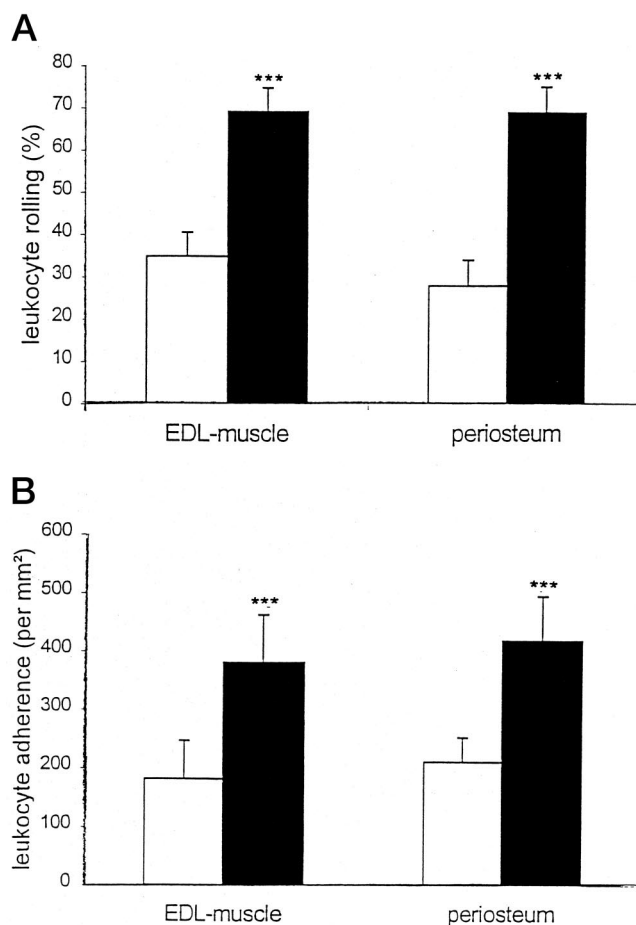
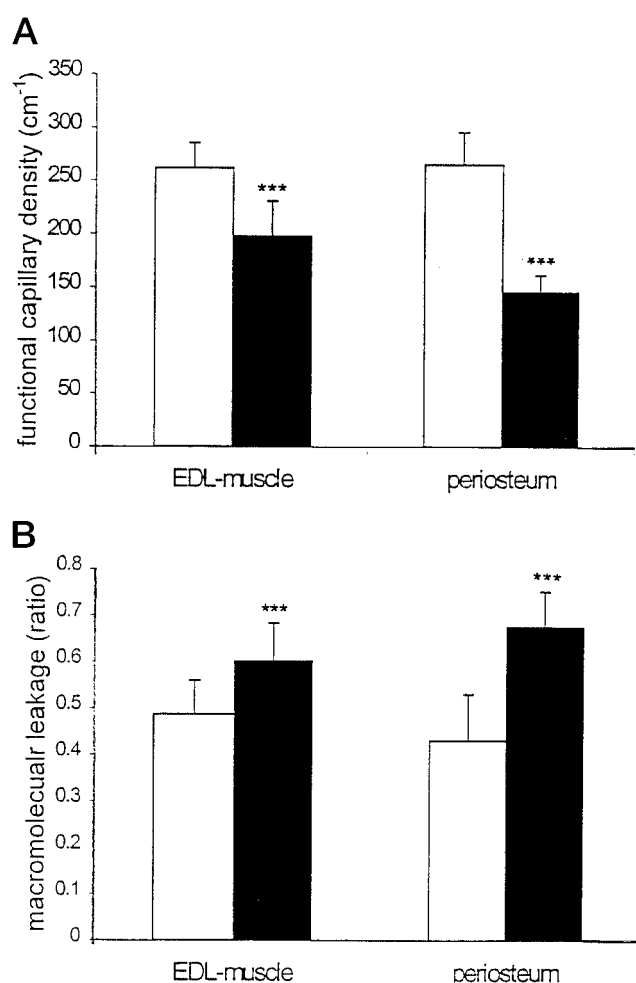


**Fig. 2.** (A) Microvascular permeability (leakage of fluorescein isothiocyanate-labeled dextran, assessed densitometrically by the ratio of extravascular to intravascular fluorescence intensity) of EDL muscle and periosteum in sham-operated (open bar) and fractured rats (filled bar). Values were mean  $\pm$  SD. \*\*\* $p < 0.001$  versus sham-operated rats (*t* test). (B) Functional capillary density (length of red blood cell-perfused capillaries per observation area; cm<sup>-1</sup>) of EDL muscle and periosteum in sham-operated (open bar) and fractured rats (filled bar). Values are mean  $\pm$  SD. \*\*\* $p < 0.001$  versus sham-operated rats (*t* test).

**Fig. 3.** Fraction of rolling leukocytes (A, percentage of total leukocyte flux) and number of permanently adherent leukocytes (B, per square millimeter of endothelial surface) in postcapillary venules of EDL muscle and periosteum in sham-operated (open bar) and fractured rats (filled bar). Values were mean  $\pm$  SD. \*\*\* $p < 0.001$  versus sham-operated rats (*t* test).

compared with sham-operated animals and primarily restricted to endothelium of postcapillary periosteal venules (Fig. 3).

**Edema Formation**

In the sham-operated rats, no significant difference between the water content of left and right EDL muscle was

**Table 2** Immediate Microvascular Changes Including Diameter, Volumetric Blood Flow in Capillaries and Venules, and Red Blood Cell Velocity Measured in EDL Muscle and Periosteum of Sham-Operated and Fractured Rats<sup>a</sup>

	D ( $\mu$ m)		VBF ( $\mu$ m <sup>3</sup> /s)		V <sub>RBC</sub> ( $\mu$ m/s)	
	Capillaries	Venules	Capillaries	Venules	Capillaries	Venules
EDL muscle						
Sham	5.5 $\pm$ 0.2	28.7 $\pm$ 11.6	5.7 $\pm$ 0.9	103.1 $\pm$ 96.7	233.8 $\pm$ 18.6	172.2 $\pm$ 40.8
Fracture	5.9 $\pm$ 0.4*	42.0 $\pm$ 11.3**	3.7 $\pm$ 1.0**	160.1 $\pm$ 91.1	134.6 $\pm$ 27.7***	116.6 $\pm$ 27.1**
Periosteum						
Sham	9.6 $\pm$ 1.3	29.8 $\pm$ 3.3	19.7 $\pm$ 9.8	97.0 $\pm$ 28.9	218.9 $\pm$ 10.1	166.0 $\pm$ 30.8
Fracture	10.4 $\pm$ 1.3	42.8 $\pm$ 5.0***	21.6 $\pm$ 11.0	160.0 $\pm$ 87.1	110.7 $\pm$ 32.2***	112.3 $\pm$ 18.9***

<sup>a</sup> Values are expressed as mean  $\pm$  SD.  
\*  $p < 0.05$ ; \*\*  $p < 0.01$ ; \*\*\*  $p < 0.001$  vs. sham-operated rats (*t* test).

**Table 3** Skeletal Muscle Edema Formation<sup>a</sup>

	EDL Water Content (%)		Edema Index
	Left	Right	
Sham-operated	77.9 ± 4.7	74.9 ± 3.4	1.03 ± 0.09
Fracture	80.5 ± 3.1*	75.1 ± 4.0	1.07 ± 0.08*

<sup>a</sup> Intramuscular water content was calculated in the left (experimental) and right (contralateral) EDL muscle. Edema index was calculated by the ratio of EDL muscle wet-to-dry weight of experimental vs. contralateral EDL muscle. Values were expressed as mean ± SD.

\*  $p < 0.05$ ; \*\*  $p < 0.01$ ; \*\*\*  $p < 0.001$  vs. sham-operated rats (t test).

observed as indicated by a low EI. However, closed tibial fracture caused a significant increase in EDL muscle water content and EI, demonstrating fracture-induced skeletal muscle edema formation (Table 3).

## DISCUSSION

From the clinical point of view, it is well accepted that the healing of open and closed diaphyseal fracture critically depends on severity of associated soft tissue damage.<sup>1</sup> This may be because the extrasosseous blood supply to the bone is adversely affected. Both clinical<sup>16</sup> and experimental evidence<sup>17</sup> support the notion that skeletal muscle provides an important collateral source of blood to cortical bone. Furthermore, it has been shown that the periosteum and overlying muscles share circulatory channels and have collateral circulation.<sup>18,19</sup>

This study using in vivo fluorescence microscopy demonstrates for the first time that even a simple closed noncomminuted fracture results in profound impairment of nutritive perfusion in both surrounding skeletal muscle and periosteum, as a markedly reduced FCD,  $V_{RBC}$ , and VBF were found. Moreover, these experimental results show that the microvascular response of skeletal muscle and periosteum to closed fracture can be visualized and quantitatively analyzed. The fracture-induced increase in macromolecular leakage in periosteum and skeletal muscle microvessels may be because fracture-induced damage to EDL muscle and periosteum is associated with disruption of microvessels, subsequent hypoxia, and loss of endothelial integrity. These insults in turn may cause an acute disturbance of the transcapillary fluid balance and increase in endothelial permeability resulting in increased edema and elevated tissue pressure. The microvascular thrombosis in surrounding EDL muscle and periosteal regions remote from the central fracture site obviously caused by (or developing in response to) the fracture may result in reduced blood supply to the bone and indicate a “no-reflow” phenomenon similar to ischemia/reperfusion injury. The markedly increased diameter of venules in skeletal muscle and periosteum found after fracture may be indicative of posttraumatic/postischemic vasodilation. Thereby, the capillary filtration pressure and subsequent edema formation may be reduced, because of a decreased transcapillary pressure

gradient. Furthermore, the fact that the capillary VBF was decreased in EDL muscle but increased in periosteum after fracture points to a shift in nutritive perfusion for the benefit of injured periosteum. If, however, the severity and extent of these early microcirculatory disturbances (1 hour after fracture) will be of prognostic significance in fracture healing needs to be shown in future studies.

The increased leukocyte-endothelial cell interaction is thought to be a key feature of postischemic or posttraumatic inflammation.<sup>15,20</sup> These initial adhesive interactions between leukocytes and endothelial cells, leading to leukocyte rolling and subsequent adherence, may be the result of rapid expression of selectin and integrin cell adhesion molecules, initiated by fracture-induced endothelial dysfunction.<sup>9,21</sup> The markedly increased leukocyte-endothelium cell interaction may lead to release of proinflammatory cytokines, thereby increasing trauma-induced inflammation and leukocyte-mediated tissue injury. Apart from direct inflammatory effects, the accumulation and the adherence of leukocytes are known to significantly increase hydraulic flow pressure, which adversely affects nutritive perfusion.<sup>22</sup>

As an additional marker of muscle injury, edema weight gain of the EDL muscle was determined. The present data are in agreement with the former reports showing that closed soft tissue trauma leads to a significant increase in skeletal muscle water content and edema.<sup>15</sup> It has been shown that maximum edema formation coincides with maximum microvascular permeability and leukocyte-endothelial cell interaction, again supporting the concept of leukocyte-mediated tissue injury.<sup>21</sup>

In conclusion, results of the current study describe for the first time direct in vivo visualization and quantification of fracture-induced microhemodynamic changes within the surrounding soft tissue. However, if and to what extent these immediate microvascular derangements in skeletal muscle and periosteum trigger the healing response of injured bone and significantly influence the long-term outcome of fractures with severe soft tissue trauma exceeds the settings of the present investigation and merits further study. Nonetheless, application of this model allows local and temporal interrelation of microvascular parameters in skeletal muscle and periosteum after fracture and trauma. It provides a useful experimental approach for the pathophysiologic analysis of tissue-confined microvascular changes after complex injuries to the extremities. Thus, these data may also allow dissection of the microcirculatory and cellular interactions between periosteum and surrounding skeletal muscle in complex pathways that determine posttraumatic tissue survival, and may allow design of specific therapeutic approaches that prevent tissue death secondary to severe soft tissue injury. In this context, these results may have further clinical perspective in view of developing therapeutic strategies to counteract the manifestations of nutritional dysfunction and inflammatory reaction in traumatized skeletal muscle and periosteum.

## ACKNOWLEDGMENTS

We thank Britt Wildemann, MD, and Gerhard Schmidmaier for their excellent technical assistance.

## REFERENCES

- Oestern HJ, Tschern H. Pathophysiology and classification of soft tissue damage in fractures [in German]. *Orthopade*. 1983;12:2–8.
- Gustilo RB, Merkow RL, Templeman D. The management of open fractures. *J Bone Joint Surg Am*. 1990;72:299–304.
- Kregor PJ, Senft D, Parvin D, et al. Cortical bone perfusion in plated fractured sheep tibiae. *J Orthop Res*. 1995;13:715–724.
- Hjortdal VE, Hansen ES, Henriksen TB, Kjolseth D, Soballe K, Djurhuus JC. The microcirculation of myocutaneous island flaps in pigs studied with radioactive blood volume tracers and microspheres of different sizes. *Plast Reconstr Surg*. 1992;89:116–124.
- Freitelson JBA, Kulenovic E, Beck DJ, et al. Endogenous norepinephrine regulates blood flow to the intact rat tibia. *J Orthop Res*. 2002;20:391–396.
- Bonnarens F, Einhorn TA. Production of a standard closed fracture in laboratory animal bone. *J Orthop Res*. 1984;2:97–101.
- Tyml K, Budreau CH. A new preparation of rat extensor digitorum longus muscle for intravital investigation of the microcirculation. *Int J Microcirc Exp*. 1991;10:335–343.
- Rücker M, Roesken F, Vollmar B, Menger MD. A novel approach for comparative study of periosteum, muscle, subcutis, and skin microcirculation by intravital fluorescence microscopy. *Microvasc Res*. 1998;56:30–42.
- Carlos TM, Harlan JM. Leukocyte-endothelial adhesion molecules. *Blood*. 1994;84:2068–2101.
- Menger MD, Kerger H, Geisweid A, et al. Leukocyte-endothelium interaction in the microvasculature of postischemic striated muscle. *Adv Exp Med Biol*. 1994;361:541–545.
- Saetzler RK, Jallo J, Lehr HA, et al. Intravital fluorescence microscopy: impact of light-induced phototoxicity on adhesion of fluorescently labeled leukocytes. *J Histochem Cytochem*. 1997;45:505–513.
- Steinbauer M, Harris AG, Abels C, Messmer K. Characterization and prevention of phototoxic effects in intravital fluorescence microscopy in the hamster dorsal skinfold model. *Langenbecks Arch Surg*. 2000;385:290–298.
- Klyszcz T, Junger M, Jung F, Zeintl H. Cap image: a new kind of computer-assisted video image analysis system for dynamic capillary microscopy. *Biomed Tech (Berl)*. 1997;42:168–175.
- Zeintl H, Sack FU, Intaglietta M, Messmer K. Computer assisted leukocyte adhesion measurement in intravital microscopy. *Int J Microcirc Clin Exp*. 1989;8:293–302.
- Schaser KD, Vollmar B, Menger MD, et al. In vivo analysis of microcirculation following closed soft-tissue injury. *J Orthop Res*. 1999;17:678–685.
- Byrd HS, Cierny G III, Tebbetts JB. The management of open tibial fractures with associated soft tissue loss: external pin fixation with early flap coverage. *Plast Reconstr Surg*. 1981;68:73–79.
- Richards RR, McKee MD, Paitich CB, Anderson GI, Bertoia JT. A comparison of the effects of skin coverage and muscle flap coverage on the early strength of union at the site of osteotomy after devascularization of a segment of canine tibia. *J Bone Joint Surg Am*. 1991;73:1321–1330.
- Whiteside LA, Lesker PA. The effects of extraperiosteal and subperiosteal dissection: I—on blood flow in muscles. *J Bone Joint Surg Am*. 1978;60:23–26.
- Whiteside LA, Lesker PA. The effects of extraperiosteal and subperiosteal dissection: II—on fracture healing. *J Bone Joint Surg Am*. 1978;60:26–30.
- Granger DN, Kubes P. The microcirculation and inflammation: modulation of leukocyte-endothelial cell adhesion. *J Leukoc Biol*. 1994;55:662–675.
- Weiss SJ. Tissue destruction by neutrophils. *N Engl J Med*. 1989;320:365–376.
- Bagge U, Blixt A, Strid KG. The initiation of post-capillary margination of leukocytes: studies in vitro on the influence of erythrocyte concentration and flow velocity. *Int J Microcirc Clin Exp*. 1983;2:215–227.

### **3.1.4 Intravitalmikroskopische und biomechanische Untersuchungen zur Analyse der Interaktion von traumatischem Weichteilschaden und Frakturheilung**

Es ist bislang unklar, über welche Pathomechanismen und mit welcher zeitlichen Kinetik ein ausgeprägter Weichteilschaden die periostale Perfusion und letztendlich die Frakturheilung negativ beeinflusst. Auf Grundlage der klinischen Problematik bei simultanem Auftreten von Fraktur und schwerer Schädigung des muskuloskeletalen Weichteilmantels war die exakte Bestimmung des pathogenetischen Einflusses eines standardisierten, schweren geschlossenen Weichteilschadens auf die Frakturheilung Ziel dieser Arbeiten.

Das Ausmaß der funktionellen Beeinträchtigung der Frakturheilung wurde mit biomechanischen Verfahren quantitativ analysiert. Darüber hinaus demonstrieren die Untersuchungen erstmalig die Mikrozirkulationsstörungen und die Leukozytenaktivierung in Periost und umliegendem Skelettmuskel bei kombinierter Verletzung, d.h. Fraktur mit simultanem schwerem Weichteilschaden (154, 155).

Im Einzelnen zeigen diese Arbeiten, dass sowohl die geschlossene Weichteilverletzung als auch die Fraktur im Vergleich zu den Kontrollen eine lang anhaltende nutritive Perfusionsstörung, endotheliale Permeabilitätsstörung und Entzündungsreaktion über den gesamten Untersuchungszeitraum bewirkte. Die geschlossene Tibiaschaftfraktur mit geschlossenem Weichteiltrauma führte im Vergleich zu einfacher Fraktur zu einer signifikanten Akzentuierung der kapillären Dysfunktion und Leukozytenadhärenz im Skelettmuskel in der Frühphase nach Trauma. Zusätzlich konnte ein signifikanter funktioneller Zusammenhang (positive Korrelation) zwischen dem Ausmaß der frühen nutritiven Perfusionsdefizite (funktionelle Kapillardichte) und Verminderung der biomechanischen Stabilität in der Frühphase der Frakturheilung (3 Wochen) nachgewiesen werden.

Die Ergebnisse demonstrieren erstmals *in vivo* die Interaktion von traumatischem Weichteilschaden, nutritiver Perfusionsstörung und Frakturheilung. Sie zeigen, dass diese frühen Mikrozirkulationsstörungen der Weichteile zur Verminderung der biomechanischen Stabilität im Verlauf der Frakturheilung führen. Die Resultate lassen die protrahierte Manifestation einer Mikrozirkulationsstörung und Leukozytenaktivierung im Skelettmuskel als kausale, pathogenetische Determinanten für die verzögerte Heilung von Frakturen mit schwerem Weichteilschaden vermuten (154, 155).

# EFFECT OF SOFT TISSUE DAMAGE ON FRACTURE HEALING: INTRAVITAL MICROSCOPIC AND BIOMECHANICAL INVESTIGATIONS IN RATS

+\*Klaus-D. Schaser; \* Zhang, L; \*\* Mittlmeier T, \* Ostapowicz D; \* Schmidmaier G, \* Duda G; \* Haas NP; \* Bail HJ  
+Dept. of Trauma & Reconstructive Surgery, Charite, Campus Virchow, Humboldt-Universität zu Berlin, Berlin, Germany,

**Introduction:** Among the different factors adversely influencing the bone healing response the associated soft tissue trauma is now increasingly attracting major interest, as it significantly impairs fracture repair and decisively determines patient's prognosis (1). Furthermore, severe concomitant soft tissue trauma has been proposed to precede and causatively underlie perturbed bone healing, frequently resulting in non-union, pseudarthrosis. To date, however, the temporal and functional relationship between skeletal muscle microcirculatory deteriorations and biomechanics of fracture healing following fracture with severe closed soft tissue injury (CSTI) are not known. Using intravitalmicroscopic analysis and biomechanical testings the present study was aimed to quantitatively assess the impact of microcirculatory disturbances in skeletal muscle following closed soft tissue damage on fracture healing.

**Methods:** Standardized closed fracture of left tibia (AO type A<sub>2</sub> & A<sub>3</sub>; no significant closed soft tissue damage) in isoflurane-anesthetized (isoflurane 1.5 vol%, N<sub>2</sub>O 0.5 l/min and O<sub>2</sub> 0.3 l/min) SD-rats (n=48) was induced using a modified weight-drop-technique (2) and intramedullary stabilized by manual insertion of a 1.0 mm k-wire. All procedures were performed with the ethical and according to the NIH guidelines. In 24 of these rats an additional standardized closed soft tissue trauma at the anterolateral tibial compartment was induced using the controlled cortical impact technique (3). The rats were assigned (n=6) to 4 groups (2h, 48h, 1 and 3 weeks after the trauma). The left extensor digitorum longus (EDL) muscle was surgically exposed for in vivo fluorescence microscopy (IVM). Non-injured, sham-operated rats (n=6) served as controls. The EDL-muscle was scanned by IVM in 2mm steps, i.e. 8 observation areas. For contrast enhancement of the vascular network and for in vivo staining of leukocytes FITC-dextran and rhodamine 6G was injected intravenously prior to each observation. Microhemodynamic analysis included the determination of microvessel diameters (D in µm), functional capillary density (FCD: length of perfused capillaries per observation area, cm<sup>-1</sup>), leukocyte-endothelial cell interactions (number of sticking leukocytes per mm<sup>2</sup> of endothelial surface) and microvascular permeability (macromolecular leakage). Biomechanical torsional testings (destructive with intact soft tissue envelope, expressed in % of the contralateral non-injured tibia, ZWICK, Ulm, Germany) were performed in additional 40 rats at 3 and 6 weeks following induction of either fracture (n=10 per time point) or fracture with soft tissue trauma (n=10 per time point).

**Results:** Microcirculation of EDL-muscle in control rats demonstrated a homogeneous perfusion with no capillary or endothelial dysfunction. Closed tibial fracture resulted in a significant reduction of functional capillary density in EDL-muscle. Microvascular diameter, leukocyte adherence and macromolecular leakage were markedly increased, indicating trauma-induced inflammation and endothelial disintegration (Tab.1). In comparison, these changes were pronounced 2h and 48h following injury in rats receiving combined fracture and soft tissue trauma. Peak level in capillary leakage coincided with the maximum leukocyte adherence at 48 hours post trauma. Following fractures with soft tissue trauma, the microvascular deteriorations in skeletal muscle were accompanied by a significantly decreased total failure load and the energy absorption of rat tibia in the early fracture healing period (3 weeks) (Tab. 2). Regression analysis between quality of initial capillary perfusion and biomechanical stability (total energy absorption at 3 weeks after fracture) revealed a positive functional association (Fig. 1).

	FCD (cm <sup>-1</sup> )	Leukocyte adherence (1/mm <sup>2</sup> )	Mikrovascular permeability (Leakage in %)	Diameter (µm) Capillary	Venule
Control(sham)	261.2±25.6	181.5±65.3	0.41±0.08	5.5 ± 0.1	25.3±7.9
2h: Fx	191.7±31.4 <sup>a</sup>	350.9±68.7	0.56±0.04 <sup>a</sup>	5.9±0.5	40.3±10.3 <sup>a</sup>
2h: Fx&CSTI	149.8±15.1 <sup>a,b</sup>	636.5±121.9 <sup>a,b</sup>	0.61±0.05 <sup>a</sup>	6.6±0.4 <sup>a,b</sup>	44.6±6 <sup>a</sup>
48h: Fx	185.2±21.3 <sup>a</sup>	504.5±149.7 <sup>a</sup>	0.61±0.04 <sup>a</sup>	6.8±1.5 <sup>a</sup>	46.1±3.9 <sup>a</sup>
48h: Fx&CSTI	154.8±12.9 <sup>a,b</sup>	512.6±82.8 <sup>a</sup>	0.60±0.06 <sup>a</sup>	7.3±1.0 <sup>a</sup>	41.7±5.6 <sup>a</sup>
1w: Fx	187.4±25.8 <sup>a</sup>	405.2±120.4 <sup>a</sup>	0.55±0.09	7.9±1.0 <sup>a</sup>	46.9±6.3 <sup>a</sup>
1w: Fx&CSTI	184.8±19.2 <sup>a</sup>	494.5±80.1 <sup>a</sup>	0.56±0.07	7.2±0.7 <sup>a</sup>	42.5±8.8 <sup>a</sup>
3w: Fx	221.4±17.2 <sup>a</sup>	456.3±67.2 <sup>a</sup>	0.43±0.06	6.9±0.8	42.6±4.0 <sup>a</sup>
3w: Fx&CSTI	196.8±12.8 <sup>a</sup>	388.0±85.1 <sup>a</sup>	0.49±0.03	6.6±0.6 <sup>a</sup>	43.6±6.2 <sup>a</sup>

Table 1: Microvascular parameters in rat EDL-muscle following sham-operation, fracture (Fx) and combined fracture and closed soft tissue injury (Fx&CSTI).<sup>a</sup> p<0.05 vs. Controls, ANOVA and post hoc Bonferroni correction; <sup>b</sup> p<0.05 vs. fracture (Fx), t-test

Table 2: Results of biomechanical testing assessed in % of the

	Torsional moment at failure (% contralat. tibia)	stiffness (% contralat. tibia)	energy absorption (% contralat. tibia)
3 W: Fx	54.7±15.3 <sup>a</sup>	51.9±21.1	122.0±75.5 <sup>a</sup>
3 W: Fx & CSTI	36.1±13.7	52.9±27.4	47.4±32.1
6 W: Fx	112.5±32.8 <sup>a,b</sup>	116.0±33.2 <sup>a,b</sup>	141.0±58.2 <sup>a</sup>
6 W: Fx & CSTI	97.5±42.4 <sup>a,b</sup>	106.3±36.2 <sup>a,b</sup>	99.1±69.8

contralateral, non-injured tibia. <sup>a</sup> p<0.05 vs. 3 weeks (3W)-Fracture (Fx) & CSTI; <sup>b</sup> p<0.05 vs. 3 weeks (3W)-fracture (Fx); t-test

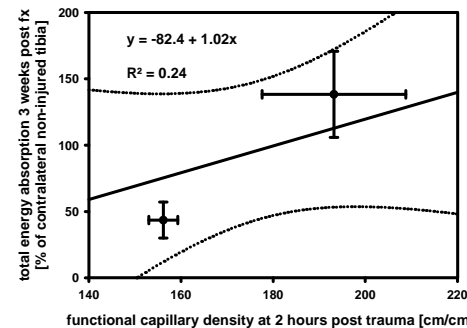


Figure 1. Regression analysis between functional capillary density at 2 hours post trauma and total energy absorption at 3 weeks post fracture as well as fracture with soft tissue trauma. Values are means ± SD. R<sup>2</sup>, coefficient of determination

**Conclusion:** The results of the present study demonstrate for the first time the in vivo-interaction of soft tissue trauma and fracture healing. It is shown that initial trauma-induced microcirculatory disturbances and leukocyte activation lead to a significant impairment in early bone healing. These data further indicate a prognostic significance of the initial microvascular dysfunction in surrounding soft tissue for delayed fracture repair. The involvement of decreased skeletal muscle perfusion in impaired bone repair and biomechanical stability provides an attractive mechanism by which soft tissue trauma is linked to decreased fracture healing response in presence of concomitant severe soft tissue damage. During management of muskuloskeletal trauma this interaction may have therapeutic implications in view of protecting posttraumatic microcirculation and preserving damaged soft tissues in order to counteract decreased fracture healing.

Ref: <sup>1</sup>Tscherne H. et al., Unfallh., (1983) 62: 163-175. <sup>2</sup>Bonnarens et al. J Orthop Res (1984), 2: 97-101, <sup>3</sup>Schaser KD et al. J Orthop Res (1999), 17, 678-685

\*\* Dept. of Trauma & Reconstructive Surgery, University Rostock, Rostock, Germany

# Einfluß des traumatischen Weichteilschadens auf die Frakturheilung: intravitalmikroskopische und biomechanische Untersuchungen an der Ratte

## Effect of soft tissue damage on fracture healing: intravital microscopic and biomechanical investigations in rats

K. Schaser<sup>1</sup>, L. Zhang<sup>1</sup>, T. Mittlmeier<sup>2</sup>, D. Ostapowicz<sup>1</sup>, G. Schmidmaier<sup>1</sup>, G. Duda<sup>1</sup>, N. P. Haas<sup>1</sup>, H. J. Bail<sup>1</sup>

<sup>1</sup> Klinik für Unfall- und Wiederherstellungschirurgie der Charité, Campus Virchow, Humboldt Universität zu Berlin

<sup>2</sup> Unfall- und Wiederherstellungschirurgie, Universität Rostock

### Abstract

**Introduction:** Among the different factors adversely influencing the bone healing response the associated soft tissue trauma is now increasingly attracting major interest, as it significantly impairs fracture repair and decisively determines patient's prognosis. Using intravital-microscopic analysis and biomechanical testings the present study was aimed to quantitatively assess the impact of microcirculatory disturbances in skeletal muscle following closed soft tissue damage on fracture healing. **Methods:** Standardized closed fracture of left tibia in anesthetized Sprague-Dawley rats (n = 48) was induced using a modified weight-drop-technique and intramedullary stabilized by manual k-wire insertion. In 24 of these rats an additional standardized closed soft tissue trauma at the anterolateral tibial compartment was induced using the controlled cortical impact technique. The rats were assigned (n = 6) to 4 groups (2 h, 48 h, 1 and 3 weeks after the trauma). Non-injured, sham-operated rats (n = 6) served as controls. The left extensor digitorum longus (EDL) muscle was surgically exposed for in vivo fluorescence microscopy. Biomechanical torsional testings were performed in additional 40 rats at 3 and 6 weeks following induction of either fracture (n = 10 per time point) or fracture with soft tissue trauma (n = 10 per time point). **Results:** Closed tibial fracture resulted in a significant reduction of functional capillary density in EDL-muscle. Microvascular diameter, leukocyte adherence and macromolecular leakage were markedly increased, indicating trauma-induced inflammation and endothelial disintegration. In comparison, these changes were pronounced 2 h and 48 h following injury in rats receiving combined fracture and soft tissue trauma. Following fractures with soft tissue trauma, the microvascular deteriorations in skeletal muscle were accompanied by a significantly decreased total failure load and the energy absorption of rat tibia in the early fracture healing period (3 weeks). **Conclusion:** The results of the present study demonstrate for the first time the in vivo-interaction of soft tissue trauma and fracture healing. It is shown that initial microcirculatory disturbances and leukocyte activation lead to a significant impairment in early fracture healing. The involvement of decreased skeletal muscle perfusion in impaired bone repair and biomechanical stability provides an attractive mechanism by which soft tissue trauma is linked to decreased fracture healing response in presence of concomitant severe soft tissue damage. Consequently, this interaction may have therapeutic implications in view of protecting posttraumatic microcirculation and preserving damaged soft tissue envelope in order to counteract decreased fracture healing.

## Einleitung

Frakturen mit schweren Weichteilschäden und deren Folgezustände bestimmen entscheidend die Prognose komplexer Extremitätenverletzungen. Die klinische Erfahrung zeigt, daß die Weichteilschädigung dabei zentrale Bedeutung für das Frakturmanagement besitzt. Durch welche spezifischen Pathomechanismen ein schwerer Weichteilschaden zu einer verzögerten Frakturheilung führt ist unklar. Direkte quantitative Untersuchungen welche die Biomechanik der Frakturheilung in Abhängigkeit von der mikrovaskulären Perfusion der umliegenden Weichteile untersuchen fehlen bislang. Ziel der Untersuchungen war die quantitative Analyse des pathogenetischen Einfluß der Mikrozirkulationsstörungen im Skelettmuskel nach geschlossenem Weichteilschaden (gWTS) auf die Frakturheilung im Tiermodell der Ratte.

## Material & Methoden

Am linken Unterschenkel von 48 SD-Ratten wurde mittels der Controlled-Impact-Technik eine standardisierte geschlossene Weichteilverletzung (G III nach Tscherne) gesetzt. Bei 24 dieser Tiere wurde zusätzlich eine standardisierte geschlossene Tibiaschaftfraktur (modifiziertes Frakturmodell n. Einhorn et al.) erzeugt und mittels intramedullärer Kirschner-Drahtosteosynthese stabilisiert. Zur intravitalen Fluoreszenzmikroskopie wurde der *Musc. ext. digit.long.* (EDL) am Unterschenkel präpariert. Die Untersuchung erfolgte 2 h, 48 h, 1 und 3 Wochen nach Trauma bzw. Trauma mit Fraktur (jeweils n = 6). Nicht-traumatisierte Ratten (n = 6) dienten als Kontrollen. Gemessen wurden die mikrovaskulären Durchmesser, funktionelle Kapillardichte (FCD), mikrovaskuläre Permeabilität (leakage), sowie die Leukozyten-Endothelzell-Interaktion. Biomechanische, torsionale Testungen (destruktiv mit intaktem Weichteilmantel, angegeben in Prozent der gesunden Gegenseite; ZWICK, Ulm) erfolgten an jeweils weiteren 20 Tieren sowohl mit Fraktur als auch Fraktur und Weichteilschaden (nach 3 und 6 Wochen, jeweils n = 10).

## Resultate

In den Kontrolltieren fand sich eine homogene mikrovaskuläre Perfusion des Skelettmuskel ohne Hinweis auf kapilläre Dysfunktion oder erhöhte Leukozyten-Endothelzell-Interaktion. Sowohl die geschlossene Weichteilverletzung als auch Fraktur bewirkte im Vergleich zu den Kontrollen eine langanhaltende nutritive Perfusionsstörung, endotheliale Permeabilitätsstörung und Entzündungsreaktion über den gesamten Untersuchungszeitraum. Die geschlossene Tibiaschaftfraktur mit geschlossenem Weichteiltrauma führte im Vergleich zu einfacher Fraktur zu einer signifikanten Akzentuierung der kapillären Dysfunktion und Leukozytenadhärenz im Skelettmuskel in der Frühphase nach Trauma (■ Tabelle 1). Diese mikrovaskuläre Funktionsstörung im Skelettmuskel war ferner mit einer in der Frühphase der Frakturheilung (3 Wochen) signifikant reduzierter Versagenslast und Energieabsorption bei Frakturen mit Weichteilschaden assoziiert (■ Tabelle 2).

## Schlußfolgerung

Die Ergebnisse demonstrieren erstmals *in-vivo* die Interaktion von traumatischem Weichteilschaden, nutritiver Perfusionsstörung und Frakturheilung. Sie zeigen, daß diese frühen Mikrozirkulationsstörungen der Weichteile zur Verminderung der biomechanischen Stabilität im Verlauf der Frakturheilung führen. Die Resultate lassen ferner die protrahierte Manifestation einer Mikrozirkulationsstörung und Leukozytenaktivierung im Skelettmuskel als kausale, pathogenetische Determinanten für die verzögerte Heilung von Frakturen mit schwerem Weichteilschaden vermuten. Effektive Behandlungsstrategien von Frakturen mit schwerem Weichteilschaden sollten



■ **Tabelle 1.** ■

	FCD (cm <sup>-1</sup> )	Leukozytenadhärenz (1/mm <sup>2</sup> )	Mikrovask. Permeab. (Leakage in %)	Diameter (µm)	
				Kapillare	Venole
Kontrollen	261,2 ± 25,6	181,5 ± 65,3	0,41 ± 0,08	5,5 ± 0,1	25,3 ± 7,9
2 h: Fx	191,7 ± 31,4 <sup>a</sup>	350,9 ± 68,7	0,56 ± 0,04 <sup>a</sup>	5,9 ± 0,5	40,3 ± 10,3 <sup>a</sup>
2 h: Fx & gWTS	149,8 ± 15,1 <sup>a,b</sup>	636,5 ± 121,9 <sup>a,b</sup>	0,61 ± 0,05	6,6 ± 0,4 <sup>a,b</sup>	44,6 ± 6,8 <sup>a</sup>
48 h: Fx	185,2 ± 21,3 <sup>a</sup>	504,5 ± 149,7 <sup>a</sup>	0,61 ± 0,04 <sup>a</sup>	6,8 ± 1,5 <sup>a</sup>	46,1 ± 3,9 <sup>a</sup>
48 h: Fx & gWTS	154,8 ± 12,9 <sup>a,b</sup>	512,6 ± 82,8 <sup>a</sup>	0,60 ± 0,06	7,3 ± 1,0 <sup>a</sup>	41,7 ± 5,6 <sup>a</sup>
1 w: Fx	187,4 ± 25,8 <sup>a</sup>	405,2 ± 120,4 <sup>a</sup>	0,55 ± 0,09 <sup>a</sup>	7,9 ± 1,0 <sup>a</sup>	46,9 ± 6,3 <sup>a</sup>
1 w: Fx & gWTS	184,8 ± 19,2 <sup>a</sup>	494,5 ± 80,1 <sup>a</sup>	0,56 ± 0,07	7,2 ± 0,7 <sup>a</sup>	42,5 ± 8,8 <sup>a</sup>
3 w: Fx	221,4 ± 17,2 <sup>a</sup>	456,3 ± 67,2 <sup>a</sup>	0,43 ± 0,06 <sup>a</sup>	6,9 ± 0,8	42,6 ± 4,0 <sup>a</sup>
3 w: Fx & gWTS	196,8 ± 12,8 <sup>a</sup>	388,0 ± 85,1 <sup>a</sup>	0,49 ± 0,03	6,6 ± 0,6 <sup>a</sup>	43,6 ± 6,2 <sup>a</sup>

<sup>a</sup> p < 0,05 vs. Kontrollen, ANOVA; <sup>b</sup> p < 0,05 vs. Fraktur ohne geschlossenen Weichteilschaden (Fx ohne gWTS), t-Test

■ **Tabelle 2.** ■

	Drehmoment (% zur Gegenseite)	Steifigkeit (% zur Gegenseite)	Energieabsorption (% zur Gegenseite)
3 W: Fx	54,7 ± 15,3 <sup>a</sup>	51,9 ± 21,1	122,0 ± 75,5 <sup>a</sup>
3 W: Fx & gWTS	36,1 ± 13,7	52,9 ± 27,4	47,4 ± 32,1
6 W: Fx	112,5 ± 32,8 <sup>a,b</sup>	116,0 ± 33,2 <sup>a,b</sup>	141,0 ± 58,2 <sup>a</sup>
6 W: Fx & gWTS	97,5 ± 42,4 <sup>a,b</sup>	106,3 ± 36,2 <sup>a,b</sup>	99,1 ± 69,8

<sup>a</sup> p < 0,05 vs. 3 Wochen (3W)-Fraktur (Fx) & geschlossenen Weichteilschaden (gWTS); <sup>b</sup> p < 0,05 vs. 3 Wochen (3W)-Fraktur (Fx); t-Test

daher die Protektion der posttraumatischen Mikrozirkulation und des geschädigten Weichteilmantels zum Ziel haben, um in der Frühphase der Frakturheilung bessere biomechanische Stabilität erreichen und einer verzögerten Frakturheilung entgegenwirken zu können.

*Korrespondenzadresse:* Dr. med. Klaus-D. Schaser, Unfall- & Wiederherstellungschirurgie, Charité, Medizinische Fakultät der Humboldt Universität zu Berlin, Campus Virchow, Augustenburger Platz 1, 13353 Berlin, Germany, Tel.: +49-30-450 552098; Fax: +49-30-450 552958, e-mail: klaus-dieter.schaser@charite.de

## **3.2 Therapeutische Ansätze zur Reduktion der mikrovaskulären Dysfunktion im Skelettmuskel der Ratte nach geschlossenem Weichteiltrauma**

Pathophysiologisch zeigen das postischämische Reperfusionssyndrom, der traumatisch-hämorrhagische Schock (generalisierte Mikrozirkulationsstörung und systemische Entzündung im Sinne einer "Ganzkörperischämie - Reperfusion") und das geschlossene Weichteiltrauma ähnliche mikrovaskuläre Reaktionsmuster. Der Einsatz von Substanzen, die eine Verbesserung der Organperfusion und Reduktion der postischämischen Leukozytenadhärenz bewirken, scheint daher auch beim traumatischen Weichteilschaden viel versprechend.

Konkret wurden hier hypertone-hyperonkotische Lösungen, N-Acetylcystein als Antioxidans, Glutathionprecursor und Radikalfänger (3, 23, 29, 101, 147, 151) und Cyclooxygenase (COX)-2-Inhibitoren (12, 166) hinsichtlich der Therapieeffektivität zur Verringerung des Sekundärschadens untersucht (81, 102, 103, 106, 189).

### **3.2.1 Reduktion der Mikrozirkulationsstörung im Skelettmuskel der Ratte nach geschlossenem Weichteiltrauma durch „small volume resuscitation“**

Bei komplexen Extremitätenverletzungen wird eine traumatisch bedingte Minderperfusion der Weichteilschadens- und Frakturregion als grundlegender pathogenetischer Faktor für verzögerte Heilung angesehen (34, 53, 56, 83, 96, 98, 178). Die Reduktion der posttraumatischen mikrovaskulären Perfusionsstörungen könnte damit einen kausaltherapeutischen Ansatz zur Behandlung des geschlossenen Weichteiltraumas darstellen. Unter dem Aspekt, dass hämorrhagischer Schock und Weichteiltrauma vergleichbare systemische und lokale mikrovaskuläre Perfusionsstörungen zeigen, scheint die Behandlung des Weichteiltraumas mit Substanzen, die zur Aufhebung schockspezifischer Mikrozirkulationsstörungen führen, sinnvoll.

In Versuchen, die eine sofortige Applikation einer „small volume resuscitation“ (7.2% hypertone NaCl und 10% Hydroxyethylstärke, Hyperhaes®) untersuchten, gelang der Nachweis der Verringerung des Sekundärschadens nach isolierter geschlossener Weichteilschädigung. Diese intravitalmikroskopischen und Laser-

Doppler-Flowmetrischen Untersuchungen zeigten eine nahezu komplette Wiederherstellung der posttraumatisch deutlich reduzierten funktionellen Kapillardichte auf nahezu das Niveau unverletzter Kontrolltiere. Zusätzlich konnte auch eine Abnahme der posttraumatisch gesteigerten mikrovaskulären Permeabilität und der endothelialen Leukozytenadhärenz als Zeichen einer reduzierten endothelialen Permeabilitätsstörung und zellulären Entzündungsreaktion demonstriert werden.

Weitere Laser-Doppler-Flowmetrische Untersuchungen des Blutflusses und Ödembestimmungen des verletzten EDL-Muskels der Ratte mittels Trocken-Feuchtwicht bestätigten diese Therapieerfolge.

Die in diesen und vorherigen Untersuchungen aufgezeigten mikrovaskulären Pathomechanismen in der Ausbildung des Sekundärschadens nach Weichteiltrauma konnten somit als therapeutische Angriffspunkte identifiziert und erfolgreich genutzt werden.

## Small volume hypertonic hydroxyethyl starch reduces acute microvascular dysfunction after closed soft-tissue trauma

T. Mittlmeier, B. Vollmar, M. D. Menger, L. Schewior, M. Raschke, K.-D. Schaser

From Humboldt University, Berlin, Germany

**A** major pathway of closed soft-tissue injury is failure of microvascular perfusion combined with a persistently enhanced inflammatory response. We therefore tested the hypothesis that hypertonic hydroxyethyl starch (HS/HES) effectively restores microcirculation and reduces leukocyte adherence after closed soft-tissue injury. We induced closed soft-tissue injury in the hindlimbs of 14 male isoflurane-anaesthetised rats. Seven traumatised animals received 7.5% sodium chloride-6% HS/HES and seven isovolaemic 0.9% saline (NS). Six non-injured animals did not receive any additional fluid and acted as a control group. The microcirculation of the extensor digitorum longus muscle (EDL) was quantitatively analysed two hours after trauma using intravital microscopy and laser Doppler flowmetry, i.e. erythrocyte flux. Oedema was assessed by the wet-to-dry-weight ratio of the EDL.

In NS-treated animals closed soft-tissue injury resulted in massive reduction of functional capillary density (FCD) and a marked increase in microvascular permeability and leukocyte-endothelial cell interaction as compared with the control group. By contrast, HS/HES was effective in restoring the FCD to 94% of values found in the control group. In addition, leukocyte rolling decreased almost to control levels and leukocyte adherence was found to be reduced by ~50%. Erythrocyte flux in NS-treated animals decreased to  $90 \pm 8\%$  (mean SEM), whereas values in the

HS/HES group significantly increased to  $137 \pm 3\%$  compared with the baseline flux. Oedema in the HS/HES group ( $1.06 \pm 0.02$ ) was significantly decreased compared with the NS-group ( $1.12 \pm 0.01$ ).

HS/HES effectively restores nutritive perfusion, decreases leukocyte adherence, improves endothelial integrity and attenuates oedema, thereby restricting tissue damage evolving secondary to closed soft-tissue injury. It appears to be an effective intervention, supporting nutritional blood flow by reducing trauma-induced microvascular dysfunction.

*J Bone Joint Surg [Br]* 2003;85-B:126-32.

Received 7 November 2000; Accepted after revision 26 February 2002

Clinically, there is emerging consensus that high levels of morbidity after complex injuries to the limbs are directly related to the severity of soft-tissue injury.<sup>1,2</sup> Previous studies have shown that the propagation of closed soft-tissue injury is preceded by a drastic reduction of functional capillary density (FCD) and a marked increase in leukocyte-endothelial-cell interaction as well as microvascular leakage.<sup>2-4</sup> Similar microcirculatory disturbances have been found to promote tissue damage in skeletal muscle in response to a variety of stimuli such as ischaemia-reperfusion<sup>5,6</sup> or infection.<sup>7</sup> A major limitation, however, in the treatment of severe soft-tissue damage in trauma patients, is the general lack of effective tools for the rapid restoration of tissue perfusion and reduction of trauma-induced inflammation. At present, the clinical management of severe soft-tissue trauma mainly relies on serial radical debridement of tissue which is necrotic or becomes necrotic during the clinical course.<sup>1</sup>

The ability of hypertonic-hyperoncotic solutions (i.e. exerting a higher than physiological plasma osmotic and oncotic pressure) to restore tissue perfusion and organ function efficiently and rapidly after haemorrhagic shock<sup>8-10</sup> and severe injury<sup>11-13</sup> is now well recognised, but there is no information regarding their ability to improve efficiently the microcirculation of skeletal muscle after severe blunt trauma to the limbs. These observations have led to the hypothesis that hypertonic-hyperoncotic fluids may simultaneously exert a significant protective effect on post-traumatic microvascular haemodynamics, the leukocyte

T. Mittlmeier, MD  
Trauma and Reconstructive Surgery, University of Rostock, Schillingallee 35, 18055 Rostock, Germany.

M. Raschke, MD  
L. Schewior, MD  
K.-D. Schaser, MD  
Trauma and Reconstructive Surgery Charité, Humboldt University, Campus Virchow-Klinikum, Augustenburger Platz 1, D-13353 Berlin, Germany.

B. Vollmar, MD  
M. D. Menger, MD  
Institute for Clinical and Experimental Surgery, University of Saarland, Hamburg/Saar, Germany.

Correspondence should be sent to Dr K.-D. Schaser.

©2003 British Editorial Society of Bone and Joint Surgery  
doi:10.1302/0301-620X.85B1.11870 \$2.00

response, and the formation of oedema in skeletal muscle which, in turn, may positively influence tissue perfusion.

We have therefore determined quantitatively the acute effectiveness of treatment with hypertonic hydroxyethyl starch (HS/HES) on the microcirculation, the leukocyte-endothelium interaction and the formation of oedema in skeletal muscle after severe closed soft-tissue trauma and compared this with treatment with normal saline (NS).

## Materials and Methods

### Animal model, impact device and surgical preparation.

All experimental procedures were performed with the permission of the local animal rights protection authorities and in accordance with NIH guidelines for the use of laboratory animals. We induced severe standardised closed soft-tissue injury in the anterolateral tibial compartment of the left hindlimb of anaesthetised male Sprague-Dawley rats (isoflurane 1.5 vol.%, N<sub>2</sub>O 0.5 l/min and O<sub>2</sub> 0.3 l/min) using the computer-assisted controlled impact-injury technique. The controlled impact-injury device, which was originally developed for the induction of severe brain injury,<sup>14</sup> employs a high-pressure pneumatic impactor which reproduces the clinical situation of severe closed soft-tissue injury caused by high-velocity trauma. The impact parameters were selected as follows: impact velocity of 7 m/s, deformation depth of 11 mm and impact duration of 100 ms with an impactor diameter of 11 mm. The optimal absorption of impact energy by the soft tissue of the rat hindlimb was guaranteed by fixation of the limb in plastic form (exactly moulded like the hindlimb) tightly mounted to the table of the impact device. The left carotid artery and right jugular vein were cannulated with polyethylene catheters (PE50, 0.58 mm inner diameter; Portex, Hythe, UK) for continuous haemodynamic monitoring and intravenous administration of fluid and fluorescence markers. The extensor digitorum longus (EDL) of the left hindlimb was prepared for intravital fluorescence microscopy modified to the technique as previously described<sup>15</sup> allowing horizontal positioning of the EDL and constant focus level for the microscopic procedure.

**Experimental groups and protocol.** We induced severe closed soft-tissue injury in 14 rats. Six non-traumatised, sham-operated animals served as a control group. The rats were allocated randomly to three treatments: trauma followed by hydroxyethyl starch (HS/HES); trauma followed by normal saline (NS); and controls with no trauma. Before the EDL was surgically exposed, the intramuscular pressure within the antero- and posterolateral tibial compartment (8 mm beneath the skin surface) was measured percutaneously (45 minutes after injury) using a microsensor catheter (0.7 mm outside diameter, Codman microsensors; Johnson & Johnson Professional Inc, Raynham, Massachusetts).

After a period of stabilisation of 15 minutes, the macrohaemodynamics, arterial blood gases and blood chemistry were determined and laser Doppler flowmetry was per-

formed. These procedures took place 1.5 hours after trauma before treatment. Seven traumatised animals were then infused intravenously over 15 minutes with 7.2% sodium chloride-10% HS/HES (4 ml/kg body-weight; Hyperhaes, Fresenius GmbH, Bad Homburg, Germany)<sup>10,11,16</sup> and seven with the equivalent volume of NS (0.9% NaCl; Braun Melsungen AG, Melsungen, Germany). There was no significant difference in the administered volume per animal between the NS (1.3 ± 0.1 ml) and the HS/HES (1.2 ± 0.1 ml). The six non-injured, sham-operated rats in the control group received no additional fluid. The concentration of HS/HES was 10% with a molecular weight of 200 000 and a degree of substitution of 0.6, i.e. the ratio of substituted (hydroxylated) glucose units to the total number of glucose molecules.<sup>17</sup> HS/HES is a derivative of amylopectin and was chosen as the colloid component instead of dextran or albumin because of its enhanced ability to protect endothelial cells from inflammatory activation and subsequent dysfunction.<sup>17</sup> Furthermore, dextran is known to induce severe anaphylaxis<sup>18</sup> and albumin may increase leakage from microvessels, adversely affecting haemostasis and possibly increasing mortality.<sup>19</sup>

After the period of infusion the macrohaemodynamics, arterial blood gases, and blood chemistry were again determined and laser Doppler flowmetry of all animals performed once more, two hours after injury, 30 minutes after treatment. The EDL was then sequentially scanned proximally to distally in 2 mm increments by intravital fluorescence microscopy to allow recording of microcirculatory images for nutritive capillaries and postcapillary venules. Microcirculatory recordings for nutritive capillaries and postcapillary venules of at least eight video-frames of each EDL muscle were taken and the values averaged per animal.

At the end of each experiment, the animals were killed and laser Doppler flowmetry of the non-perfused EDL muscle performed finally to assess the biological zero.<sup>20</sup> Thereafter, the EDLs of both hindlimbs were removed for determination of the oedematous weight gain.

**Intravital fluorescence microscopy.** For visualisation of the microcirculation of the EDL we used an intravital fluorescence microscope (Optiphot; Nikon, Tokyo, Japan) with a water-immersion objective (203, Nikon). The surface of the EDL was epi-illuminated by a high-pressure mercury lamp (100 W) and fluorescence emission of fluorescein-isothiocyanate (FITC)-dextran (450 to 490 nm/>580 nm) and rhodamine (530 to 560 nm/>580 nm) was detected by means of an appropriate filter system. Microcirculatory images were recorded using a CCD videocamera (FK 6990-IQ; Pieper, Schwete, Germany) and transferred to an SVHS videorecorder (HR-S4700EG/E; JVC, Friedberg, Germany) for off-line analysis. The final magnification on the video screen was 940-fold.

For contrast enhancement of the microvascular network and for *in vivo* staining of leukocytes a single bolus of FITC-labelled dextran (5%, 150000 mol wt; 15 mg/kg body-weight; Sigma Chemical, Deisenhofen, Germany) and

**Table I.** Mean ( $\pm$  SEM) arterial blood pressure (mmHg) and heart rate (beats/min) of isoflurane anaesthetised animals, continuously recorded and averaged for the entire study period

Group	Mean arterial blood pressure	Heart rate
Control	107 $\pm$ 5	254 $\pm$ 10
NS	90 $\pm$ 4	304 $\pm$ 10
HS/HES	95 $\pm$ 2	299 $\pm$ 18

rhodamine 6G (0.1%, 0.15 mg/kg body-weight; Sigma Chemical) was injected intravenously.<sup>21</sup> Duration of continuous light exposure per observation area was limited to 60 seconds at maximum.

**Microcirculatory analysis.** The videotaped microcirculatory images were analysed off-line for the diameters of microvessels, FCD, microvascular permeability (macromolecular leakage) and red blood cell velocity ( $V_{RBC}$ ) using a computerised microcirculation image-analysis system (CapImage; Zeintl, Heidelberg, Germany).<sup>22</sup> FCD was quantified by the length of FITC-dextran-perfused capillaries per observation area ( $cm^{-1}$ ). Microvascular permeability (macromolecular leakage) was expressed as the ratio of fluorescence-intensity, selected from the perivascular area to the corresponding intravascular area (plasma gaps between erythrocytes).

Using the PC-associated image-analysis system we determined centreline red blood cell velocity ( $V_{RBC-centreline}$ ) in the capillaries and venules of skeletal muscle.<sup>22</sup> The mean red blood cell velocity for each vessel ( $V_{RBC-mean}$ ) and video field was calculated as  $V_{mean} = V_{centreline} / 1.6$ . Venular wall shear rate as a function of the disperse force on rolling leukocytes was calculated as follows: shear rate =  $8 \times V_{mean} / D$ , where  $V_{mean}$  is mean erythrocyte velocity and D is venular diameter.<sup>23</sup>

The number of rolling and adherent leukocytes as well as the total leukocyte flux were counted for 30 seconds along a vessel segment of 100  $\mu m$ . Leukocyte rolling was defined as the slow passage of leukocytes rolling along the vessel wall with a velocity less than 40% of centreline velocity<sup>24</sup> and expressed as the percentage of rolling cells to total leukocyte flux. Adherence of leukocytes was defined by non-moving leukocytes with a stable contact to the endothelial lining of postcapillary venules for at least 20 seconds. Assuming cylindrical microvessel geometry, leukocyte adherence was expressed as the number of non-moving leukocytes per endothelial surface ( $cells/mm^2$ ), calculated from the diameter and length (100  $\mu m$ ) of the vessel segment analysed.

**Laser Doppler flowmetry.** Erythrocyte flux was measured using a dual-channel laser Doppler monitor (DRT4; Moore Instruments, Axminster, UK; needle probe DP4, 780-820 nm, external diameter 0.8 mm) and expressed as percentage of baseline (pretreatment flux values). By means of a three-dimensional micromanipulator, the EDL was sequentially scanned in increments of 1 mm reaching at least 20 measurements per EDL.

**Table II.** Time-related changes in arterial haematocrit (%), acid-base excess (BE), arterial pH, serum sodium, potassium and chloride concentrations (nmol/l), creatine kinase (CK) and arterial lactate at baseline, in response to trauma and at 30 minutes after treatment. Values are expressed as mean  $\pm$  SEM

Group	Baseline	1.5 hours after trauma (before treatment)	2 hours after trauma (30 minutes after treatment)
<b>Haematocrit (%)</b>			
Control	41.1 $\pm$ 1.2	–	–
NS	39.5 $\pm$ 1.6	37.9 $\pm$ 1.2	35.3 $\pm$ 1.4
HS/HES	41.1 $\pm$ 1.2	39.6 $\pm$ 1.0	28.9 $\pm$ 1.4*†‡
<b>BE (mmol/l)</b>			
Control	2.8 $\pm$ 0.7	–	–
NS	4.4 $\pm$ 0.8	0.03 $\pm$ 0.7	-1.0 $\pm$ 1.5*
HS/HES	2.0 $\pm$ 0.8	0.3 $\pm$ 1.4	-1.6 $\pm$ 0.9*
<b>pH</b>			
Control	7.43 $\pm$ 0.02	–	–
NS	7.44 $\pm$ 0.01	7.38 $\pm$ 0.02	7.36 $\pm$ 0.04
HS/HES	7.43 $\pm$ 0.02	7.39 $\pm$ 0.03	7.35 $\pm$ 0.02*
<b>Serum Na<sup>+</sup> (nmol/l)</b>			
Control	140.5 $\pm$ 1.5	–	–
NS	139.8 $\pm$ 0.5	137.7 $\pm$ 1.1	139.7 $\pm$ 1.0
HS/HES	138.7 $\pm$ 1.1	136.7 $\pm$ 0.4	146.9 $\pm$ 0.69*†‡
<b>Serum K<sup>+</sup> (nmol/l)</b>			
Control	4.1 $\pm$ 0.7	–	–
NS	4.1 $\pm$ 0.2	4.8 $\pm$ 0.2	4.5 $\pm$ 0.2
HS/HES	4.5 $\pm$ 0.2	4.8 $\pm$ 0.3	4.3 $\pm$ 0.3
<b>Serum Cl<sup>-</sup> (nmol/l)</b>			
Control	102.7 $\pm$ 0.6	–	–
NS	103.8 $\pm$ 0.5	102.7 $\pm$ 0.7	107.2 $\pm$ 1.2
HS/HES	102.9 $\pm$ 0.9	103.3 $\pm$ 0.4	119.0 $\pm$ 0.6*†‡
<b>CK (U/L)</b>			
Control	67.6 $\pm$ 5.7	–	–
NS	90.3 $\pm$ 11.8	188.3 $\pm$ 15.8*	174.6 $\pm$ 28.5*
HS/HES	80.5 $\pm$ 9.2	245.0 $\pm$ 37.8*	238.7 $\pm$ 54.9*
<b>Lactate (mg/dl)</b>			
Control	19.5 $\pm$ 2.1	–	–
NS	16.3 $\pm$ 0.7	14.0 $\pm$ 1.8	12.2 $\pm$ 1.9
HS/HES	20.3 $\pm$ 2.3	19.9 $\pm$ 1.7	17.1 $\pm$ 3.2

\*p < 0.01 versus baseline

†p < 0.01 versus 1.5 hours after trauma

‡p < 0.05 versus NS

**Blood sampling.** Arterial blood samples were taken before (baseline) and at 1.5 hours and at two hours after injury, 30 minutes after administration of either HS/HES or NS. Arterial blood gases were assessed using a blood-gas analyser (ABL 300; Radiometer, Copenhagen, Denmark). Plasma electrolyte concentrations were measured using a potentiometric test. Based on enzymatic ultraviolet methods the levels of plasma lactate were obtained by a colorimetric test (540 nm) whereas the activity of creatine kinase (CK) was determined by a multiple-point kinematic test (670 nm) (Vitros products chemistry; Eastman Kodak Company, Rochester, New York).

**Determination of the formation of skeletal muscle oedema.** Oedematous weight gain was assessed by measuring the wet-to-dry-weight ratio of injured and non-injured EDLs. After determination of wet weight the EDLs were dried for 24 hours in a laboratory oven (80°C) and weighed again (dry weight). Stable dry weight was found after 24

**Table III.** Intramuscular pressure percutaneously measured in mm Hg 45 minutes after trauma in the ventral and dorsal tibial compartment of rat hindlimbs and oedematous weight gain of the EDL as expressed by the oedema index (wet-to-dry-ratio of experimental *versus* contralateral EDL)

Group	Intramuscular pressure		Oedema index
	Ventral	Dorsal	
Control	6.3 ± 0.4	5.1 ± 0.6	1.01 ± 0.03
NS	21.5 ± 0.8*	11.7 ± 0.6	1.11 ± 0.01*
HS/HES	20.7 ± 0.4*	9.1 ± 0.6*	1.06 ± 0.02†

\*p < 0.05 *versus* control

†p < 0.05 *versus* NS

hours in all animals. The formation of oedema was finally expressed by the wet-to-dry-weight ratio of injured *versus* non-injured EDL (oedema index).

**Statistical analysis.** All time points within a group were analysed by a paired *t*-test, including Bonferroni correction for repeated measurements which involved dividing the threshold p value by 3 (k = 3 as the number of pairwise comparisons performed between the three repeated measures on the same rat). For differences between NS, HS/HES and control groups we performed ANOVA for independent samples followed by the *post-hoc* Tukey-test for multiple-comparison procedures. Erythrocyte flux between the HS/HES and NS groups was compared using the unpaired *t*-test. All values were given as mean ± SEM. Statistical significance was set at p < 0.05.

## Results

**Macrohaemodynamics and blood parameters.** The mean arterial blood pressure and heart rate of the experimental groups remained stable within the normal range without significant changes between groups throughout the entire study period when compared with the non-injured animals (Table I). Before treatment there were no significant differences between the two experimental groups as to blood gases and blood chemistry. In both experimental groups trauma led to a significant increase in the levels of creatine kinase and a slight development of metabolic acidosis (Table II). Treatment with HS/HES, however, was associated with a significant decrease in haematocrit and pH when compared with administration of NS. Simultaneously, haemodilution with HS/HES was paralleled by a significant increase in the concentration of serum sodium and chloride when compared with NS-treated animals (Table II).

**Intramuscular pressure.** As early as one hour after the induction of closed soft-tissue injury intramuscular pressure within the anterior and posterior tibial compartment was significantly increased in groups receiving NS or HS/HES when compared with the control group. However, at no time point of analysis did the closed soft-tissue injury result in intramuscular pressure exceeding 30 mm Hg indicating a compartment syndrome (Table III).

**Post-traumatic skeletal muscle microcirculation and small volume infusion of HS/HES.** The post-traumatic

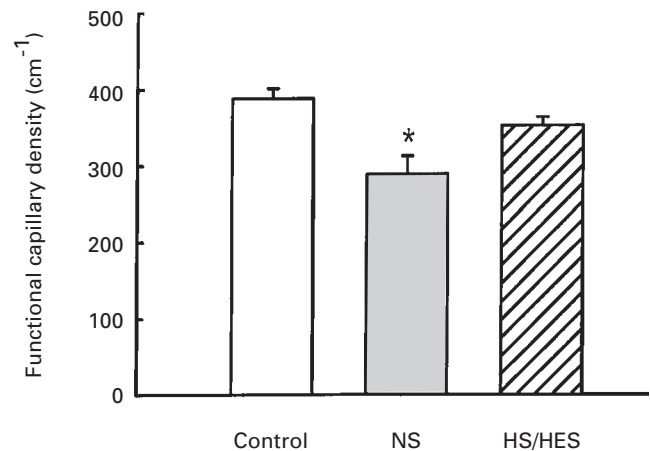


Fig. 1a

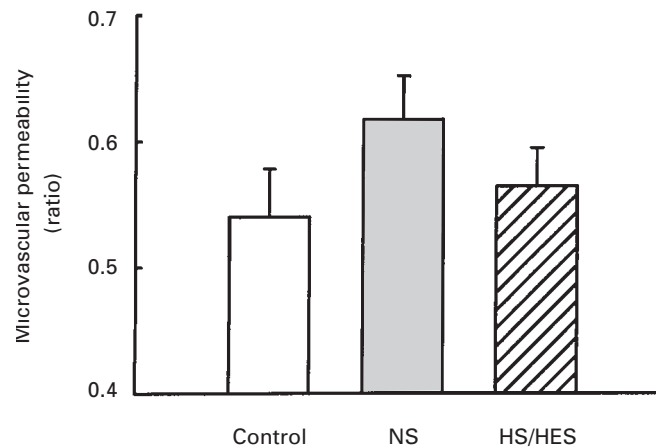


Fig. 1b

Graphs showing a) mean (±SEM) FCD (length of erythrocyte perfused capillaries per observation area) and b) mean (±SEM) microvascular permeability (venular macromolecular leakage of FITC-dextran) analysed densitometrically by the ratio of extra- to intravascular fluorescence intensity in rat skeletal muscle under control conditions and at two hours after trauma, i.e. 30 minutes after treatment with either NS or HS/HES (p < 0.05 *v* control).

microcirculation in skeletal muscle in NS-treated animals was characterised by a significant reduction in the FCD and a trend towards enhanced microvascular permeability as compared with the control group (Fig. 1). In the NS-treated group, impairment of nutritive perfusion was further accompanied by a marked increase in trauma-induced leukocyte-endothelial cell interaction compared with the control group. Both leukocyte rolling and adherence were primarily restricted to the endothelium of postcapillary venules and increased by nearly two- and sixfold (Fig. 2). These microvascular deteriorations were significantly improved when animals were treated with HS/HES. As early as 30 minutes after administration of HS/HES the FCD was restored to 94.7% of values found in the sham-operated control group (Fig. 1). Analysis of microvessel diameter revealed a signif-

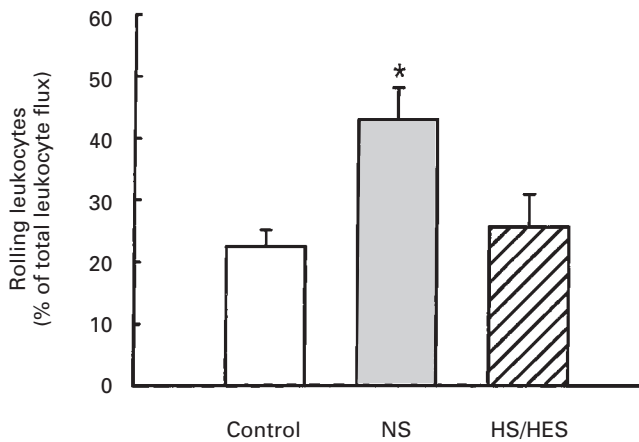


Fig. 2a

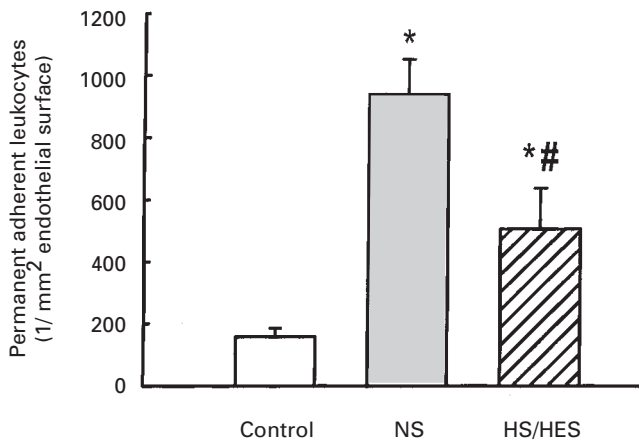


Fig. 2b

Leukocyte-endothelial cell interaction in postcapillary venules of rat EDL under control conditions (non-injured animals) and after treatment with either NS or HS/HES at two hours after injury. Leukocytes were stained in vivo by rhodamine 6G. Figure 2a – Mean (±SEM) number of rolling leukocytes and b) mean (±SEM) number of adherent leukocytes per mm<sup>2</sup> endothelial surface ( $p^* < 0.05$  v control,  $p\# < 0.05$  v NS).

icant increase in capillary diameter in the EDL of NS-treated animals when compared with the control group whereas in animals of the HS/HES group, the luminal diameter of the capillaries remained relatively unchanged (Table IV). Red blood cell velocity in both nutritive capillaries and postcapillary venules did not change significantly on treatment with HS/HES when compared with NS. Trauma-induced leukocyte rolling in HS/HES-treated animals decreased almost to the baseline levels of the non-traumatised control group, and leukocyte adherence was significantly attenuated by approximately 50% compared with the NS group (Fig. 2). Venular shear rate showed no significant difference between both groups (Table IV).

**Laser Doppler flowmetry.** Post-traumatic erythrocyte flux in the EDL of animals receiving HS/HES showed a signifi-

**Table IV.** Mean (± SEM) luminal diameter and mean (± SEM) red blood cell velocity in capillaries and venules as well as calculated postcapillary wall shear rate in rat skeletal muscle after severe closed soft-tissue trauma

Group	Diameter (µm)		Red blood cell velocity (mm/sec)		Shear rate (1/sec) (venules)
	Capillaries	Venules	Capillaries	Venules	
Control	5.0 ± 0.1	22.3 ± 1.9	0.20 ± 0.01	0.23 ± 0.03	88.1 ± 13.8
NS	5.4 ± 0.2*	24.1 ± 1.4	0.17 ± 0.04	0.25 ± 0.03	117.0 ± 13.3
HS/HES	5.1 ± 0.4	20.5 ± 1.3	0.15 ± 0.01	0.28 ± 0.04	94.3 ± 13.5

\* $p < 0.05$  v control

cant increase by one-third of preinfusion flux values, whereas flux values after treatment with NS declined below the baseline level (preinfusion flux values) (Fig. 3).

**Formation of oedema.** In the non-injured, sham-operated control group, negligible oedema within skeletal muscle was found two hours after trauma. The NS-treated traumatised animals, however, showed a significant increase in the oedema index. By contrast, formation of oedema in the HS/HES-treated group was significantly decreased (Table III).

## Discussion

**Intramuscular pressure.** The fact that closed soft-tissue injury was equally pronounced in both groups points to a standardised induction of closed soft-tissue injury by the controlled impact-injury technique as a precondition for comparing effects of different treatments.

**Systemic haemodynamics and blood parameters.** Contrary to previous studies of traumatic haemorrhagic shock and hypotension in which hypertonic-hyperosmotic solutions were shown rapidly and efficiently to restore severely depressed macrohaemodynamics,<sup>8,12,13,25</sup> in our study the mean arterial blood pressure and heart rate were not affected by infusion of HS/HES. Normovolaemic conditions and the missing systemic fluid imbalance between the intra- and extracellular space have already been discussed as possible factors accounting for the lack of macrohaemodynamic changes.<sup>25,26</sup>

The significant decrease in haematocrit in HS/HES-treated animals presumably reflects the ability of HS/HES to initiate a rapid shift of fluid from the intracellular to the extracellular-intravascular compartment,<sup>9</sup> thereby causing marked haemodilution and improvement of blood fluidity. Furthermore, apart from reduction in endothelial cell swelling this osmotic gradient also seems to draw fluid from the erythrocytes. This possibly decreases red blood cell volume, reduces hydraulic flow pressure and may in part contribute to rheological improvement in microvascular perfusion and faster washout of toxic metabolites including free radicals and proinflammatory cytokines. The apparently negative side-effect of a significantly decreased pH in the HS/HES group is thought to be related to a hyperchloraemic metabolic acidosis<sup>16</sup> since lactate levels and arterial blood gases were within the normal range and did not differ between groups.



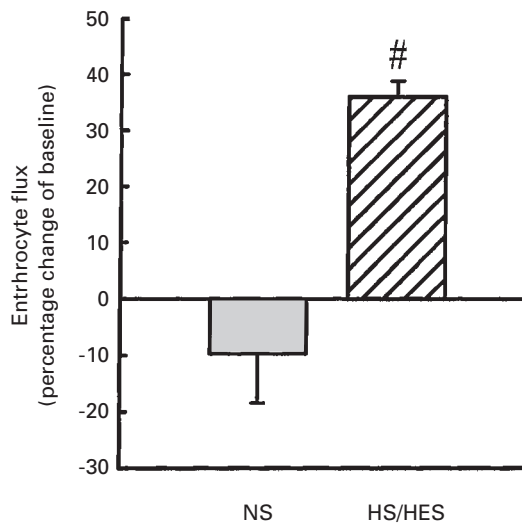


Fig. 3

Mean ( $\pm$ SEM) change in blood flow (erythrocyte flux measured by laser Doppler flowmetry) of rat EDL two hours after trauma and 30 minutes after treatment with either HS/HES or NS ( $p\# < 0.05$  v NS).

The observation that hypertonic-hyperosmotic infusions are detrimental under some circumstances,<sup>27</sup> yet protective in others<sup>8,12,13,25</sup> indicates potential risks of treatment with such fluids. These are specifically relevant in critically injured, dehydrated and high-risk patients<sup>28</sup> and seem to be related to an increased plasma osmolarity and hypokalaemia causing cardiac arrhythmia and a metabolic acidosis induced by an increased plasma chloride anion load, thereby augmenting pre-existing acidosis.<sup>16</sup> In severely injured patients, however, there is now increasing consensus that selective and only primary application of these fluids appears to have a good risk-to-benefit ratio and gives better patient survival<sup>12,18</sup> when tailored to the underlying circulatory state.<sup>10,16</sup>

**Post-traumatic skeletal muscle microcirculation.** The observation that microvascular disturbances of skeletal muscle may be considered to be a starting point for developing tissue damage after severe standardised closed soft-tissue injury confirms previous studies.<sup>3,4</sup> They are likely to be the consequence of several factors, including direct destruction of microvessels, microvascular thrombosis and decreased nutritive capillary perfusion, persistently enhanced leakage and leukocyte-endothelial cell interaction leading to increased oedema and tissue pressure. Together, these factors appear progressively to impede the viability and function of the entire skeletal muscle.

In our study we have shown that HS/HES acutely ameliorates the post-traumatic microcirculation by increasing the FCD and endothelial integrity. These beneficial effects on nutritional blood flow possibly illustrate the essential principle of small volume resuscitation which is thought to function primarily by an osmotically-induced fluid shift into the intravascular compartment.<sup>9,10</sup> On the microcirculatory

level this could attenuate tissue oedema, reduce intercapillary distance and tissue pressure, and enhance blood fluidity because of a decreased hydraulic flow resistance. From this it may be argued that HS/HES exerts its beneficial effects in closed soft-tissue injury by maintaining adequate perfusion or even reopening capillaries which otherwise would remain collapsed. In studies showing reversal of shock- or ischaemia-induced capillary narrowing by hypertonic-hyperosmotic solutions this has been interpreted as direct evidence of the ability of HS/HES to reduce swelling of endothelial cells.<sup>9,29</sup> In our study, however, luminal capillary diameters were found to be unchanged in response to HS/HES. This suggests that the cellular basis of the HS/HES-mediated protection of the post-traumatic microcirculation differs partly from the HS/HES-induced mechanisms responsible for reversal of shock-<sup>8,9</sup> or ischaemia-induced capillary dysfunction.<sup>26,29</sup>

Previous studies have shown that although endothelial integrity is deranged immediately after closed soft-tissue injury, microvascular permeability displays a gradual increase with significant peak levels not earlier than 24 hours after injury.<sup>3,4</sup> Thus, it is conceivable that two hours after closed soft-tissue injury, i.e. one hour of treatment with HS/HES, macromolecular leakage is just about to increase and initial changes are too small to reveal a significant difference.

Treatment of severe closed soft-tissue injury with HS/HES did not significantly affect capillary and venular red blood cell velocity. These findings are in line with previous studies. Using hyperosmolar saline dextran for the treatment of reperfusion injury in striated muscle of hamsters, Nolte et al<sup>26</sup> also found no effect on blood flow velocity when compared with normal saline.

In addition, HS/HES was also shown significantly to reduce the accumulation and adherence of leukocytes to the endothelium of postcapillary venules, which have been shown to be critically involved in the generation of postischaemic<sup>6,30,31</sup> and post-traumatic microvascular injury.<sup>4</sup> These leukocyte-mediated pathways, including production of reactive O<sub>2</sub> radicals, expression of adhesion molecules, and increase in hydraulic flow pressure because of microvascular adherence<sup>30</sup> are promoting a persistent pro-inflammatory state with subsequent tissue damage. Although HS/HES induced significant haemodilution (haematocrit 28% v 35%) red blood cell velocity was only slightly shifted to higher values and calculated venular wall shear rates were comparable between both experimental groups. Therefore it is likely that the difference in the number of rolling and adherent leukocytes did not solely result from changes in physical forces or rheological characteristics, counteracting leukocyte-endothelial cell contact. Direct evidence for this selective inhibitory effect of HS/HES on leukocyte-endothelial cell interaction in traumatised skeletal muscle has not been provided so far. Specifically, the lower microvascular haematocrit associated with a decreased margination of leukocytes within the bloodstream

causing less endothelial contact appears to be one principal cause for reduced leukocyte adherence after treatment with HS/HES.<sup>29,32</sup>

Erythrocyte flux as assessed by laser Doppler flowmetry is calculated from the product of velocity and concentration of moving blood cells.<sup>20</sup> Red blood cell velocity in capillaries and postcapillary venules remained unchanged in response to HS/HES when compared with NS (Table IV). Therefore, the significant HS/HES-induced increase in erythrocyte flux possibly reflects the enhanced total blood cell movement (concentration) caused by the increase in length and number of perfused capillaries, i.e. the FCD.

However, the results should be interpreted with reference to the fact that only acute effects of HS/HES on the microcirculation were analysed. Further investigations are required to analyse whether the initial boosting effects of HS/HES on the post-traumatic microcirculation are only transient in nature or will indeed last and significantly improve the net biological response over time.

In conclusion, our findings provide evidence that acute microvascular deteriorations, trauma-induced inflammatory response and tissue oedema after closed soft-tissue injury may be effectively reversed by small volume infusion of HS/HES. They reinforce the concept that the post-traumatic microcirculation may serve as a target for therapeutic interventions. Therefore, the appropriate use of HS/HES after severe closed soft-tissue injury appears to be an effective primary intervention which may support tissue perfusion and protect soft tissue from regional shock phenomena by prevention of microvascular dysfunction.

This work was supported by grants from the AO-ASIF Foundation, Switzerland and the Else-Kröner-Fresenius Foundation, Germany. B. Vollmar is a recipient of the Heisenberg-Stipendium of the Deutsche Forschungsgesellschaft (Vo 450/6-1).

No benefits in any form have been received or will be received from a commercial party related directly or indirectly to the subject of this article.

## References

1. Levin LS, Condit DP. Combined injuries – soft tissue management. *Clin Orthop* 1996;327:172-81.
2. Tscherne H, Oestern HJ. A new classification of soft-tissue damage in open and closed fractures. *Unfallheilkunde* 1982;85:111-5.
3. Mittlmeier T, Schaser K, Kroppenstedt S, et al. Microvascular response to closed soft tissue injury. *Trans Orthop Res Soc* 1997;44:317.
4. Schaser K, Vollmar B, Menger MD, et al. In vivo analysis of microcirculation following closed soft tissue injury. *J Orthop Res* 1999;17:678-85.
5. Allen DM, Chen LE, Seaber AV, Urbaniak JR. Pathophysiology and related studies of the no reflow phenomenon in skeletal muscle. *Clin Orthop* 1995;314:122-33.
6. Menger MD, Pelikan S, Steiner D, Messmer K. Microvascular ischemia-reperfusion injury in striated muscle: significance of “reflow paradox”. *Am J Physiol* 1992;263:H1901-6.
7. Lam C, Tym IK, Martin C, Sibbald W. Microvascular perfusion is impaired in a rat model of normotensive sepsis. *J Clin Invest* 1994;94:2077-83.
8. Vollmar B, Lang G, Menger MD, Messmer K. Hypertonic hydroxyethyl starch restores hepatic microvascular perfusion in hemorrhagic shock. *Am J Physiol* 1994;266:H1927-34.
9. Mazzoni MC, Borgstrom P, Intaglietta M, Arfors KE. Capillary narrowing in hemorrhagic shock is rectified by hyperosmotic saline-dextran reinfusion. *Circ Shock* 1990;31:407-18.
10. Kreimeier U, Christ F, Frey L, et al. Small-volume resuscitation for hypovolemic shock: concept, experimental and clinical results. *Anaesthesist* 1997;46:309-28.
11. Holcroft JW, Vassar MJ, Perry CA, Gannaway WL, Kramer GC. Use of a 7.5% NaCl/6% Dextran 70 solution in the resuscitation of injured patients in the emergency room. *Prog Clin Biol Res* 1989;299:331-8.
12. Mattox KL, Maningas PA, Moore EE, et al. Prohospital hypertonic saline/dextran infusion for post-traumatic hypotension: the U.S.A. multicenter trial. *Ann Surg* 1991;213:482-91.
13. Vassar MJ, Fischer RP, O'Brien PE, et al. A multicenter trial for resuscitation of injured patients with 7.5% sodium chloride: the effect of added dextran 70. The multicenter group for the study of hypertonic saline in trauma patients. *Arch Surg* 1993;128:1003-11.
14. Dixon CE, Clifton GL, Lighthall JW, Yaghai AA, Hayes RL. A controlled cortical impact model of traumatic brain injury in the rat. *J Neurosci Methods* 1991;39:253-62.
15. Tymi K, Budreau CH. A new preparation of rate extensor digitorum longus muscle for intravital investigation of the microcirculation. *Int J Microcirc Clin Exp* 1991;10:335-43.
16. Vassar MJ, Perry CA, Holcroft JW. Analysis of potential risks associated with 7.5% sodium chloride resuscitation of traumatic shock. *Arch Surg* 1990;125:1309-15.
17. Treib J, Baron JF, Grauer MT, Strauss RG. An international view of hydroxyethyl starches. *Intensive Care Med* 1999;25:258-68.
18. Allhoff T, Lenhart FP. Severe dextran-induced anaphylactic/anaphylactoid reaction despite preventive hapten administration. *Infusionsther Transfusionsmed* 1993;20:301-6.
19. Reviewers. CIGA. Human albumin administration in critically ill patients: systematic review of randomised controlled trials. *BMJ* 1998;317:235-40.
20. Bonner R, Nossal R. Model of Laser-Doppler measurements of blood flow in tissue. *Appl Optics* 1981;20:2097-2107.
21. Menger MD, Lehr HA. Scope and perspectives of intravital microscopy – bridge over form in vitro to in vivo. *Immunol Today* 1993;14:519-22.
22. Klysz T, Junger M, Jung F, Zeintl H. Cap image – a new kind of computer-assisted video image analysis system for dynamic capillary microscopy. *Biomed Tech (Berl)* 1997;42:168-75.
23. Bienvenu K, Granger N. Molecular determinants of shear rate-dependent leukocyte adhesion in postcapillary venules. *Am J Physiol* 1993;264:H1504-8.
24. Atherton A, Born GV. Quantitative investigations of the adhesiveness of circulating polymorphonuclear leukocytes to blood vessel walls. *J Physiol* 1972;222:447-74.
25. Velasco IT, Rocha e Silva M, Oliveira MA, Oliveira MA, Silva RI. Hypertonic and hyperoncotic resuscitation from severe hemorrhagic shock in dogs: a comparative study. *Crit Care Med* 1989;17:261-4.
26. Nolte D, Bayer M, Lehr HA, et al. Attenuation of postischemic microvascular disturbances in striated muscle by hyperosmolar saline dextran. *Am J Physiol* 1992;263:H1411-6.
27. Bickell WH, Bruttig SP, Millnamow GA, O'Benar J, Wade CE. Use of hypertonic saline/dextran versus lactated Ringer's solution as a resuscitation fluid after uncontrolled aortic hemorrhage in anesthetized swine. *Ann Emerg Med* 1992;21:1077-85.
28. Holcroft JW, Vassar MJ, Turner JE, Derlet RW, Kramer GC. 3% NaCl and 7.5% NaCl/dextran 70 in the resuscitation of severely injured patients. *Ann Surg* 1987;206:279-88.
29. Menger MD, Thierjung C, Hammersen F, Messmer K. Dextran vs hydroxyethylstarch in inhibition of postischemic leukocyte adherence in striated muscle. *Circ Shock* 1993;41:248-55.
30. Rubin BB, Romaschin A, Walker PM, Gute DC, Korthuis RJ. Mechanism of postischemic injury in skeletal muscle: intervention strategies. *J Appl Physiol* 1996;80:369-87.
31. Weiss SJ. Tissue destruction by neutrophils. *N Engl J Med* 1989;320:365-76.
32. Bagge U, Blixt A, Strid KG. The initiation of post-capillary margination of leukocytes: studies in vitro on the influence of erythrocyte concentration and flow velocity. *Int J Microcirc Clin Exp* 1983;2:215-27.

### **3.2.2 Therapieeffektivität hypertoner-hyperonkotischer Lösungen bei Störungen der Mikrozirkulation nach Weichteiltrauma und hämorrhagischem Schock**

Wie initiale Studien zeigen konnten, kommt es beim traumatischen geschlossenen Weichteilschaden zur protrahierten Ausbildung eines „lokalen Schockzustandes“ mit vergleichbaren, jedoch regionalen Mikrozirkulationsstörungen. Inwieweit jedoch ein zusätzlich zur Weichteilverletzung vorliegender Schock zu einer Akzentuierung der traumatisch induzierten Mikrozirkulationsstörungen führt, war bislang unklar. Außerdem sollten hyperosmolare-hyperonkotische Lösungen hinsichtlich ihrer Fähigkeit zur „Resuscitation“ und lokalen Protektion der Mikrozirkulation nach schwerem geschlossenem Weichteiltrauma und gleichzeitig induziertem hämorrhagischen Schock untersucht werden. Diese Untersuchungen konnten nachweisen, dass hypertone-hyperonkotische Lösungen zu einer Reduktion der durch hämorrhagischen Schock verstärkten mikrovaskulären Perfusionsstörungen und Leukozyten-Endothelzellinteraktion im traumatisierten Skelettmuskel führen (46).

Erstmals wurde in dieser Studie eine massive Schock-induzierte Zunahme der NADH-Autofluoreszenz beobachtet, was auf ein mikrovaskuläres Perfusionsversagen hinweist. Eine Regressionsanalyse zwischen funktioneller Kapillardichte und NADH demonstrierte eine signifikante inverse Korrelation. Deutlich reduzierte NADH-Autofluoreszenzwerte nach Behandlung mit hyperonkotischer und hypertoner-hyperosmolarer Lösung im Vergleich zu unbehandelten oder NaCl-behandelten Schocktieren bestätigten eine verbesserte nutritive Perfusion und Sauerstoffversorgung des Gewebes (46).

Hämorrhagische Schocksituationen und komplexe Extremitätenverletzungen mit ausgedehnten Weichteilschäden weisen bei polytraumatisierten Patienten eine hohe Koinzidenz auf. In diesem Zusammenhang könnten diese Ergebnisse zur Entwicklung neuer spezifischer Therapieansätze in der klinischen Praxis dienen und der prognostisch relevanten Interaktion von traumatischer Weichteilverletzung und traumatisch-hämorrhagischer Schocksituation Rechnung tragen.

Philip Gierer  
Brigitte Vollmar  
Klaus-Dieter Schaser  
Christian Andreas  
Georg Gradl  
Thomas Mittlmeier

## Efficiency of small-volume resuscitation in restoration of disturbed skeletal muscle microcirculation after soft-tissue trauma and haemorrhagic shock

Received: 16 April 2003  
Accepted: 8 September 2003  
Published online: 14 November 2003  
© Springer-Verlag 2003

The paper was presented at the International Symposium on Significance of Musculo-Skeletal Soft Tissue on Pre-Operative Planning, Surgery and Healing, 13–14 February 2003, Berlin, Germany

P. Gierer (✉) · C. Andreas · G. Gradl · T. Mittlmeier  
Department of Trauma  
and Reconstructive Surgery,  
University of Rostock,  
Schillingallee 35, 18057 Rostock, Germany  
e-mail: philip.gierer@med.uni-rostock.de  
Tel.: +49-381-4946053  
Fax: +49-381-4946052

P. Gierer · B. Vollmar · C. Andreas  
Department of Experimental Surgery,  
University of Rostock,  
Rostock, Germany

K.-D. Schaser  
Department of Trauma  
and Reconstructive Surgery, Charité,  
Campus Virchow,  
Humboldt University,  
Berlin, Germany

**Abstract** *Background and aims:* Despite advances in primary care, trauma in conjunction with shock remains the leading cause for morbidity and mortality of young adults in western countries. Herein, we report on the efficiency of small-volume resuscitation to improve compromised perfusion of traumatised skeletal muscle tissue in shock. *Methods:* In pentobarbital anaesthetised, mechanically ventilated rats, closed soft-tissue trauma of the right hind limb was induced, followed by induction of haemorrhagic shock [mean arterial blood pressure (MAP) 40 mmHg for 1 h]. For resuscitation, animals received saline (four-times the shed blood volume/20 min), 10% hydroxyethyl starch (HES) 200/0.5 (equal to shed blood volume/5 min) or 7.2% sodium chloride/6% hydroxyethyl starch 200/0.5 (HyperHES; 10% of shed blood volume/2 min). At 2 h of resuscitation, traumatised skeletal muscle tissue was analysed by in vivo microscopy. Non-resuscitated animals served as shock controls. *Results:* Despite incomplete restoration of systemic blood pressure, HyperHES was su-

perior to saline, but not to HES, with respect to amelioration of nutritive perfusion. Inflammatory cell response within the traumatised skeletal muscle tissue escaped from the anti-adhesive properties of HyperHES when applied for resuscitation from hypovolaemic shock, and did not differ from values in HES-treated and saline-treated animals. *Conclusion:* Resuscitation with HyperHES is as effective as HES in improving capillary perfusion in traumatised skeletal muscle during haemorrhagic shock. However, because values of functional capillary density in the HyperHES-treated and HES-treated animals were still markedly below those reported in traumatised skeletal muscle of normovolaemic animals, further tools are needed to enhance efficiency in treatment of local skeletal muscle tissue injury during haemorrhagic shock.

**Keywords** Intravital fluorescence microscopy · Nutritive perfusion · Microcirculation · NADH fluorescence · Leukocyte–endothelial cell interaction

### Introduction

Car accidents are the most frequent cause of polytraumatising injuries in the European countries. These patients often suffer from lesions of the central organs, bone fractures and concomitant soft-tissue trauma. Beside

this complex injury pattern, polytraumatised patients often undergo massive blood loss leading to hypovolaemia and shock. Despite major advancements in the early management of critically injured patients, the rapid substitution of volume remains the important cornerstone in first aid therapy to restore circulating blood volume, to

bring back adequate nutritive organ perfusion and to secure oxygen supply to tissue. Previous studies have demonstrated that resuscitation from haemorrhagic shock with crystalloid solutions did not sufficiently improve microvascular blood flow in various organs [1, 2, 3, 4]. In contrast, small-volume resuscitation, i.e. the rapid application of a small amount of hypertonic–hyperoncotic solution, has been shown to be of high efficiency in the treatment of haemorrhage and shock. For example, HyperHES, i.e. 7.2% NaCl/6% hydroxyethyl starch was found to be capable of restoring microvascular perfusion to central organs [3, 4] and to prevent leukocyte adherence to the venular endothelium with, thus, the potential to limit secondary tissue damage [5].

To date, however, it has not been investigated as to whether small-volume resuscitation is of benefit for traumatised skeletal muscle during haemorrhagic shock conditions. The objective of this study was to assess the effects of resuscitation with HyperHES on nutritive perfusion and local inflammatory cell response in skeletal muscle after soft-tissue trauma and haemorrhagic shock.

## Materials and methods

### Animal model

The experimental protocol was approved by the local animal rights protection authorities and followed the National Institutes of Health guidelines for the care and use of laboratory animals. Male Sprague–Dawley rats [body weight (bw) 250–300 g] were anaesthetised with 6% pentobarbital sodium (55 mg/kg bw i.p.; Narcoren, Merial, Hallbergmoos, Germany) and placed on a heating pad for maintenance of body temperature at 37°C. Following tracheotomy the animals were mechanically ventilated (tidal volume 1 ml/100 g bw; 50 breaths/min). Catheters (PE-50; Portex, Hythe, Kent, UK) were placed in the right carotid artery and left jugular vein for continuous monitoring of central haemodynamics (Sirecust; Siemens, Germany).

By means of a pneumatically controlled impact device, a standardised soft-tissue trauma was induced on the lateral compartment of the right hind limb, simulating high-velocity trauma of the lower extremity [6]. The controlled-impact technique was initially developed as a model of experimental traumatic brain injury in rats, reproducing the pathophysiological and morphological responses of severe closed head injury as found in humans [7, 8]. The controlled-impact device consisted of a compressed nitrogen gas source, an adjustable impactor, a displacement transducer, and a personal computer-assisted interface for data transmission and analysis of time/displacement parameters of the impact. The following impact parameters were selected: impact velocity of 7 m/s, deformation depth of 11 mm and impact duration of 100 ms, with an impact diameter of 11 mm. The left hind limb was placed in a plastic mould (Technovit; Kulzer, Wertheim, Germany) shaped like the hind limb to guarantee optimal energy transmission to the tissue by avoiding hind-limb movement during impact.

Subsequently, the right extensor digitorum longus (EDL) muscle was microsurgically prepared to allow us direct access for in vivo high-resolution multifuorescence microscopy. The preparation technique was first described by Tysl and Budreau [9] and modified for in vivo microscopy by Schaser et al. [6]. During preparation, the tissues were superfused with 37°C warm physio-

logical saline solution to prevent drying. After final exposure of the EDL muscle, the tissue was covered with a cover glass.

### Shock and resuscitation

For induction of haemorrhagic shock, the animals were bled to a mean arterial blood pressure (MAP) of 40 mmHg within 10 min. MAP was maintained at that level for 1 h by further bleeding or re-infusion of the shed blood. For resuscitation, the animals received 0.9% saline (saline; Braun Melsungen, Melsungen; Germany), 10% hydroxyethyl starch (HES) 200/0.5 (Fresenius Kabi, Bad Homburg, Germany) or 7.2% saline/6% HES 200/0.5 (HyperHES; Fresenius Kabi). While saline was applied at a volume equal to four-times the shed blood volume within 20 min, the volume of HES applied was equal to the shed blood volume and was given over 5 min. Animals undergoing small-volume resuscitation received 10% of the shed blood volume as HyperHES within 2 min.

### Experimental protocol

After baseline recordings (inclusion criteria: MAP 95–105 mmHg, haematocrit 40–45%, pCO<sub>2</sub> 35–40 mmHg, pO<sub>2</sub> >100 mmHg, pH 7.35–7.45), soft-tissue trauma was induced, followed by haemorrhagic shock of 1 h. Two hours after resuscitation with saline (*n*=7), HES (*n*=7) or HyperHES (*n*=7) in vivo microscopy of the EDL muscle was performed. In an additional group of animals in vivo microscopy of the EDL muscle was performed at the end of the 1-h shock period (*n*=7). At the end of the experiments the animals were killed by exsanguination.

### In vivo fluorescence microscopy

After intravenous injection of fluorescein-isothiocyanate (FITC)-labelled dextran (15 mg/kg bw, Sigma, Deisenhofen, Germany) and rhodamine 6G (0.15 mg/kg bw, Sigma), in vivo microscopy was performed with a Nikon microscope (E600-FN, Nikon, Tokyo, Japan) equipped with a 100-W mercury lamp and filter sets for blue (excitation/emission 465–495 nm/>505 nm), green (510–560 nm/>575 nm) and ultraviolet (340–380 nm/>400 nm) epi-illumination. By use of a water-immersion objective (Plan Fluor ×20/0.75, Nikon) a final magnification of 304-fold was achieved. Images were recorded by means of a charge-coupled device video camera (FK 6990-IQ-S, Pieper, Schwerte, Germany) and transferred to an S-VHS video system for subsequent off-line analysis.

### Microcirculatory analysis

For quantitative off-line analysis a computer-assisted microcirculation image-analysis system was used (CapImage, Zeintl, Heidelberg, Germany). As previously described [5, 6], functional capillary density was defined as the total length of red blood cell-perfused capillaries per observation area and given in centimetres per square centimetre. For assessment of leukocyte–endothelial cell interaction in post-capillary venules, flow behaviour of leukocytes was analysed with respect to free-floating, rolling and adherent leukocytes. Rolling leukocytes were defined as those cells moving along the vessel wall at a velocity of less than 40% of that of leukocytes at the centreline and were expressed as a percentage of the total leukocyte flux. Venular leukocyte adherence was defined as the number of leukocytes not moving or detaching from the endothelial lining of the vessel wall during an observation period of 20 s. Assuming cylindrical microvessel geometry, leukocyte adherence was expressed as non-moving cells per endothelial surface (number per square millimetre), calculated from the

**Table 1** Systemic haemodynamics after soft-tissue trauma and haemorrhagic shock/resuscitation. Values are given as mean  $\pm$  SEM. *Saline* resuscitation with 0.9% saline ( $n=7$ ); *HES* resuscitation with 10% hydroxyethyl starch 200/0.5 ( $n=7$ ); *HyperHES* resuscitation with 7.2% saline/6% hydroxyethyl starch 200/0.5 ( $n=7$ )

Group	Baseline	Shock		Resuscitation				
		10 min	60 min	2 min	5 min	20 min	90 min	120 min
Mean arterial blood pressure (mmHg)								
Saline	101 $\pm$ 1	41 $\pm$ 1	39 $\pm$ 1	80 $\pm$ 8	96 $\pm$ 7	86 $\pm$ 9	103 $\pm$ 4	100 $\pm$ 3
HES	102 $\pm$ 1	40 $\pm$ 1	39 $\pm$ 1	87 $\pm$ 9	96 $\pm$ 7	92 $\pm$ 6	98 $\pm$ 7	97 $\pm$ 5
HyperHES	100 $\pm$ 0	39 $\pm$ 1	39 $\pm$ 1	50 $\pm$ 5* <sup>#</sup>	70 $\pm$ 6* <sup>#</sup>	79 $\pm$ 4	80 $\pm$ 3*	82 $\pm$ 3*
Heart rate (beats/min)								
Saline	348 $\pm$ 13	331 $\pm$ 21	320 $\pm$ 14	340 $\pm$ 13	336 $\pm$ 9	361 $\pm$ 9	394 $\pm$ 10	406 $\pm$ 10
HES	341 $\pm$ 12	328 $\pm$ 15	321 $\pm$ 14	330 $\pm$ 19	338 $\pm$ 10	364 $\pm$ 13	393 $\pm$ 11	398 $\pm$ 14
HyperHES	344 $\pm$ 20	340 $\pm$ 16	301 $\pm$ 16	308 $\pm$ 15	328 $\pm$ 14	354 $\pm$ 13	359 $\pm$ 25	391 $\pm$ 27

\* $P<0.05$  vs saline, <sup>#</sup> $P<0.05$  vs HES

diameter and length of the vessel segment analysed. In post-capillary venules, centreline red blood cell velocity was determined by the line shift method (CapImage). NADH fluorescence of skeletal muscle tissue was densitometrically assessed after 2 s of ultraviolet epi-illumination by computer-assisted grey level determination [10]. To avoid interference of grey levels by microvascular structures, we limited the analysis strictly to the intercapillary space.

#### Laboratory analysis

Arterial blood samples were withdrawn for analysis of blood gases (Rapidlab 348, Bayer Vital, Fernwald, Germany) and blood cell count with a Coulter Counter (AcTdiff, Coulter, Hamburg, Germany).

#### Statistical analysis

Results were given as mean  $\pm$  SEM. Statistical evaluation for differences between groups was performed by Friedman repeated-measures analysis of variance (ANOVA), followed by the appropriate post-hoc multiple comparison procedure with Bonferroni correction for repeated measurements (SigmaStat, Jandel, San Rafael, Calif., USA). To assess the correlation between NADH fluorescence and functional capillary density, we used linear regression analysis. Statistical significance was set at  $P<0.05$ .

## Results

### Systemic parameters and macrohaemodynamics

At baseline and during shock, the animals did not differ with respect to MAP, heart rate, haematocrit, systemic leukocyte count and pH (Table 1 and Table 2). With onset of resuscitation from haemorrhagic shock all animals revealed a rapid and steep rise in MAP (Table 1). While both saline-treated and HES-treated animals regained almost baseline parameters of approximately 100 mmHg, MAP was not completely restored in HyperHES-treated animals and was found to be significantly lower than the values in saline-treated and HES-treated animals at 2, 5, 90 and 120 min after resuscitation (Table 1). Heart rate dropped slightly upon shock induction and increased over time during resuscitation, however, without major differ-

**Table 2** Haematocrit, leukocyte count and pH after soft-tissue trauma and haemorrhagic shock/resuscitation. Values are given as mean  $\pm$  SEM. *Saline* resuscitation with 0.9% saline ( $n=7$ ); *HES* resuscitation with 10% hydroxyethyl starch 200/0.5 ( $n=7$ ); *HyperHES* resuscitation with 7.2% saline/6% hydroxyethyl starch 200/0.5 ( $n=7$ )

Group	Baseline	Shock 60 min	Resuscitation 120 min
Haematocrit (%)			
Saline	42.9 $\pm$ 0.7	35.2 $\pm$ 1.1	27.5 $\pm$ 0.5
HES	43.7 $\pm$ 0.7	33.4 $\pm$ 1.6	24.1 $\pm$ 1.2
HyperHES	44.8 $\pm$ 0.7	35.1 $\pm$ 0.8	29.8 $\pm$ 0.9 <sup>#</sup>
Leukocyte count ( $10^9/l$ )			
Saline	5.8 $\pm$ 0.4	3.6 $\pm$ 0.5	7.8 $\pm$ 1.3
HES	6.8 $\pm$ 0.8	4.9 $\pm$ 0.6	4.1 $\pm$ 0.5*
HyperHES	5.9 $\pm$ 0.7	4.5 $\pm$ 0.3	6.0 $\pm$ 0.7
pH			
Saline	7.48 $\pm$ 0.01	7.40 $\pm$ 0.02	7.31 $\pm$ 0.03
HES	7.46 $\pm$ 0.01	7.41 $\pm$ 0.01	7.39 $\pm$ 0.01
HyperHES	7.46 $\pm$ 0.01	7.42 $\pm$ 0.02	7.43 $\pm$ 0.03*

\* $P<0.05$  vs saline, <sup>#</sup> $P<0.05$  vs HES

ences between the groups (Table 1). Shock caused a marked fall in haematocrit. Infusion of any of the three fluids led to a further decrease in haematocrit, which was found most pronounced in the HES-treated animals (Table 2).

### Nutritive capillary perfusion

Closed soft-tissue trauma in combination with haemorrhagic shock caused a tremendous impairment of nutritive capillary perfusion, with an average value of 78 $\pm$ 17 cm<sup>2</sup>/cm<sup>2</sup> (Fig. 1). While resuscitation with HES, but in particular with HyperHES, caused an almost twofold increase in functional capillary density, resuscitation with saline ameliorated skeletal muscle capillary perfusion, but did not reach the values of the HES-treated or HyperHES-treated animals (Fig. 1). In line with nutritive perfusion failure during shock, high NADH autofluorescence of skeletal muscle tissue was observed, indicating pro-

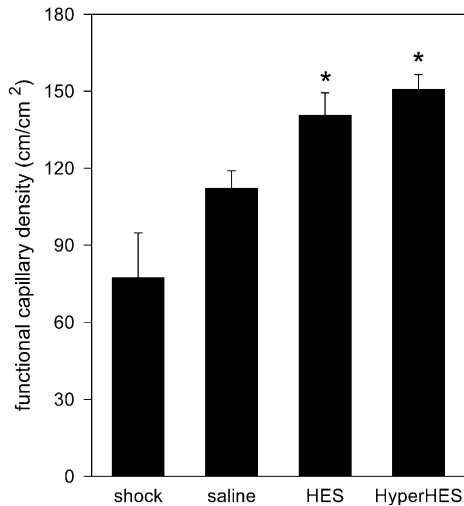


**Fig. 1** Functional capillary density of skeletal muscle tissue after soft-tissue trauma and resuscitation from haemorrhagic shock. Resuscitation was performed with 0.9% saline ( $n=7$ ), 10% HES 200/0.5 ( $n=7$ ) or HyperHES ( $n=7$ ). Animals without resuscitation served as shock group ( $n=7$ ). Values are given as mean  $\pm$  SEM. \* $P<0.05$  vs shock

nounced tissue hypoxia [ $119\pm 21$  arbitrary units (aU)]. Resuscitation-associated reperfusion of nutritive capillaries restored oxygen supply and, thus, caused a slight reduction of tissue NADH levels in saline-treated animals ( $115\pm 21$ aU) and a marked reduction of tissue NADH levels in HES-treated ( $89\pm 16$ aU) and HyperHES-treated ( $100\pm 16$ aU) animals. Regression analysis revealed a linear negative correlation between mean values of functional capillary density and NADH autofluorescence of skeletal muscle tissue, with a regression coefficient of  $r=-0.84$  (Fig. 2).

#### Venular leukocyte–endothelial cell interaction and red blood cell velocity

From shock to resuscitation, interaction of leukocytes with the endothelium of post-capillary venules was found to be further increased, reflecting a characteristic reperfusion-associated event (Table 3). In all groups studied, the fraction of rolling leukocytes was markedly increased upon resuscitation from shock. Quantitative analysis of venular leukocyte adherence revealed significantly higher numbers of firmly adherent cells in the animals treated with saline, HES, and HyperHES when compared with shock (Table 3). Between groups, HyperHES revealed some tendency towards lower numbers of firmly adherent leukocytes (Table 3).

While red blood cell velocity in post-capillary venules was found to be reduced to  $91\pm 22$   $\mu\text{m/s}$  upon shock, resuscitation caused a significant increase in venular red

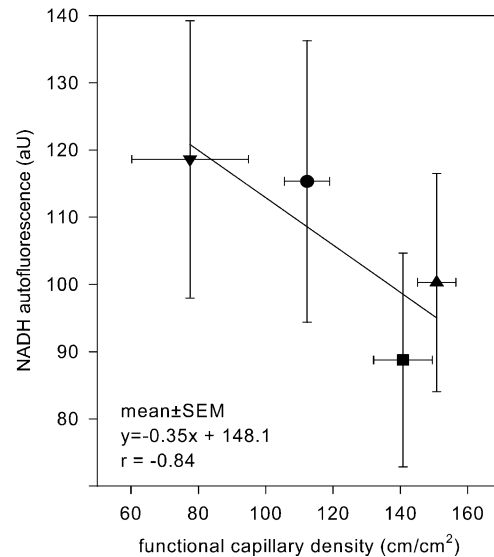


**Fig. 2** Regression analysis between values of functional capillary density and NADH autofluorescence of skeletal muscle tissue. Values are given as mean  $\pm$  SEM, obtained at the end of the 1-h shock period (triangle down) and at 2 h after resuscitation with saline (circle), HES (square) or HyperHES (triangle up).  $r$  regression coefficient

**Table 3** Venular leukocyte–endothelial cell interaction after soft-tissue trauma and haemorrhagic shock/resuscitation. Values are given as mean  $\pm$  SEM. Saline resuscitation with 0.9% saline ( $n=7$ ); HES resuscitation with 10% hydroxyethyl starch 200/0.5 ( $n=7$ ); HyperHES resuscitation with 7.2% saline/6% hydroxyethyl starch 200/0.5 ( $n=7$ )

Group	Leukocyte rolling (%)	Leukocyte adherence ( $n/\text{mm}^2$ )
Shock	16 $\pm$ 5	183 $\pm$ 21
Saline	52 $\pm$ 10*	419 $\pm$ 89*
HES	33 $\pm$ 7	379 $\pm$ 70*
HyperHES	49 $\pm$ 8*	311 $\pm$ 35*

\* $P<0.05$  vs shock

blood cell velocity to values above 200  $\mu\text{m/s}$  (saline  $328\pm 76$   $\mu\text{m/s}$ ; HES  $262\pm 84$   $\mu\text{m/s}$ ; HyperHES  $202\pm 42$   $\mu\text{m/s}$ ;  $P<0.05$  vs shock).

## Discussion

In the present model of closed soft-tissue trauma and haemorrhagic shock, resuscitation with HyperHES and HES was found to be more effective than saline to improve nutritive perfusion of skeletal muscle tissue. In contrast, HyperHES and HES, as with saline, failed to block reperfusion-associated local inflammatory cell response sufficiently. As underlined by the linear negative regression between functional capillary density and

NADH autofluorescence of skeletal muscle tissue, resuscitation-induced improvement of nutritive perfusion is associated with increased oxygen supply to tissue.

*Skeletal muscle microcirculation after trauma and shock:* As given by the results of the present study, haemorrhagic shock in combination with closed soft-tissue trauma caused marked tissue perfusion failure. While values of functional capillary density of the EDL muscle were reported to approximate 240 cm/cm<sup>2</sup> at 1.5 h after trauma induction [6], haemorrhagic shock substantially aggravated perfusion failure of traumatised muscle tissue, as indicated by mean values of functional capillary density of 80 cm/cm<sup>2</sup>. Comparably, as shown by our group for the haemorrhaged liver [10], nutritive perfusion failure of skeletal muscle tissue is paralleled by high values of NADH autofluorescence, indicating insufficient oxygen supply with, thus, tissue hypoxia. NADH is a naturally occurring intracellular fluorophore and one of the main means of transferring energy from the tricarboxylic acid cycle to the respiratory chain in the mitochondria. Inhibition of the respiratory chain due to inadequate oxygen supply is reflected by increased NADH levels [11, 12]. Besides direct tissue destruction caused instantaneously by the impact itself, trauma-induced microvascular dysfunction propagates ischaemia, representing the most decisive trigger for post-traumatic tissue damage [6]. Moreover, as given by the present results, shock-induced lowering of perfusion pressure is associated with a reduction of blood cell velocity and, consequently, cessation of microvascular blood flow. Shock-induced swelling of endothelial cells elevates hydraulic resistance, which leads to impaired skeletal muscle microvascular perfusion and hinders resuscitation efforts to restore shock-impaired flow [13]. By means of in vivo microscopy of rabbit skeletal muscle, Mazzoni et al. [14] demonstrated that an endothelial cell swelling-induced reduction of luminal diameter of ~20% significantly increases capillary resistance and contributes to further flow retardation. Although haemorrhagic shock resulted in a fall of systemic haematocrit, local haem-concentration in individual capillaries may have occurred as a result of increased microvascular permeability [15], additionally affecting flow conditions. Taken together, multiple, closely linked and overlapping factors might have contributed to the marked impairment of skeletal muscle microcirculation following trauma and shock.

*Small-volume resuscitation and central haemodynamics:* Upon resuscitation all the animals showed a rapid increase in MAP; however, the rise of MAP during early resuscitation was significantly more pronounced in the saline-treated and HES-treated animals than in the HyperHES-treated animals. The extent of restoration of central haemodynamics is nicely reflected by the concomitant increase in red blood cell velocity in post-capillary venules. Following infusion of HyperHES, MAP remained below pre-shock values, a finding that is

consistent with the reports of others [16]. There is major evidence from the literature that MAP is restored by small-volume resuscitation to only 70% of control values, while cardiac output exceeds control values by 30–40% [16].

*Small-volume resuscitation and microcirculation of traumatised skeletal muscle tissue:* In line with previous reports of our group and others [1, 2, 3, 4, 16], conventional crystalloid volume substitution might have restored systemic blood pressure, however, it did not sufficiently reverse local nutritive perfusion failure. In contrast, HES and, in particular, HyperHES, were found almost to double the values of functional capillary perfusion to approximately 150 cm/cm<sup>2</sup>. However, it has to be mentioned that these values are still markedly below those reported for traumatised skeletal muscle tissue in normovolaemic animals [5]. This finding most probably reflects the more severe injury to tissue in the case of local trauma in conjunction with the systemic insult of haemorrhagic shock. Since it has become an established fact that the primary factor rendering patients at risk of developing multiple organ dysfunction syndrome after shock and trauma is the persistence of impaired microcirculation [17], there is need for more potent therapeutic tools to restore adequate tissue perfusion.

Small-volume resuscitation is based on the instantaneous mobilisation of endogenous fluid along the osmotic gradient from the intracellular to the intravascular compartment [18, 19], with a preferential shift of water from the microvascular endothelium and the red blood cells [20]. The rectification of shock-narrowed capillaries is considered the pivotal mechanism for restoration of nutritional blood flow. Direct evidence for this mechanism was found by in vivo microscopy in skeletal muscle of rabbits, demonstrating reversal of shock-induced capillary narrowing with hypertonic–hyperoncotic dextran, but not with isotonic Ringer's lactate solution [14]. In the present model that combines local trauma and systemic hypovolaemia, microvascular disturbances of the skeletal muscle tissue are likely the result of several factors, including direct destruction of microvessels, microvascular thrombosis and local bleeding, as well as reduced nutritive perfusion, enhanced leakage and leukocyte–endothelial cell interaction, leading to increased oedema and tissue pressure [5, 6, 21]. Thus, the basis of small-volume resuscitation-mediated protection might partly differ when compared with HyperHES-induced mechanisms responsible for reversal of haemorrhagic shock alone. This might account for the fact that HyperHES did not normalise tissue perfusion and only marginally affected leukocyte–endothelial cell interaction, in contrast to the obvious anti-adhesive properties of HyperHES when applied either in the presence of local trauma under normotensive conditions [5] or in the



absence of trauma under conditions of haemorrhagic shock [3, 4].

In previous experiments, we could demonstrate that progressive tissue damage following soft-tissue injury is secondary to delayed and progressive microvascular perfusion failure [6]. With this in mind, we should aim our primary efforts at restoration of circulating blood

volume and improvement of compromised tissue perfusion. Since the present study demonstrates that primary intervention by hypertonic-hyperoncotic fluid resuscitation enhances, but does not normalise, tissue perfusion, further tools are needed to enhance efficiency in the treatment of local skeletal muscle tissue injury during haemorrhagic shock.

## References

1. Wang P, Ba ZF, Burkhardt J, Chaudry IH (1992) Measurement of hepatic blood flow after severe hemorrhage: lack of restoration despite adequate resuscitation. *Am J Physiol* 262:G92–G98
2. Wang P, Hauptman JG, Chaudry IH (1990) Hemorrhage produces depression in microvascular blood flow which persists despite fluid resuscitation. *Circ Shock* 32:307–318
3. Vollmar B, Lang G, Menger MD, Messmer K (1994) Hypertonic hydroxyethyl starch restores hepatic microvascular perfusion in hemorrhagic shock. *Am J Physiol* 266:H1927–H1934
4. Vollmar B, Preissler G, Menger MD (1996) Small-volume resuscitation restores hemorrhage-induced microcirculatory disorders in rat pancreas. *Crit Care Med* 24:445–450
5. Mittlmeier T, Vollmar B, Menger MD, Schewior L, Raschke M, Schaser KD (2003) Small volume hypertonic hydroxyethyl starch reduces acute microvascular dysfunction after closed soft-tissue trauma. *J Bone Joint Surg Br* 85:126–132
6. Schaser KD, Vollmar B, Menger MD, Schewior L, Kroppenstedt SN, Raschke M, Lubbe AS, Haas NP, Mittlmeier T (1999) In vivo analysis of microcirculation following closed soft-tissue injury. *J Orthop Res* 17:678–685
7. Dixon CE, Clifton GL, Lighthall JW, Yaghami AA, Hayes RL (1991) A controlled cortical impact model of traumatic brain injury in the rat. *J Neurosci Methods* 39:253–262
8. Lighthall JW, Dixon CE, Anderson TE (1989) Experimental models of brain injury. *J Neurotrauma* 6:83–97
9. Tymi K, Budreau C (1991) A new preparation of the rat extensor digitorum longus muscle for intravital investigation of the microcirculation. *Int J Microcirc Clin Exp* 10:335–343
10. Vollmar B, Burkhardt M, Minor T, Klauke H, Menger MD (1997) High-resolution microscopic determination of hepatic NADH fluorescence for in vivo monitoring of tissue oxygenation during hemorrhagic shock and resuscitation. *Microvasc Res* 54:164–173
11. Chance B, Cohen P, Jöbsis F, Schoener B (1962) Intracellular oxidation–reduction states in vivo. The microfluorometry of pyridine nucleotide gives a continuous measurement of the oxidation state. *Science* 137:499–508
12. Ince C, Coremans JM, Bruining HA (1992) In vivo NADH fluorescence. *Adv Exp Med Biol* 317:277–296
13. Mazzoni MC, Borgstrom P, Intaglietta M, Arfors KE (1989) Luminal narrowing and endothelial cell swelling in skeletal muscle capillaries during hemorrhagic shock. *Circ Shock* 29:27–39
14. Mazzoni MC, Borgstrom P, Intaglietta M, Arfors KE (1990) Capillary narrowing in hemorrhagic shock is rectified by hyperosmotic saline–dextran reinfusion. *Circ Shock* 31:407–418
15. Menger MD, Rucker M, Vollmar B (1997) Capillary dysfunction in striated muscle ischemia/reperfusion: on the mechanisms of capillary “no-reflow”. *Shock* 8:2–7
16. Kreimeier U, Bruckner UB, Niemczyk S, Messmer K (1990) Hyperosmotic saline dextran for resuscitation from traumatic-hemorrhagic hypotension: effect on regional blood flow. *Circ Shock* 32:83–99
17. Kreimeier U, Frey L, Messmer K (1993) Small volume resuscitation. *Curr Opin Anaesth* 6:400–408
18. Kreimeier U, Christ F, Frey L, Habler O, Thiel M, Welte M, Zwissler B, Peter K (1997) Small volume resuscitation for hypovolemic shock. Concept, experimental and clinical results. *Anaesthesist* 46:309–328
19. Kreimeier U, Peter K, Messmer K (2001) Small volume—large benefits? *Anaesthesist* 50:442–449
20. Mazzoni MC, Borgstrom P, Arfors KE, Intaglietta M (1988) Dynamic fluid redistribution in hyperosmotic resuscitation of hypovolemic hemorrhage. *Am J Physiol* 255: H629–H637
21. Menth-Chiari WA, Curl WW, Rosencrance E, Smith TL (1998) Contusion of skeletal muscle increases leukocyte–endothelial cell interactions: an intravital-microscopy study in rats. *J Trauma* 45:709–714

### **3.2.3 Prävention und Therapie des Sekundärschadens nach geschlossenem Weichteiltrauma durch N-Acetylcystein**

Ziel dieser Studien war die erstmalige Prüfung der Effizienz des Antioxidans, Radikalfängers und Glutathionprekursors N-Acetylcystein zur Therapie und Prävention des Sekundärschadens nach Weichteiltrauma. Ausgangspunkt für diese Untersuchungen bildeten Literaturbefunde und klinische Erfahrungsberichte über effektive Therapieerfolge in der Behandlung von postischämischen Reperfusionsschäden im Skelettmuskel (23, 41, 75, 139, 185, 186) und anderen Organen (17, 30, 35, 43, 58, 72, 173).

In den hierzu durchgeführten intravitalmikroskopischen und Laser-Doppler-Flowmetrischen Studien ließ sich eine durch N-Acetylcystein-induzierte komplette Wiederherstellung der posttraumatisch signifikant gestörten kapillären Durchblutung in der Frühphase nach Weichteiltrauma dokumentieren (151, 153). Ferner zeigten sich neben reduzierten Werten für mikrovaskuläre Permeabilität und intramuskuläre Ödemmanifestation deutliche N-Acetylcystein-abhängige anti-inflammatorische/-adhäsive Effekte auf die Leukozyten-Endothelzell-interaktion.

Die kausale Rolle der posttraumatischen lokalen Entzündungsreaktion für den sekundären Gewebeuntergang konnte durch eine signifikante positive Korrelation der endothelialen Leukozytenadhärenz und der Reduktion der Immunreaktivität für das muskelspezifische Intermediärcytofilament Desmin (indirektes Nekrosezeichen) belegt werden.

Zusätzlich fanden sich nach geschlossenem Weichteilschaden geringere Kreatinkinasewerte im Serum von N-Acetylcystein-therapierten Tieren im Vergleich zu unbehandelten Kontrolltieren, was eine N-Acetylcystein-vermittelte Gewebsschutz mit verminderter sekundärer Muskelschädigung reflektiert (151, 153).

## Acute effects of *N*-acetylcysteine on skeletal muscle microcirculation following closed soft tissue trauma in rats

Klaus-D. Schaser<sup>a,\*</sup>, Herman J. Bail<sup>a</sup>, Lioba Schewior<sup>a</sup>, John F. Stover<sup>b</sup>,  
Ingo Melcher<sup>a</sup>, Norbert P. Haas<sup>a</sup>, Thomas Mittlmeier<sup>c</sup>

<sup>a</sup> Department of Trauma and Reconstructive Surgery, Charité, Campus Virchow-Klinikum, Humboldt-Universität zu Berlin, Augustenburger Platz 1, 13353 Berlin, Germany

<sup>b</sup> Division of Surgical Intensive Care Medicine, Department of Surgery, University Hospital Zuerich, Raemistrasse 100, 8091 Zuerich, Switzerland

<sup>c</sup> Department of Trauma and Reconstructive Surgery, Universität Rostock, Schillingallee 35, 18055 Rostock, Germany

Accepted 19 May 2004

### Abstract

Trauma-induced microcirculatory dysfunction, formation of free radicals and decreased endothelial release of nitric oxide (NO) contribute to evolving tissue damage following skeletal muscle injury. Administration of *N*-acetylcysteine (NAC) known to scavenge free radicals and generate NO is considered a valuable therapeutic approach. Thus, the objective of this study was to quantitatively analyze the acute effects of NAC on skeletal muscle microcirculation and leukocyte–endothelial cell interaction following severe standardized closed soft tissue injury (CSTI). Severe CSTI was induced in the hindlimbs of 14 male anesthetized Sprague–Dawley rats using the controlled impact injury technique. Rats were randomly assigned ( $n = 7$ ) to high-dose intravenous infusion of NAC (400 mg/kg body weight) or isovolemic normal saline (NS). Non-injured, sham-operated animals ( $n = 7$ ) were subjected to the same surgical procedures but did not receive any additional fluid. Creatin kinase (CK) activity was assessed at baseline, 1 h before and 2 h following posttraumatic NAC or NS infusion. Microcirculation of the extensor digitorum longus (EDL) muscle was analyzed using intravital microscopy and Laser-Doppler flowmetry (LDF). Edema index (EI) was calculated by measuring the EDL wet-to-dry weight ratio ( $EI = \text{injured/contralateral limb}$ ). EDL-muscles were analyzed for desmin immunoreactivity and granulocyte infiltration. Microvascular deteriorations observed following NS-infusion were effectively reversed by NAC: Functional capillary density was restored to levels found in sham-operated animals and leukocyte adherence was significantly ( $p < 0.05$ ) reduced compared to the NS group. NAC significantly ( $p < 0.05$ ) increased erythrocyte flux determined by Laser-Doppler flowmetry. Posttraumatic serum CK levels and EI were significantly ( $p < 0.05$ ) decreased by NAC. During the posttraumatic acute phase, single infusion of NAC markedly reduced posttraumatic microvascular dysfunction, attenuated both leukocyte adherence and tissue infiltration. NAC also decreased CSTI-induced edema formation and myonecrosis as reflected by attenuated serum CK levels and attenuated loss of desmin immunoreactivity. NAC may serve as an effective therapeutic strategy by supporting microvascular blood supply and tissue viability in the early posttraumatic period. Additional studies aimed at long-term analysis and investigation of injury severity— or dosage dependency are needed.

© 2004 Orthopaedic Research Society. Published by Elsevier Ltd. All rights reserved.

**Keywords:** Microcirculation; Skeletal muscle; Trauma; *N*-acetylcysteine; Rats

### Introduction

Severe soft tissue trauma strongly influences morbidity following complex injuries to the extremities as evidenced by prolonged healing of fractures and return

of limb function as well as sustained susceptibility to local wound infections [15,25,45]. Persistently enhanced trauma-induced microcirculatory impairment, increased microvascular permeability, “no reflow” phenomenon of nutritive capillaries and leukocyte-mediated tissue destruction contribute to evolving tissue damage secondary to ischemia/reperfusion [16,28–30] or trauma [41,42] in skeletal muscle injury. Direct trauma to microvessels results in membrane damage, endothelial cell

\* Corresponding author. Tel.: +49-30-450-552098; fax: +49-30-450-552958.

E-mail address: klaus-dieter.schaser@charite.de (K.-D. Schaser).

swelling, perivascular hemorrhage, and uncontrolled clot formation, leading to additional local ischemia, which, in turn, induces further degradation of membrane phospholipids, accumulation of free radicals [34], and inflammation-induced oxidative stress [49]. Increased oxidative stress, in turn, severely impairs the endogenous anti-oxidant defense where glutathione (GSH) is the most important component [7,17,39]. In addition, posttraumatic and postischemic reduction in endothelial nitric oxide (NO) synthesis known for its strong vasodilating potential [24,32,38] may aggravate evolving tissue damage.

Thus, early administration of radical scavengers, replenishing of diminished cellular GSH-stores and replacement of NO are promising therapeutic approaches to reduce posttraumatic soft tissue damage. Pharmacological studies have shown that *N*-acetylcysteine (NAC) is an anti-oxidant [2], precursor of glutathione [39], and donor of nitric oxide (NO) [8,17,21,33]. Therefore, we hypothesized that NAC could ameliorate local microcirculatory impairment, reduce leukocyte–endothelial cell interaction, and attenuate structural damage in the early and acute posttraumatic period following traumatic skeletal muscle injury in rats subjected to severe standardized closed soft tissue injury (CSTI) [41].

## Material and methods

### Animal model and surgery

Experiments were performed in accordance to the NIH guidelines for laboratory animal use and were approved by the local animal right protection authorities.

Severe CSTI was induced in the antero-lateral compartment of the left mid thigh in male anesthetized and spontaneously breathing (isoflurane 1.5 vol.%, N<sub>2</sub>O 0.5 l/min and O<sub>2</sub> 0.3 l/min) Sprague–Dawley rats (weight 250–300 g) as previously described [41]. Since severe CSTI predominantly occurs in high-energy accident victims, the impact parameters were adapted accordingly. CSTI was performed with the high-pressure computer-assisted controlled impact injury (CI) technique by accelerating a pneumatically driven 11 mm bolt with a flat tip to an impact velocity of 7 m/s (=25 km/h), inducing a penetration depth of 11 mm at a contact time of 0.1 s [41]. These settings resulted in a reproducible non-lethal focal injury (blunt trauma) to the left extensor digitorum longus (EDL) muscle without inducing a concomitant bone fracture or manifest compartment syndrome.

For continuous hemodynamic monitoring of heart rate (HR) and mean arterial blood pressure (MABP), and for administration of fluid and fluorescence markers the left carotid artery and right jugular vein were cannulated with PE-catheters (PE50, 0.58 mm inner diameter, Portex, Hythe, Kent, UK).

For *in vivo* analysis of microcirculation using intravital fluorescence microscopy (IVM), the left EDL muscle was surgically exposed modified to the previously described technique [46], allowing horizontal scanning of the entire EDL muscle surface at a constant focus level and analyze of stable microcirculation for a period of 3 h at maximum.

### Experimental protocol

For microcirculatory measurements and determination of skeletal muscle edema weight gain severe standardized CSTI was induced in 14

rats. Non-injured, sham-operated animals served as sham-group ( $n = 7$ ). Immunohistochemical studies were performed in additional 7 sham-operated animals (*sham*,  $n = 7$ ) and 14 rats at 3 h following CSTI and induction of therapy with either normal saline (NS) ( $n = 7$ ) or *N*-acetylcysteine (NAC,  $n = 7$ ).

Compartment syndrome was ruled out by measuring the intramuscular pressure ( $P_{im}$  in mmHg) in the anterior and posterior tibial compartment. For this, a special microsensor catheter (0.7 mm outside diameter, CODMAN® microsensors, Johnson & Johnson Professional, Inc., Raynham, MA, USA) was percutaneously inserted (8 mm vertically beneath skin surface) before surgical exposure of the EDL muscle [41].

After surgery, the prepared EDL-muscle was allowed to stabilize for 15 min before values for macrohemodynamics, arterial blood gases, blood chemistry, and Laser-Doppler flowmetry (LDF) were collected (1 h after trauma, before treatment). Following CSTI, rats were randomly assigned to an intravenous infusion of NAC (Fluimucil®, Zambon, Gräfelfing, Germany) in a dosage of 400 mg/kg body weight (2.45 mmol/kg; equivalent to 2 ml/kg) ( $n = 7$ ) or an equivalent volume of NS (0.9% NaCl, Braun Melsungen AG, Melsungen, Germany,  $n = 7$ ; mean volume per animal:  $0.61 \pm 0.03$  ml) for 15 min. High-dose treatment with NAC was chosen based on previous studies showing beneficial effects following intravenous administration in postischemic reperfusion disorders [22] and is at the upper limit of a the standard infusion regimen under human circumstances [17]. Non-injured, sham-operated animals ( $n = 7$ ) received no additional fluid. Following the infusion (1.5 h after CSTI), LDF values were assessed, blood samples were analyzed, and EDL muscle microcirculation was investigated using intravital fluorescence microscopy (2 h after CSTI).

After sacrificing the animals at the end of each experiment and assessing the biological zero values of the non-perfused EDL muscle using LDF necessary to assess changes caused by the Brownian molecular motion [5], the left and right EDL muscles were removed for gravimetric analysis of edema formation (Fig. 1) and immunohistological analysis in a separate group of rats.

Due to the facts that the used animal model is acute in nature not allowing survival of rats with painful incapacitation of the hind limb for ethical reasons and that the stability of the microsurgically prepared EDL-muscle is only of short duration, the study period had to be restricted to 3 h after trauma.

### Intravital microscopy

*In vivo* microvascular imaging was performed with epi-illumination intravital multifluorescence microscopy using a modified high-resolution NIKON-microscope (Optiphot, NIKON, Tokyo, Japan) equipped with a high-pressure mercury lamp (100 W) and a selective filter block system allowing to detect fluorescence emission of fluorescein-isothiocyanate (FITC)-dextran (excitation/emission wavelength: 450–490 nm/>580 nm) and rhodamine (530–560 nm/>580 nm). Intravital microscopy enabled well contrasted and focused images of high quality in regard to image red and white blood cells as well as determine individual segments of the microvascular bed (Figs. 3 and 4), i.e., capillaries and venules [41]. Microvascular images and videosequences were recorded using a CCD-camera (FK 6990-IQ, Pieper, Schwerte, Germany) and transferred to an SVHS-videorecorder (HR-S4700EG/E, JVC, Friedberg, Germany) for off-line analysis (final magnification on the video screen: 940-fold).

For contrast enhancement between erythrocytes and plasma, FITC-dextran (5%, 150,000 molecular weight; 15 mg/kg body weight; Sigma Chemical, Deisenhofen, Germany) was injected intravenously prior to each investigation [30]. For *in vivo* imaging of leukocytes [50], rats were given a bolus of rhodamine 6G (0.1%, 0.15 mg/kg body weight; Sigma Chemical). To decrease the development of boundary reflection error and to minimize loss of fluorescence intensity due to progressive metabolization, hepatic extraction and excretion the time period for performing intravital microscopic observations was standardized. Therefore recordings of microvascular images were started 1–3 min after injection (complete contrast enhancement of the peripheral capillary bed and equilibration of the transendothelial extravasation rate) and have been completed 15–20 min after injection of the FITC-dextran and rhodamine bolus, respectively. For limitation of phototoxic effects duration of continuous light exposure per observation area was restricted to 60 s at maximum [36,40].

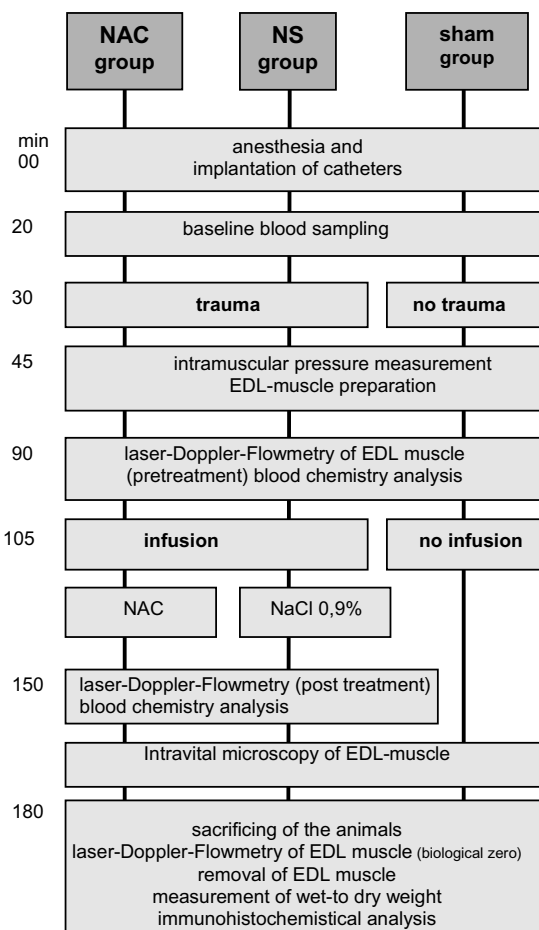


Fig. 1. Schematic drawing of the experimental protocol depicting time course of interventions in sham-operated, and *N*-acetylcysteine (NAC) and normal saline (NS)-treated rats.

#### Microcirculatory analysis

Quantification of posttraumatic skeletal muscle microcirculation and microvascular parameters was performed off-line by a frame-to-frame analysis using a computer-assisted microcirculation image analysis program [20,52]. Microcirculatory analysis was performed by the same investigator blinded to the status of the studied rats.

#### Microvascular diameter ( $D$ in $\mu\text{m}$ )

For diameter measurements the user selects a videoimage for analysis. The length of a line which is then placed perpendicular between the inner two edges of the microvessel is calculated as the luminal diameter.

#### Functional capillary density (FCD in $\text{cm}^{-1}$ )

FCD is defined as the length of erythrocyte-perfused capillaries per observation area. Since only erythrocyte-perfused capillaries are counted this parameter is used as an indicator for nutritive tissue perfusion and oxygen delivery. Using the image-analysis system the perfused capillaries within the area are traced by the user and the length is calculated.

#### Microvascular permeability (macromolecular leakage in %)

The microvascular permeability (macromolecular leakage) is used to assess the integrity of the endothelial barrier. Under normal conditions the plasma marker FITC-dextran (150,000 molecular weight) is unable to pass the endothelium, producing a high-contrast image. Consequently, endothelial dysfunction induced by different noxious

stimuli will result in diffusion of FITC-dextran into the perivascular-interstitial space consecutively increasing the perivascular fluorescence intensity and the ratio of extra- to intravascular fluorescence intensity. Leakage measurement relies on computer-assisted quantification of fluorescence intensity using a densitometric technique (digital video-image analysis). Mean gray level is measured by assessing the number and area of all pixel-points with a certain intensity which is defined by the amount of fluorescence. Leakage (assessed in 4 fields per image at minimum) was expressed as the ratio of fluorescence-intensity, selected from perivascular area to the corresponding intravascular area (plasma gaps within the microvascular flow). For assessment of corresponding perivascular values the fluorescence intensity is measured within an extravascular area in the immediate vicinity to the microvascular vessel wall in a distance from the vessel wall not exceeding the corresponding microvascular diameter. Furthermore, extravascular measurement sites were located at the same level like the intravascular plasma gap relative to the longitudinal axis of the microvascular segment.

#### Centerline red blood cell velocity ( $V_{\text{RBC-centerline}}$ )

The centerline red blood cell velocity is measured from a line shift diagram, which is created from a 10–15 s video sequence in which there is no tissue movement. A line is drawn along the length of the vessel in the centerline blood flow and the pixels under this line are stored in the computer over a 10 s observation period and are aligned vertically. Dark cells (erythrocytes) moving along the line produce slanted stripes. From the length and slope of these stripes the image analysis program calculates the red blood cell velocity. In this line shift diagram, the  $y$ -axis represents the distance along the line and the  $x$ -axis shows the time. The mean red blood cell velocity for each vessel and video-field ( $V_{\text{RBC-mean}}$ ) was calculated as previously described [4,30] as  $V_{\text{mean}} = V_{\text{centerline}}/1.6$ .

#### Leukocyte-endothelial cell interactions

Leukocyte adherence was determined by counting the number of rolling and adherent as well as free-flowing (non-adherent) leukocytes for 30 s along a 100  $\mu\text{m}$  venular segment. To prevent tangential sections through the investigated microvascular segment the level with the largest microvascular diameter was microscopically focussed. Thus, in vivo labeled leukocytes adhering to the endothelium of the vessel wall over or beneath the exactly adjusted focus level are projected to the image plane with less but sufficient sharp contours.

Leukocyte rolling was defined as white blood cells repeatedly contacting, reversibly adhering and loosely interacting to the endothelial vessel wall with a flow velocity significantly less than centerline velocity [3] and expressed in percent of the total leukocyte flux. Permanent leukocyte adherence (sticking) was defined as the number of non-moving leukocytes tightly adhering and firmly attaching to the same spot on the endothelial lining of a 100  $\mu\text{m}$  vessel segment for at least 20 s and expressed as number of adherent cells per  $\text{mm}^2$  endothelial surface, assuming cylindrical microvessel geometry.

#### Venular wall shear rate ( $SR$ )

The wall shear rate as a function of the disperse force on rolling leukocytes was calculated for each venule:  $SR = 8 \times V_{\text{mean}}/D$  in ( $\text{s}^{-1}$ ), where  $V_{\text{mean}}$  is the mean erythrocyte velocity and  $D$  is venular diameter [4].

#### Laser-Doppler flowmetry

This technique employs a monochromatic laser light beam which detects blood cell movement in the tissue by analyzing the Doppler shift of backscattered light. Thereby, the average blood flow (erythrocyte flux) within a particular tissue volume is obtained. Changes in erythrocyte flux (arbitrary units) were determined using a dual channel laser Doppler monitor (DRT4, Moore Instruments, Axminster, UK; needle probe DP4, 780–820 nm, external diameter 0.8 mm). Erythrocyte flux in the surgically exposed EDL-muscle was calculated as the product of erythrocyte velocity and concentration [5] and was assessed before (1 h after CSTI) and following treatment with NAC and NS (1.5 h after CSTI), and expressed relative to pre-infusion values. For prevention of motion artefacts and sequential scanning of the EDL-muscle surface in 1 mm incremental steps along the longitudinal axis of the EDL-muscle (reaching 20 measurements per EDL-muscle at

minimum) the laser-needle probe was attached to a three-dimensional micromanipulator.

#### Blood sampling

Arterial blood gases (paCO<sub>2</sub>, paO<sub>2</sub> and pH), plasma concentration of hemoglobin (Hb), and serum creatine kinase (CK)-levels were determined before CSTI (baseline), before (1 h after CSTI) and 1 h following NAC or NS infusion (2 h after CSTI). Arterial blood gases and hemoglobin were assessed using a blood gas analyser (ABL 300, Radiometer, Copenhagen, Denmark). Activity of CK was determined by a multiple-point-kinematic test (670 nm) (Vitros products chemistry, East Man Kodak company, Rochester, York, USA).

#### Quantification of edema formation (edema weight gain)

Posttraumatic skeletal muscle edema formation was assessed gravimetrically by measuring the wet-to-dry weight ratio of the left (traumatized) and contralateral (non-injured) EDL-muscle (edema index: EI = left/contralateral EDL) after the NAC or NS infusion at 2.5 h after CSTI. After determination of wet weight, EDL muscles were dried for 24 h in a laboratory oven (80 °C) and weighed again to assess the dry weight.

#### Immunohistochemistry

Specimens were freshly acquired, fixed in 4% formaldehyde, processed to paraffin and cut into 3 µm transverse and longitudinal sections. Immunohistochemical staining for muscle specific class III intermediate filament desmin (monoclonal mouse anti-human desmin, clone D33; DAKO, Glostrup, Denmark) and rat neutrophilic granulocytes (mouse anti-rat granulocyte antibody, Clone: HIS48; Pharmingen, San Diego, CA, USA) was performed by immersion in citrate puffer (100 mM, pH = 6) and microwave heating for antigen retrieval. Following incubation with primary antibodies (HIS48 1:30, anti-desmin 1:50) the biotinylated secondary antibody was added for 60 min at room temperature. After incubation with avidin-biotin complex the sections were subjected to diaminobenzidine substrate.

#### Desmin immunoreactivity to assess myonecrosis

As a part of the cytoskeleton, desmin forms a network across the muscle fibre bordering at the plasma and nuclear membrane and is particularly localized in the subplasmalemmal region and the Z-band. Indicating muscle cell viability the muscle-specific intermediate cytofilament desmin unmasks necrosis of myofibers as a rapid post-traumatic and visible loss of the faint, irregular desmin positivity in their sarcoplasm [35].

#### Leukocyte infiltration

Neutrophilic granulocyte extravasation and infiltration into skeletal muscle tissue was analyzed by immunostaining using the HIS 48 antibody, known to selectively stain rat granulocytes.

To draw a histomorphometrical comparison to the extent of myonecrosis (detectable as the loss of desmin intermediate cytofilament immunopositivity), planimetric analysis of desmin immunopositivity (area measurement, given as the area with loss of immunopositivity vs. area with detectable immunopositivity) was performed (ratio: non-immunoreactive/immunoreactive). To assess leukocyte infiltration into the tissue at least 15 randomly selected fields of 60,000 µm<sup>2</sup> per animal were analyzed for the presence of HIS48-immunoreactivity and given as number of HIS48-immunoreactive cells per mm<sup>2</sup> tissue surface. Quantitative analysis was performed using a computer-assisted interactive image analysis system (Quantimed Image analysis, LEICA Instruments, Cambridge, UK).

#### Statistical methods

Data were analyzed by a repeated-measures analysis for three groups as previously described [27]. The sample size of seven rats per group was considered to be sufficient due to the small variations of the data observed in preceding studies using comparable sample size [41] and the fact that the normality test (Kolmogorov-Smirnov) was passed. Differences between groups were tested by ANOVA for inde-

pendent samples followed by post hoc analysis using Bonferroni-correction for multiple comparisons. To test for time effects within a group data were subjected to a multivariate analysis of variance for repeated measures and differences were tested by paired Student's *t*-test, including Bonferroni-correction for repeated measurements. Erythrocyte flux (LDF) between the NAC and NS groups was compared using the unpaired Student's *t*-test. The strength of association between microvascular leukocyte adherence and the extent of loss in desmin immunoreactivity (myonecrosis) for all groups was analyzed by linear regression analysis. All data were expressed as mean ± SD. Statistical significance was set at *p* < 0.05.

## Results

### Systemic hemodynamics and blood parameters

In all investigated groups, HR, MABP, arterial blood gases (pH, paCO<sub>2</sub>, and paO<sub>2</sub>) and plasma calcium levels remained unchanged and within normal limits (Tables 1, 2). Anaphylactic-like responses to FITC-labeled dextran or rarely observed *N*-acetylcysteine (NAC)-induced cardiorespiratory complications [37] were not observed in any of the rats. Hemoglobin was significantly decreased following administration of NAC or NS (Table 1), which was similar in all groups before the infusion period. Following CSTI the significantly increased serum CK-levels were significantly reduced following NAC-treatment (Fig. 2).

Table 1

Changes in arterial blood gases and hemoglobin (Hb) concentration determined in NS- and NAC-treated animals at baseline, 1 h (before treatment) and 1.5 h (after treatment) following closed soft tissue injury

Group	Baseline	1 h after trauma (before treatment)	2 h after trauma (45 min after treatment)
<b>pH</b>			
Sham	7.43 ± 0.02	–	–
NS	7.45 ± 0.02	7.38 ± 0.04	7.35 ± 0.09
NAC	7.44 ± 0.03	7.44 ± 0.03	7.41 ± 0.08
<b>paCO<sub>2</sub> [mmHg]</b>			
Sham	38.6 ± 4.7	–	–
NS	41.0 ± 5.6	42.9 ± 5.5	44.8 ± 10.4
NAC	40.3 ± 4.9	30.3 ± 6.8	28.6 ± 4.98
<b>paO<sub>2</sub> [mmHg]</b>			
Sham	155 ± 22.3	–	–
NS	213.9 ± 20.1	243.8 ± 90.6	218.6 ± 49.2
NAC	206.7 ± 22.9	214.1 ± 49.2	267.9 ± 39.1
<b>Hb [mg/dl]</b>			
Sham	13.5 ± 0.4	–	–
NS	13.7 ± 0.2	12.6 ± 0.9	11.8 ± 1.0 <sup>a</sup>
NAC	14.8 ± 0.6	12.1 ± 2.8	11.6 ± 2.2 <sup>a</sup>

Hb was significantly decreased at 1.5 h after trauma (<sup>a</sup>*p* < 0.05 vs. corresponding baseline) most likely due to progressive trauma-induced hemorrhage into skeletal muscle tissue.

Table 2

Mean arterial blood pressure (mmHg) and heart rate (beats/min), intramuscular pressure measured percutaneously in the ventral and dorsal tibial compartment of rat hindlimb, and edema index (wet-to-dry ratio of injured vs. contralateral EDL muscle) remained unchanged following CSTI and treatment with NAC and NS in the isoflurane-anaesthetized rats

Group	Mean arterial blood pressure (mm Hg)	Heart rate (beats/min)	Intramuscular pressure (mm Hg)		Edema index
			Ventral	Dorsal	
Sham	103 ± 5	267 ± 17	6.3 ± 0.4	5.1 ± 0.6	1.01 ± 0.03
NS	109 ± 13	253 ± 25	20.7 ± 1.1 <sup>a</sup>	9.0 ± 1.6 <sup>a</sup>	1.13 ± 0.03 <sup>a</sup>
NAC	102 ± 4	326 ± 27	19.8 ± 6.0 <sup>a</sup>	9.6 ± 2.9 <sup>a</sup>	1.09 ± 0.03 <sup>a</sup>

Sham, non-traumatized, sham-operated animals ( $n = 7$ ); NS, injured animals treated with NS ( $n = 7$ ); NAC, injured animals treated with NAC ( $n = 7$ ). Values are expressed as means ± SD. ANOVA for independent samples followed by post hoc analysis and Bonferroni-correction for multiple comparison procedures: <sup>a</sup> $p < 0.05$  vs. sham.

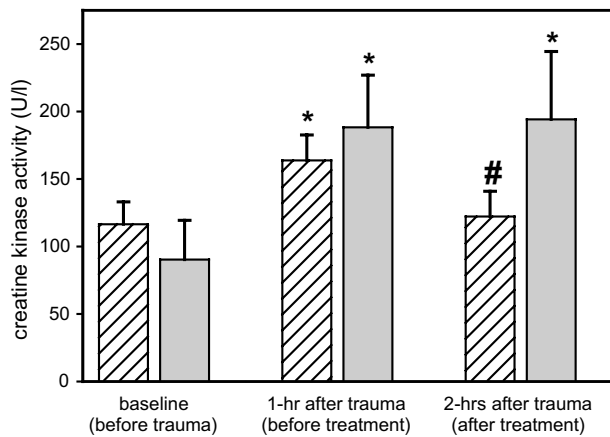


Fig. 2. Changes in creatin kinase activity in rat serum following severe closed soft tissue trauma and treatment with either normal saline (NS,  $n = 7$ ; filled bar) or *N*-acetyl cysteine (NAC,  $n = 7$ ; hatched bar). Values are mean ± SD in U/l. ANOVA for repeated measures followed by post hoc analysis and Bonferroni-correction for repeated measurements: \* $p < 0.05$  vs. corresponding baseline; paired student's *t*-test: # $p < 0.05$  vs. 1-h after trauma (before treatment).

### Intramuscular pressure

CSTI significantly increased intramuscular pressure ( $P_{im}$ ) within the anterior and posterior compartment compared to non-injured sham-operated animals (Table 2). This increase in  $P_{im}$  was equally pronounced in NAC- and NS-receiving rats indicating standardized induction of CSTI (Table 2).

Table 3

Microvascular diameters and red blood cell velocity in capillaries and venules as well as calculated venular wall shear rate in rat EDL muscle following severe closed soft tissue trauma and treatment with either NS or NAC

Group	Diameter ( $\mu\text{m}$ )		Red blood cell velocity ( $\mu\text{m/s}$ )		Shear rate ( $\text{s}^{-1}$ )
	Capillaries	Venules	Capillaries	Venules	
Sham	5.0 ± 0.2	22.8 ± 8.9	189.3 ± 24.0	254.0 ± 27.4	99.1 ± 21.5
NS	5.3 ± 0.4	23.0 ± 2.2	141.8 ± 63.6	270.4 ± 45.9	105.3 ± 21.4
NAC	5.2 ± 0.4	23.2 ± 7.6	137.0 ± 55.1	329.5 ± 108.0	129.9 ± 59.7

Sham ( $n = 7$ ), untreated (non-injured) sham animals; NS ( $n = 7$ ), injured animals treated with normal saline; NAC ( $n = 7$ ), injured animals treated with *N*-acetylcysteine.

### Skeletal muscle microcirculation

CSTI induced heterogeneous microvascular impairment similar to the postischemic “no reflow” phenomenon, characterized by capillary thrombosis, increased intercapillary distance and reduced nutritive blood flow. Posttraumatic microcirculation in the NS group was furthermore characterized by a significant reduction in the FCD (Fig. 5a), which was paralleled by slight but not significant increase in macromolecular leakage when compared to sham-operated animals (Fig. 5b). NAC administration completely restored FCD and slightly exceeded the levels found in non-traumatized sham-operated animals. In addition, posttraumatic microvascular permeability revealed some tendency towards lower values by the treatment with NAC (Fig. 5b). There were no significant differences in capillary and venular diameters as well as venular wall shear rate in the investigated groups (Table 3).

### Leukocyte–endothelial cell interaction

In the non-injured sham-operated animals 20% of the total leukocyte flux within the analysed microvessel segment were found to be rolling along the endothelium of postcapillary venules (Fig. 3). Following CSTI and subsequent NS-administration leukocyte rolling was increased by nearly 2-fold (Fig. 4). Treatment with NAC significantly reduced leukocyte rolling (Fig. 6a) compared to the NS group.

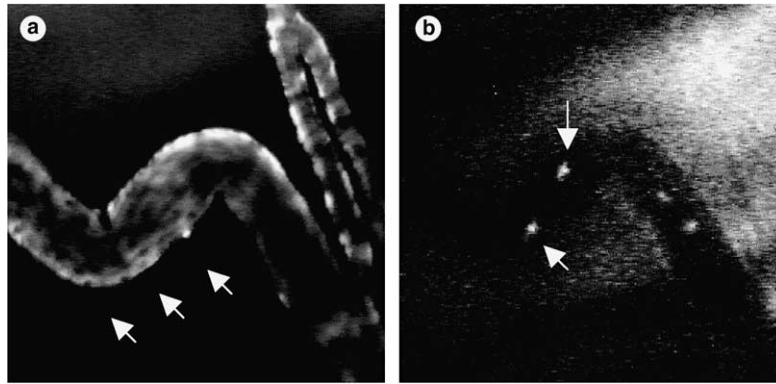


Fig. 3. Intravital fluorescence microscopic images of a postcapillary venule in a non-injured control animal following (a) injection of FITC-dextrane for contrast enhancement between plasma and erythrocytes and (b) after in vivo labeling of leukocytes using rhodamin 6G. Note the low fluorescence density (white arrows) in the perivascular area (a) and the low number of leukocytes (white arrows) adhering to the microvascular endothelium (b) of the identical venular segment (magnification: 940-fold).

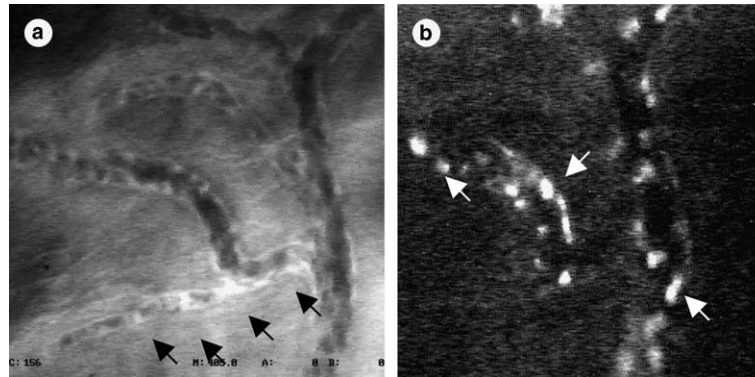


Fig. 4. Intravital fluorescence microscopic images of a postcapillary venule in an injured and normal saline (NS)-treated control animal following (a) injection of FITC-dextrane for contrast enhancement between plasma and erythrocytes and (b) after in vivo labeling of leukocytes using rhodamin 6G. Note the increased fluorescence density (black arrows) in the perivascular area (a) and the high number of leukocytes (white arrows) adhering to the microvascular endothelium (b) of the identical venular segment (magnification: 940-fold).

In the sham-group, permanently adhering leukocytes were rarely observed in collecting venules of EDL muscle. Severe CSTI significantly increased leukocyte adherence, primarily restricted to the postcapillary endothelium. NAC significantly decreased the number of sticking leukocytes compared to the rats receiving NS (Fig. 6b).

#### Laser-Doppler flowmetry

Laser-Doppler flowmetry of sham-operated animals revealed constant flux values over the 2 h study period without significant changes. Consistent with the intravital microscopic findings of drastically increased FCD in the NAC-group Laser-Doppler flowmetry revealed a significantly increased erythrocyte flux in response to NAC compared to the declined flux values of the NS-group (Fig. 7).

#### Edema formation

CSTI significantly increased edema formation (expressed by the edema index) compared to the non-injured sham-operated animals (Table 2). Posttraumatic NAC infusion decreased the edema index compared to the rats receiving NS, which, however, remained pathologically elevated compared to non-injured sham-group.

#### Immunohistochemistry

Immunohistochemical staining of granulocytes by HIS48 demonstrated distinct labeling of the cell surface membranes. Posttraumatic leukocyte infiltration was significantly decreased in NAC-treated rats compared to NS ( $p < 0.05$ ) (Fig. 8a). Necrosis of myofibers was visible as swelling and edema with loss of irregular desmin



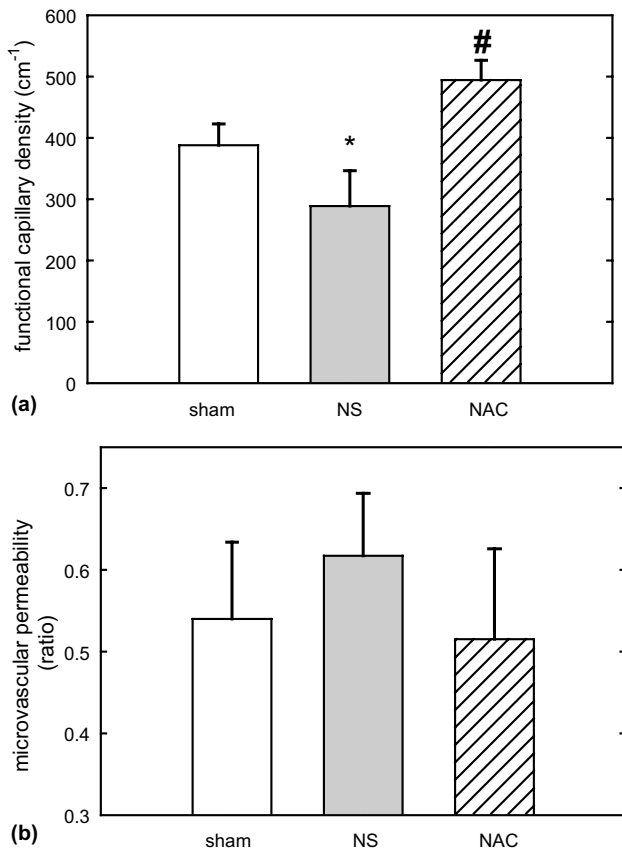


Fig. 5. Changes in capillary perfusion and transendothelial leakage following trauma and treatment. (a) Functional capillary density (length of erythrocyte perfused capillaries per observation area; given in  $\text{cm}^{-1}$ ) and (b) microvascular permeability (capillary macromolecular leakage of FITC-dextrane) analyzed densitometrically by the ratio of extra- to intravascular fluorescence intensity) in EDL muscle in non-injured, sham-operated animals ( $n = 7$ ; open bar) and at 2 h post trauma, i.e. 30 min following treatment with either NS (normal saline,  $n = 7$ ; filled bar) or NAC (*N*-acetylcysteine,  $n = 7$ ; hatched bar). Values are means (SD, ANOVA for independent samples followed by post hoc analysis and Bonferroni-correction for multiple comparison procedures: \* $p < 0.05$  vs. sham, # $p < 0.05$  vs. NS.

immunoreactivity. In the preserved viable myofibers desmin immunoreactivity depicted the cross striations in the sarcoplasm. Histo-morphometrical analysis of desmin immunoreactivity following CSTI revealed signs of markedly decreased ( $p < 0.05$ ) myofiber necrosis in response to NAC treatment (Fig. 8b).

Regression analysis of microvascular leukocyte adherence on loss of desmin immunoreactivity revealed a positive correlation (Fig. 9) between sham-operated animals, the NS and NAC groups ( $r^2 = 0.75$ ).

## Discussion

Severe traumatic soft tissue damage results in micro-circulatory impairment and tissue damage within the

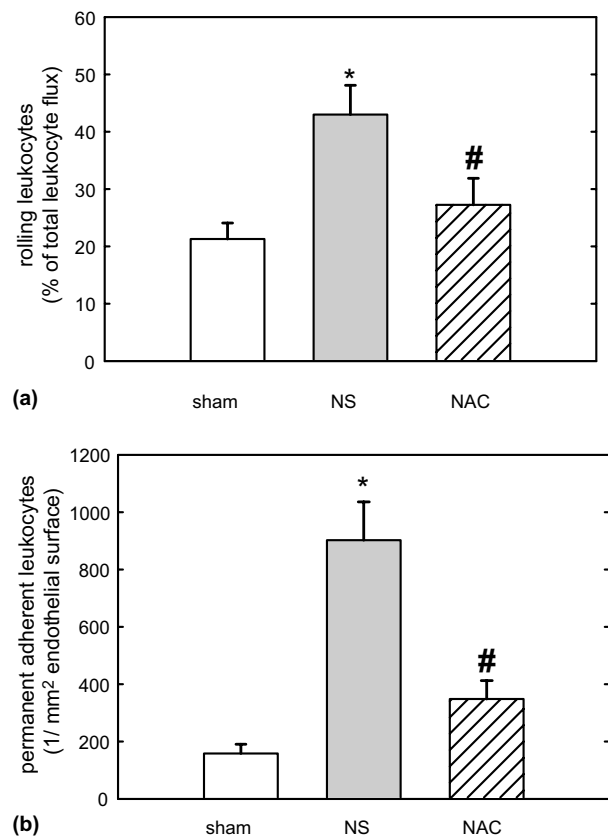


Fig. 6. Leukocyte-endothelial cell interaction in postcapillary venules of EDL muscle in sham-operated, non-injured animals ( $n = 7$ ; open bar) and after treatment of injured animals with either NS (normal saline,  $n = 7$ ; filled bar) or NAC (*N*-acetyl cysteine,  $n = 7$ ; hatched bar) at 2 h post trauma. (a) Number of rolling leukocytes in % of total leukocyte flux. (b) Number of adherent leukocytes per  $\text{mm}^2$  endothelial surface. Values are means  $\pm$  SD, ANOVA for independent samples followed by post hoc analysis and Bonferroni-correction for multiple comparison procedures: \* $p < 0.05$  vs. sham, # $p < 0.05$  vs. NS.

first hour after CSTI in rats as reflected by decreased FCD, marked adherence and infiltration of leukocytes, edema formation and myonecrosis. These results are in line with previous studies [31,41,42].

Single posttraumatic intravenous infusion of NAC significantly attenuated the immediate microcirculatory impairment, myonecrosis, edema formation and release of CK during the early posttraumatic period, indicating that NAC exerts beneficial effects on nutritive muscular blood flow and tissue oxygenation. These effects may possibly be caused by attenuating capillary dysfunction in terms of reopening thrombotically occluded capillaries or inhibiting capillary collapse and progressive microvascular injury secondary to soft tissue trauma. In this context, NAC potentiates inhibitory effects of NO on capillary platelet aggregation [43], thereby possibly reducing intravascular coagulation and microvascular thrombosis and thus restricting secondary tissue damage.

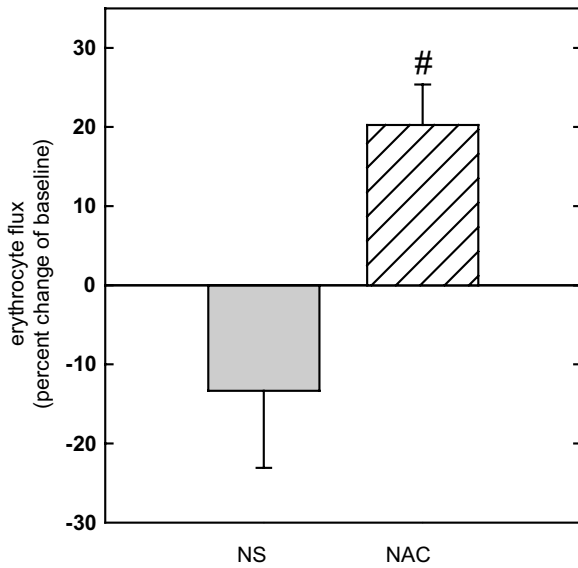


Fig. 7. Erythrocyte flux as measured by Laser-Doppler flowmetry of EDL muscle 1.5 h after trauma and 30 min following treatment with either NS (normal saline,  $n = 7$ , filled bar) or NAC (*N*-acetylcysteine,  $n = 7$ ; hatched bar). Values (mean  $\pm$  SD) are expressed as percentage change of baseline (pre-treatment flux values). Student's *t*-test:  $^{\#}p < 0.05$  vs. NS.

In addition, intravenous administration of *N*-acetylcysteine supplies cysteine to restore depleted levels of the endogenous anti-oxidant GSH which in conjunction with the ability to scavenge hypochlorous acid, hydroxyl and superoxide radicals [2] provides an attractive mechanism by which NAC might protect the structural and functional integrity of endothelial and parenchymal cell membranes. Free-radical initiated tissue damage has been identified as a major causative component in traumatic soft tissue damage [47], compartment syndrome [34] and ischemia/reperfusion injury [13]. In a rat model of free radical donor-induced soft tissue damage to the extremities van der Laan and colleagues demonstrated that NAC substantially reduced vascular permeability of  $^{99m}\text{Tc}$ -IgG and effectively preserved endothelial integrity [48]. Results of the present *in vivo* microscopic study are in line with these findings as a decrease in microvascular permeability following NAC-therapy was observed compared to rats receiving NS. Among other targets, NAC has been shown to successfully reduce oxidative tissue injury resulting from trauma and ischemia induced endothelial lipid peroxidation [2,10,12,14], thereby preserving transcapillary fluid balance and diminishing posttraumatic endothelial dysfunction. Furthermore, NAC exerts a direct anti-inflammatory effect as the neutrophilic chemotaxis and the inflammation-induced oxidative stress is effectively inhibited [18,19] which is reflected by the significantly decreased accumulation, adherence and migration of leukocytes following experimental CSTI. Our results on calculated venular wall shear rates, being comparable between both treatment

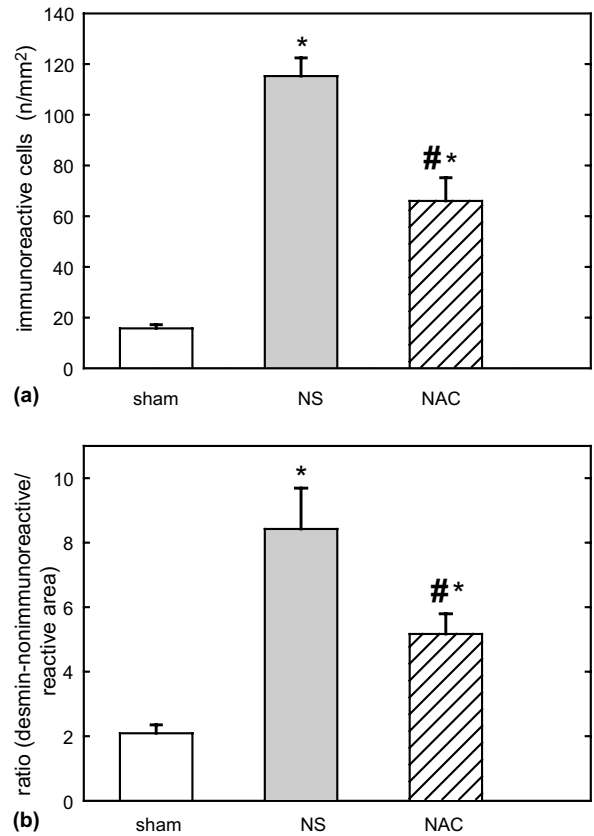


Fig. 8. Changes in neutrophilic granulocyte infiltration and desmin immunoreactivity (skeletal muscle viability) in sham-operated, non-injured animals ( $n = 7$ ; open bar) and after treatment of injured animals with either normal saline (NS,  $n = 7$ ; filled bar) or *N*-acetylcysteine (NAC,  $n = 7$ ; hatched bar) at 2 h post trauma. (a) Number of neutrophilic granulocytes per  $\text{mm}^2$  skeletal muscle area as determined by immunohistochemistry using the rat-specific HIS48 antibody and (b) desmin immunoreactivity as expressed by area measurements of non-immunoreactive vs. immunoreactive skeletal muscle area. Values are means  $\pm$  SD, ANOVA for independent samples followed by post hoc analysis and Bonferroni-correction for multiple comparison procedures:  $^*p < 0.05$  vs. sham,  $^{\#}p < 0.05$  vs. NS.

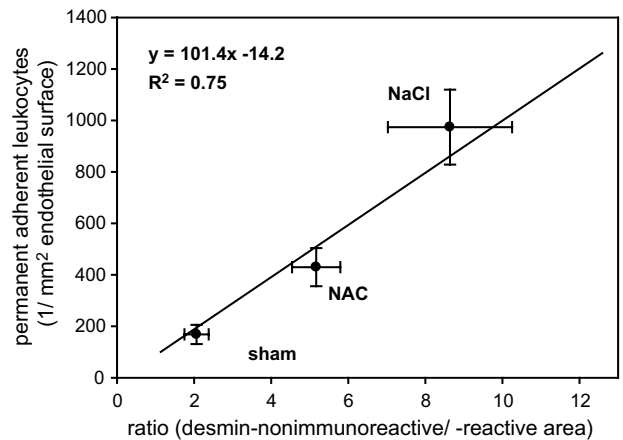


Fig. 9. Regression analysis between permanent microvascular leukocyte adherence and the loss of desmin immunoreactivity for sham-, NS-, and NAC group ( $r^2 = 0.75$ ).

groups argue that NAC-induced decrease in leukocyte adherence and subsequent infiltration into the perivascular space occurs independent from changes in physical forces or microhemodynamic/rheologic characteristics. In this context, we detected a positive functional relationship between extent of microvascular leukocyte adherence and loss of desmin immunoreactivity, supporting the concept of leukocyte-mediated tissue damage. Posttraumatic activation and adherence of leukocytes exert deleterious effects to the endothelium as well as parenchymal tissue by the release of proinflammatory mediators and toxic substances such as lysosomal enzymes, arachidonic acid metabolites and reactive oxygen species. In the present study these adverse effects could be ameliorated by the administration of NAC as both leukocyte infiltration and loss of desmin immunoreactivity, i.e., inflammation-induced myonecrosis were markedly reduced. In this context, NAC has been shown to significantly reduce the expression of adhesion molecules as e.g., ICAM-1 and P-selectin following ischemia/reperfusion injury [1,11,18,19,51] and induce shedding of selectins from the microvascular endothelium [44]. Despite the fact that no intermediate or long-term results are presently available, the NAC-induced decrease in leukocyte adherence and myonecrosis appears to be a promising approach to reduce secondary tissue destruction by neutrophilic leukocytes in the acute phase following severe soft tissue trauma.

Furthermore, NAC is involved in supporting the synthesis of NO by replenishing the sulfhydryl-groups either directly or via increasing cysteine levels [6,17,33]. This idea aroused great interest because it argues that NAC may exert its vasoactive effects by modulating NO-activity at different sites. In particular in skeletal muscle, recent studies have provided important information on a beneficial effect of NAC for the treatment of ischemia/reperfusion injury [8,21,26]. Chen and colleagues were able to demonstrate that infusion of NAC protects the contractile function of EDL muscle from reperfusion injury [8]. They concluded that the protective function of NAC may be related to reversal of microvessel spasm during the reperfusion period and NO-mediated vasodilatation, leading to increased nutritional blood flow to injured skeletal muscle. Although they did observe dosage-dependent effects with less protection at higher doses, other studies have actually found significant benefits using similar high dosages as used in the present study [22,48]. The finding of the present study that NAC treatment was not associated with a significant increase in capillary or venular diameters when compared to sham-operated or NS-treated animals may be due to the fact that intravital microscopy did not reveal a significant posttraumatic microvessel spasm as seen during postischemic reperfusion injury [8]. However, variable susceptibility of cellular targets in conjunction with differences in extent and pattern of microvascular injury

between postischemic reperfusion and closed soft tissue trauma most likely account for the variable capacity of NAC-mediated protection.

More direct support for the concept that NO replacement reduces microvascular dysfunction is provided by the intravital microscopic studies of Kubes et al. [23] who showed that nitric oxide synthetase (NOS)-inhibitors increase leukocyte adherence, protein extravasation and microvascular injury. However, it is also known that protective effects of NAC [8,26] and more importantly NO [9,21] depend on the local concentrations, the type of tissue (skeletal muscle), the site of production and the specific local targets. The observed beneficial effect of NAC administration and the known NAC-mediated NO-replacement in postischemic [8,26] and posttraumatic (this study) disorders suggests that compromised NO release by the dysfunctional endothelium possibly precedes and maintains ongoing microvascular and parenchymal injury, thereby initiating secondary tissue damage in CSTI. Despite neither NO nor its metabolites were measured in the present study, our results seem to indicate that microcirculatory derangements in skeletal muscle caused by CSTI represent a target which is susceptible to both, the anti-oxidant action and NO-donation by NAC.

In conclusion, the significantly reduced serum CK levels in conjunction with less pronounced edema formation and skeletal muscle necrosis following NAC administration could possibly reflect NO-mediated protection of severely traumatized skeletal muscle from further tissue injury. Interventions directed at inhibiting leukocyte-adherence, protecting nutritive blood flow, restricting endothelial disintegration, scavenging radicals and supplementing cellular GSH-precursor pools may allow for increased salvage of traumatized skeletal muscle by reducing the extent of secondary microcirculatory dysfunction. From the clinical perspective, the positive acute effects of NAC administration in terms of inhibiting leukocyte adherence and ameliorating microvascular perfusion need to be investigated in intermediate and long-term studies to determine whether these effects are temporarily limited or will persistently improve the injury-specific outcome. Furthermore, studies aimed at analyzing injury severity and dosage dependency of NAC are warranted. Depending on these results the NAC-treatment of soft tissue trauma may have therapeutic implications aimed at protecting skeletal muscle against trauma-induced microvascular injury.

#### Acknowledgements

This work was supported by grants from the Deutsche Forschungsgemeinschaft (DFG Scha 930/1-1) and the AO-ASIF Foundation, Switzerland.

## References

- [1] Aoki T, Suzuki Y, Nishio K, Suzuki K, Miyata A, Oyamada Y, et al. Effect of antioxidants on hyperoxia-induced ICAM-1 expression in human endothelial cells. *Adv Exp Med Biol* 1997; 411:503–11.
- [2] Aruoma OI, Halliwell B, Hoey BM, Butler J. The antioxidant action of *N*-acetylcysteine: its reaction with hydrogen peroxide, hydroxyl radical, superoxide, and hypochlorous acid. *Free Radic Biol Med* 1989;6:593–7.
- [3] Atheron A, Born GVR. Quantitative investigation of the adhesiveness of circulating polymorphonuclear leukocytes to blood vessel walls. *J Physiol* 1972;222:447–74.
- [4] Bienvenu K, Granger N. Molecular determinants of shear rate-dependent leukocyte adhesion in postcapillary venules. *Am J Physiol* 1993;33:H1504–8.
- [5] Bonner R, Nossal R. Model of Laser-Doppler measurements of blood flow in tissue. *Appl Optics* 1981;20:2097–107.
- [6] Braughler JM. Sulfhydryl group involvement in the modulation of guanosine 3',5'-monophosphate metabolism by nitric oxide, norepinephrine, pyruvate and *t*-butyl hydroperoxide in minced rat lung. *Biochem Pharmacol* 1982;31:3847–51.
- [7] Bulger EM, Maier RV. Antioxidants in critical illness. *Arch Surg* 2001;136:1201–7.
- [8] Chen LE, Seaber AV, Nasser RM, Stamler JS, Urbaniak JR. Effects of *S*-nitroso-*N*-acetylcysteine on contractile function of reperfused skeletal muscle. *Am J Physiol* 1998;274:R822–9.
- [9] Clancy RM, Amin AR, Abramson SB. The role of nitric oxide in inflammation and immunity. *Arthritis Rheum* 1998;41:1141–51.
- [10] Cuzzocrea S, Mazzon E, Costantino G, Serraino I, De Sarro A, Caputi AP. Effects of *N*-acetylcysteine in a rat model of ischemia and reperfusion injury. *Cardiovasc Res* 2000;47:537–48.
- [11] Cuzzocrea S, Mazzon E, Dugo L, Serraino I, Ciccolo A, Centorrino T, et al. Protective effects of *N*-acetylcysteine on lung injury and red blood cell modification induced by carrageenan in the rat. *FASEB J* 2001;15:1187–200.
- [12] Dunne JB, Davenport M, Williams R, Tredger JM. Evidence that *S*-adenosylmethionine and *N*-acetylcysteine reduce injury from sequential cold and warm ischemia in the isolated perfused rat liver. *Transplantation* 1994;57:1161–8.
- [13] Flaherty JT, Weisfeldt ML. Reperfusion injury. *Free Radical Biol Med* 1988;5:409–19.
- [14] Fukuzawa K, Emre S, Senyuz O, Acarli K, Schwartz ME, Miller CM. *N*-acetylcysteine ameliorates reperfusion injury after warm hepatic ischemia. *Transplantation* 1995;59:6–9.
- [15] Hansen ST. Soft-tissue injuries in the lower extremity. In: *Orthopedic trauma protocols*. 1993. p. 381–4.
- [16] Harris AG, Steinbauer M, Leiderer R, Messmer K. Role of leukocyte plugging and edema in skeletal muscle ischemia-reperfusion injury. *Am J Physiol* 1997;273:H989–96.
- [17] Harrison PM, Wendon JA, Gimson AE, Alexander GJ, Williams R. Improvement by acetylcysteine of hemodynamics and oxygen transport in fulminant hepatic failure. *N Engl J Med* 1991;324:1852–7.
- [18] Jensen T, Kharazmi A, Schiotz PO, Nielsen H, Stenvang Pedersen S, Stafanger G, et al. Effect of oral *N*-acetylcysteine administration on human blood neutrophil and monocyte function. *APMIS* 1988;96:62–7.
- [19] Kharazmi A, Nielsen H, Schiotz PO. *N*-acetylcysteine inhibits human neutrophil and monocyte chemotaxis and oxidative metabolism. *Int J Immunopharmacol* 1988;10:39–46.
- [20] Klyszcz T, Junger M, Jung F, Zeintl H. Cap image—a new kind of computer-assisted video image analysis system for dynamic capillary microscopy. *Biomed Tech* 1997;42:168–75.
- [21] Kobczik LR, Bredt DS, Stamler JS. Nitric oxide in skeletal muscle. *Nature* 1994;372:546–8.
- [22] Koeppel TA, Thies JC, Lehmann T, Gebhard MM, Herfarth C, Otto G, et al. Improvement of hepatic microhemodynamics by *N*-acetylcysteine after warm ischemia. *Eur Surg Res* 1996;28: 270–7.
- [23] Kubes P, Suzuki M, Granger D. Nitric oxide: an endogenous modulator of leukocyte adhesion. *Proc Natl Acad Sci USA* 1991;88:4651–5.
- [24] Lefer AM, Lefer DJ. The role of nitric oxide and cell adhesion molecules on the microcirculation in ischaemia-reperfusion. *Cardiovasc Res* 1996;32:743–51.
- [25] Levin LS, Condit DP. Combined injuries—soft tissue management. *Clin Orthop* 1996;327:172–81.
- [26] Liu K, Chen LE, Seaber AV, Urbaniak JR. *S*-nitroso-*N*-acetylcysteine protects skeletal muscle against reperfusion injury. *Microsurgery* 1998;18:299–305.
- [27] Looney SW, Stanley WB. Exploratory repeated measures analysis for two or more groups. *Am Stat* 1989;43:220–5.
- [28] Menger MD, Pelikan S, Steiner D, Messmer K. Microvascular ischemia-reperfusion injury in striated muscle: significance of “reflow paradox”. *Am J Physiol* 1992;263:H1901–6.
- [29] Menger MD, Rucker M, Vollmar B. Capillary dysfunction in striated muscle ischemia/reperfusion: on the mechanisms of capillary “no-reflow”. *Shock* 1997;8:2–7.
- [30] Menger MD, Steiner D, Messmer K. Microvascular ischemia-reperfusion injury in striated muscle: significance of “no reflow”. *Am J Physiol* 1992;263:H1892–900.
- [31] Menth-Chiari WA, Curl WW, Rosenrance E, Smith TL. Contusion of skeletal muscle increases leukocyte-endothelial cell interactions: an intravital microscopic study in rats. *J Trauma* 1998;45: 709–14.
- [32] Mitchell D, Tyml K. Nitric oxide release in rat skeletal muscle capillary. *Am J Physiol* 1996;270:H1696–703.
- [33] Myers PR, Minor Jr RL, Guerra Jr R, Bates JN, Harrison DG. Vasorelaxant properties of the endothelium-derived relaxing factor more closely resemble *S*-nitrosocysteine than nitric oxide. *Nature* 1990;345:161–3.
- [34] Perler BA, Tohmeh AG, Bulkeley GB. Inhibition of the compartment syndrome by the ablation of free radical-mediated reperfusion injury. *Surgery* 1990;108:40–7.
- [35] Rantanen J, Hurme T, Lukka R, Heino J, Kalimo H. Satellite cell proliferation and the expression of myogenin and desmin in regenerating skeletal muscle: evidence for two different populations of satellite cells. *Lab Invest* 1995;72:341–7.
- [36] Reed MWR, Miller FN. Importance of light dose in fluorescent microscopy. *Microvasc Res* 1988;36:104–7.
- [37] Reynard K, Riley A, Walker BE. Respiratory arrest after *N*-acetylcysteine for paracetamol overdose. *Lancet* 1992;340: 675.
- [38] Rubinstein I, Abassi Z, Coleman R, Winaver J, Better OS. Involvement of nitric oxide system in experimental muscle crush injury. *J Clin Invest* 1998;101:1325–33.
- [39] Ruffmann R, Wendel A. GSH rescue by *N*-acetylcysteine. *Klin Wochenschr* 1991;69:857–62.
- [40] Saetzler RK, Jallo J, Lehr HA, Philips CM, Vasthare U, Arfors KE, et al. Intravital fluorescence microscopy: impact of light-induced phototoxicity on adhesion of fluorescently labeled leukocytes. *J Histochem Cytochem* 1997;45:505–13.
- [41] Schaser K, Vollmar B, Kroppenstedt S, Schewier L, Raschke M, Menger MD, et al. In vivo analysis of microcirculation following closed soft tissue injury. *J Orthop Res* 1999;17:678–85.
- [42] Smith TL, Curl WW, Smith BP, Holden MB, Wise T, Marr A, et al. New skeletal muscle model for the longitudinal study of alterations in microcirculation following contusion and cryotherapy. *Microsurgery* 1993;14:487–93.
- [43] Stamler J, Mendelsohn ME, Amarante P, Smick D, Andon N, Davies PF, et al. *N*-acetylcysteine potentiates platelet inhibition by endothelium-derived relaxing factor. *Circ Res* 1989;65:789–95.

- [44] Taut FJ, Schmidt H, Zapletal CM, Thies JC, Grube C, Motsch J, et al. *N*-acetylcysteine induces shedding of selectins from liver and intestine during orthotopic liver transplantation. *Clin Exp Immunol* 2001;124:337–41.
- [45] Tscherne H, Oestern HJ. [A new classification of soft-tissue damage in open and closed fractures (author's transl.).] *Unfallheilkunde* 1982;85:111–5.
- [46] Tysl K, Budreau CH. A new preparation of rat extensor digitorum longus muscle for intravital investigation of the microcirculation. *Int J Microcirc Clin Exp* 1991;10:335–43.
- [47] van der Laan L, Kapitein PJ, Oyen WJ, Verhofstad AA, Hendriks T, Goris RJ. A novel animal model to evaluate oxygen derived free radical damage in soft tissue. *Free Radic Res* 1997;26:363–72.
- [48] van der Laan L, Oyen WJ, Verhofstad AA, Tan EC, ter Laak HJ, Gabreels Festen A, et al. Soft tissue repair capacity after oxygen-derived free radical-induced damage in one hindlimb of the rat. *J Surg Res* 1997;72:60–9.
- [49] van der Vusse GJ, van Bilsen M, Reneman RS. Ischemia and reperfusion induced alterations in membrane phospholipids: an overview. *Ann NY Acad Sci* 1994;723:1–14.
- [50] Villringer A, Dirnagel U, Them A, Shurer L, Krombach F, Einhüpl KM. Imaging of leukocytes within the rat brain cortex in vivo. *Microvasc Res* 1991;42:305–15.
- [51] Weigand MA, Plachky J, Thies JC, Spies Martin D, Otto G, Martin E, et al. *N*-acetylcysteine attenuates the increase in alpha-glutathione *S*-transferase and circulating ICAM-1 and VCAM-1 after reperfusion in humans undergoing liver transplantation. *Transplantation* 2001;72:694–8.
- [52] Zeintl H, Sack FU, Intaglietta M, Messmer K. Computer assisted leukocyte adhesion measurement in intravital microscopy. *Int J Microcirc Clin Exp* 1989;8:293–302.

### **3.2.4 Reduktion der lokalen Mikrozirkulationsstörung und Entzündungsreaktion nach geschlossenem Weichteiltrauma durch selektive Cyclooxygenase (COX)-2 Hemmung**

Obgleich die begleitende Pharmakotherapie von Weichteilverletzungen mit nicht-steroidalen anti-inflammatorischen Substanzen bereits klinischer Standard ist (14), liegen bislang keine Kenntnisse über die Quantität und Kinetik der COX-2-Expression im Skelettmuskel nach geschlossenem Weichteiltrauma vor. Ferner sind außer der bekannten Inhibition des COX-Systems (12) die spezifischen Effekte dieser Medikamente auf die mikrovaskuläre Perfusion und Endothelfunktion im traumatisierten Muskel unbekannt.

Die nachfolgenden Studien dienten dazu, das Ausmaß und den zeitlichen Verlauf der COX-1- und -2-Expression im Skelettmuskel der Ratte nach standardisiertem geschlossenem Weichteiltrauma zu analysieren.

Spezifische Western-Blot-Analysen und immunhistochemische Untersuchungen demonstrierten eine vorübergehende Zunahme der Expression von COX-1 und -2 mit Spitzenwerten bei 8-12h. Bereits nach 18h post Trauma war die Expression sowohl für COX-1 als auch -2, unabhängig von der vor oder nach Trauma begonnenen Therapie mit dem COX-2-Inhibitor Parecoxib (166), auf das Niveau unverletzter Kontrolltiere zurückgegangen. Zusätzlich war sowohl die vor als auch die nach dem Trauma durchgeführte Gabe von Parecoxib mit einer signifikanten Begrenzung der nach Weichteiltrauma zunehmenden kapillären Dysfunktion und posttraumatischen Entzündungsreaktion (Leukozyten-Endothelzell-Interaktion) assoziiert.

Diese Daten deuten auf eine kausale Bedeutung des Cyclooxygenasesystems in der Pathogenese des Sekundärschadens nach traumatischer Weichteilverletzung hin. Darüber hinaus erweitern diese Resultate die bisherigen Kenntnisse über die Wirkmechanismen von COX-2-Inhibitoren hinsichtlich ihrer therapeutisch relevanten protektiven Effekte auf die posttraumatisch gestörte Mikrozirkulation und Leukozytenaktivierung.

# SELECTIVE CYCLOOXYGENASE-2 INHIBITION REVERSES MICROCIRCULATORY AND INFLAMMATORY SEQUELAE OF CLOSED SOFT-TISSUE TRAUMA IN AN ANIMAL MODEL

BY PHILIP GIERER, MD, THOMAS MITTLMEIER, MD, REINGART BORDEL,  
KLAUS-DIETER SCHASER, MD, GEORG GRADL, MD, AND BRIGITTE VOLLMAR, MD

*Investigation performed at the Department of Experimental Surgery, University of Rostock, Rostock, Germany*

**Background:** Despite the common use of nonsteroidal anti-inflammatory drugs in the treatment of closed soft-tissue injuries, our understanding of the effect of these medications on tissue healing is incomplete. Using high-resolution multicolor fluorescence microscopy, we investigated the efficiency of preinjury and postinjury treatment with the selective cyclooxygenase (COX)-2 inhibitor parecoxib to improve compromised perfusion of traumatized muscle tissue and to minimize secondary tissue damage.

**Methods:** With use of a pneumatically driven and computer-controlled impact device, closed soft-tissue trauma of the left hindlimb was induced in anesthetized rats that had had intravenous administration of 10 mg/kg of either parecoxib sodium (seven rats) or an equal volume of saline solution (seven rats). Seven additional animals received parecoxib two hours after the trauma, and seven animals without trauma served as controls.

**Results:** Time-course studies with use of both Western blot protein analysis and immunohistochemistry demonstrated a transient upregulation of COX-2 protein expression with peak levels eight to twelve hours after trauma and a return to near baseline level at eighteen hours. Regardless of whether parecoxib was administered before or after the injury, it completely restored microcirculatory impairment within the injured muscle. This was indicated by the mean values (and standard error of the mean) for nutritive perfusion ( $434 \pm 15$  cm/cm<sup>2</sup> in animals treated before the injury and  $399 \pm 8$  cm/cm<sup>2</sup> in those treated after injury), nicotinamide adenine dinucleotide (NADH) levels ( $73 \pm 2$  aU and  $74 \pm 1$  aU, respectively), and inflammatory cell interaction ( $184 \pm 36$  and  $186 \pm 32$  n/mm<sup>2</sup>, respectively, for leukocytes, and  $1.0 \pm 0.1$  and  $0.8 \pm 0.1$  n/mm<sup>2</sup>, respectively, for platelets) at eighteen hours after trauma, which were not different from those found in noninjured muscle tissue of controls. In contrast, skeletal muscle in saline solution-treated animals revealed persistent perfusion failure ( $296 \pm 30$  cm/cm<sup>2</sup>) with tissue hypoxia (NADH,  $100 \pm 4$  aU), and enhanced endothelial interaction of both leukocytes ( $854 \pm 73$  mm<sup>-2</sup>) and platelets ( $2.3 \pm 0.5$  n/mm<sup>2</sup>) at eighteen hours after trauma.

**Conclusions and Clinical Relevance:** Treatment of skeletal muscle soft-tissue trauma with parecoxib before as well as after injury is highly effective in restoring disturbed microcirculation. Moreover, a reduced inflammatory cell response helps to prevent leukocyte or platelet-dependent secondary tissue injury. These results deserve further investigation to prove that selective COX-2 inhibitors improve performance and promote healing following closed soft-tissue injury.

Closed or open soft-tissue injury is an almost invariable consequence of musculoskeletal trauma. The severity of soft-tissue trauma is one of the most decisive prognostic determinants of the outcome of complex injury to the extremities. Due to the high frequency of high-velocity or high-energy trauma and sports-related injuries, the prevalence of severe soft-tissue trauma continues to increase. Apart from temporary immobilization and local cryotherapy, the admin-

istration of nonsteroidal anti-inflammatory drugs has become a therapeutic standard in the acute routine treatment of soft-tissue injuries<sup>1-3</sup>. The ability of nonsteroidal anti-inflammatory drugs to reduce inflammation and pain is based on the inhibition of prostaglandin synthesis by cyclooxygenase (COX)<sup>4</sup>, which is present in at least two isoforms<sup>5</sup>. COX-1 is a predominantly constitutive form and is involved in cellular homeostasis with maintenance of tissue physiology, whereas

COX-2 is a rapidly inducible isoform upregulated by reactive oxygen species, inflammatory cytokines, and mitogens<sup>6</sup>. To date, the function of COX-2 has been primarily linked to inflammatory processes, whereas the expression of COX-1 appears to be more confined to physiological functions. In this context, the use of specific COX-2 inhibitors may provide the advantage of selectively targeting inflammatory processes without disturbing tissue homeostasis.

In contrast to what is known about conventional anti-inflammatory medications<sup>1,7,8</sup>, our understanding of the effects of COX-2 inhibitors on the musculoskeletal tissues is incomplete. A normal inflammatory response might be a prerequisite for adequate healing, so it is possible that suppression of inflammation by COX-2 inhibitors might adversely affect soft-tissue healing, as has been described for ligament injuries and fractures<sup>9,10</sup>. Thus, the aim of our study was to determine whether preinjury and postinjury administration of the selective COX-2 inhibitor parecoxib, which is the water-soluble prodrug for intravenous application of valdecoxib and currently one of the most selective COX-2 inhibitors<sup>11</sup>, is indeed of therapeutic benefit in a model of closed soft-tissue injury.

## Materials and Methods

### Animal Model

The experimental protocol was approved by the local animal rights protection authorities and followed the National Institutes of Health guidelines for the care and use of laboratory animals. Male Sprague-Dawley rats (250 to 300 g) were anesthetized with an intraperitoneal injection of 55 mg/kg of 6% pentobarbital sodium (Narcoren; Merial, Hallbergmoos, Germany). Immediately prior to the injury, the animals received either 10 mg/kg of parecoxib sodium (Dynastat; Pharmacia GmbH, Erlangen) (the parecoxib-0h group) or an equal volume (0.5 mL) of saline solution (the saline group) intravenously by the caudal vein. In an additional series of animals, 10 mg/kg of parecoxib was administered intravenously two hours after the injury (the parecoxib-2h group). Anesthetized animals that did not receive soft-tissue trauma or therapy served as a time-matched control group (the sham group). According to the analysis establishing the number of replications needed to detect a given true difference between means<sup>12</sup>, a total of seven animals was included in each experimental group.

By means of a pneumatically driven and computer-controlled impact device, a standardized soft-tissue injury was induced on the lateral compartment of the left hindlimb, simulating high-velocity trauma of the lower extremity. The nature and kinetics of tissue injury with use of this impact device have been described by our group in detail previously<sup>13</sup>. The controlled-impact technique was initially developed as a model of standardized traumatic brain injury in rats, reproducing the pathophysiological and morphological responses of severe closed-head injury found in humans<sup>14,15</sup>. The controlled-impact device consists of a compressed nitrogen gas source, an adjustable impactor, a displacement transducer, and a personal computer-assisted interface for data transmis-

sion and analysis of time-displacement parameters of the impact. The impact parameters that we selected were an impact velocity of 7 m/s, a deformation depth of 11 mm, and an impact duration of 100 ms with an impactor diameter of 10 mm. The left hindlimb was placed in a plastic mold (Technovit; Kulzer, Wertheim, Germany) shaped like the hindlimb to guarantee optimal energy transmission to the tissue by avoiding hindlimb movement during the impact.

At eighteen hours after trauma induction, the animals were anesthetized again and placed on a heating pad to maintain body temperature at 37°C. Following a tracheotomy, the animals were mechanically ventilated (tidal volume of 1 mL/100 g of body weight and fifty breaths per minute). Catheters (PE-50; Portex, Hythe, Kent, United Kingdom) were placed in the right carotid artery and the left jugular vein for continuous monitoring of central hemodynamics (Sirecust; Siemens, Erlangen, Germany).

The left extensor digitorum longus muscle was microsurgically prepared to allow direct access for in vivo high-resolution multicolor fluorescence microscopy. The preparation technique was first described by Tysl and Budreau<sup>16</sup> and was modified for in vivo microscopy by our group<sup>13</sup>. During preparation, tissues were superfused with 37°C warm physiological saline solution to prevent drying. After final exposure of the extensor digitorum longus muscle, the tissue was covered with a cover glass.

After obtaining baseline recordings (the inclusion criteria included a mean arterial blood pressure of 100 to 110 mm Hg, a hematocrit of 45% to 50%, a pCO<sub>2</sub> of 35 to 40 mm Hg, and a pH of 7.35 to 7.45) and a twenty-minute stabilization period after completion of the exposure, in vivo microscopy of the extensor digitorum longus muscle was performed. At the end of the experiments, the animals were killed by exsanguination. Muscle tissue was sampled for Western blot protein analysis, histology, and immunohistochemistry.

### Platelet Preparation

Resting platelets were isolated with use of the Sepharose column as described previously<sup>17</sup>. Blood was drawn from healthy human volunteers (twenty-five to forty years old) without history of disease or anticoagulant therapy, after they had provided informed consent. After centrifugation, platelet-rich plasma was layered on a prepared Sepharose column (Amersham Pharmacia Biotech, Uppsala, Sweden). Isolated platelets were stained with 2',7'-bis(2-carboxyethyl)-5-(and-6)-carboxy-fluorescein acetoxymethyl ester (BCECF; Molecular Probes, Eugene, Oregon), passed again through the Sepharose column, and were diluted in phosphate-buffered saline solution to a final concentration of  $1 \times 10^8$  cells mL<sup>-1</sup>. Previous work in rodent models has shown that there is no difference in the use of human platelets when compared with syngeneic platelets<sup>17</sup>.

### In Vivo Fluorescence Microscopy

After intravenous injection of fluorescein-isothiocyanate (FITC)-labeled dextran (15 mg/kg of body weight) (Sigma, Deisenhofen, Germany) and rhodamine 6G (0.15 mg/kg of body weight) (Sigma), in vivo microscopy was performed with use of a mi-



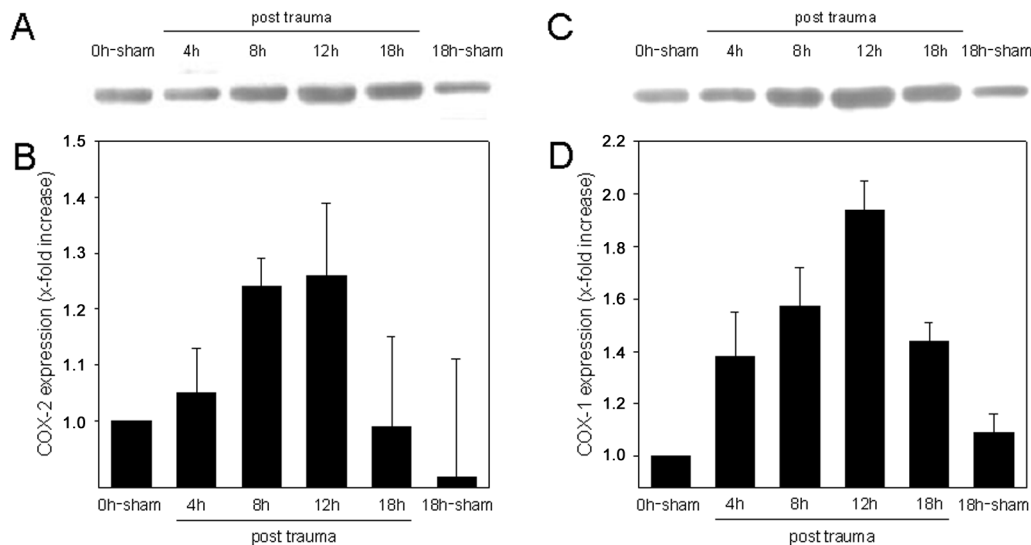


**Fig. 1**  
Representative Western blots (A and C) and densitometric analysis of cyclooxygenase (COX)-2 and COX-1 protein expression (B and D) in skeletal muscle tissue of animals prior to trauma (0h-sham) as well as at four, eight, twelve, and eighteen hours after closed soft-tissue injury. 18h-sham indicates time-matched control animals without trauma. The values are given as the mean and the standard error of the mean, and five animals per time-point were analyzed.

roscope (E600-FN; Nikon, Tokyo, Japan) equipped with a 100-W mercury lamp and filter sets for blue (excitation of 465 to 495 nm and emission of >505 nm), green (510 to 560 nm and >575 nm, respectively), and ultraviolet (340 to 380 nm and >400 nm, respectively) epi-illumination. BCECF-stained platelets were injected intra-arterially ( $1 \times 10^8$  platelets per time-point over thirty seconds) and were allowed a period of 120 seconds to recirculate until the analysis of their intravascular adhesion with use of blue light epi-illumination<sup>17</sup>. With a physiological platelet concentration in rats of approximately  $600 \times 10^3$  platelets/ $\mu$ L in whole blood and a total blood volume of 8 mL/100 g of body weight<sup>18</sup>, the labeled fraction was about 1% of all circulating platelets. By use of water-immersion objectives (Nikon) at  $\times 20/0.75$  W and  $\times 40/0.80$  W, final magnifications of 306 and 630 times were achieved. Images were recorded by means of a charge-coupled video camera (FK 6990-IQ-S; Pieper, Schwerte, Germany) and transferred to a Super-VHS video system for subsequent off-line analysis.

#### Microcirculatory Analysis

For quantitative off-line analysis, a computer-assisted microcirculation image-analysis system (version 7.4, CapImage; Zeintl, Heidelberg, Germany) was used. As previously described<sup>13,19,20</sup>, functional capillary density was defined as the total length of red blood-cell-perfused capillaries per observation area in  $\text{cm}/\text{cm}^2$ . To assess leukocyte-endothelial cell interaction in postcapillary venules, flow behavior of leukocytes was analyzed with respect to free floating, rolling, and adherent leukocytes. Rolling leukocytes were defined as those cells moving along the vessel wall at a velocity of <40% of that of leukocytes at the centerline and were expressed as a percentage of the total leukocyte flux.

Venular leukocyte adherence was defined as the number of leukocytes not moving or detaching from the endothelial lining of the venule wall during an observation period of twenty seconds. Assuming cylindrical microvessel geometry, leukocyte adherence was expressed as nonmoving cells per endothelial surface ( $\text{n}/\text{mm}^2$ ), calculated from the diameter and length of the vessel segment analyzed. In postcapillary venules, centerline red blood-cell velocity was determined with use of the line-shift method (CapImage). Platelet adhesion was analyzed within ten observation fields of skeletal muscle tissue and was given as the number of adherent thrombocytes per square millimeter. Reduced nicotinamide adenine dinucleotide (NADH) fluorescence of skeletal muscle tissue was densitometrically assessed after two seconds of ultraviolet epi-illumination by computer-assisted gray-level determination<sup>21</sup>. To avoid interference of gray levels with microvascular structures, analysis was strictly limited to the intercapillary space.

#### Laboratory Analysis

Arterial blood samples were withdrawn for analysis of blood gases (Rapidlab 348; Bayer Vital, Fernwald, Germany) and blood cell count with use of a Coulter Counter (AcTdiff; Coulter, Hamburg, Germany).

#### Western Blot Analysis

For Western blot analysis of COX isoforms, traumatized extensor digitorum longus muscle tissue was homogenized in lysis buffer (10 mM Tris, pH 7.5, 10 mM NaCl, 0.1 mM EDTA, 0.5% Triton-X 100, 0.02%  $\text{NaN}_3$ , and 0.2 mM phenylmethylsulphonylfluoride (PMSF); prior to use, the buffer received a protease inhibitor cocktail [1:100 v/v; Sigma]), incubated for thirty min-

utes on ice and centrifuged for fifteen minutes at 10 g. The soluble whole protein fraction was saved for subsequent analysis. Protein concentrations were determined with use of the bicinchoninic acid (BCA) protein assay (Sigma) with bovine serum albumin as a standard. Twenty micrograms of protein per lane were separated discontinuously on sodium dodecyl sulfate polyacrylamide gels (12%) and were transferred to a polyvinylidene difluoride membrane (Immobilon-P; Millipore, Eschborn, Germany). After blockade of nonspecific binding sites, membranes were incubated for two hours at room temperature with goat polyclonal anti-COX-1 and goat polyclonal anti-COX-2 antibodies (each 1:200; Santa Cruz Biotechnology, Heidelberg, Germany) followed by peroxidase-conjugated donkey polyclonal anti-goat IgG (1:40000; Santa Cruz Biotechnology) as a secondary antibody. Ponceau-S staining of membranes served to check for equal loading of lanes.

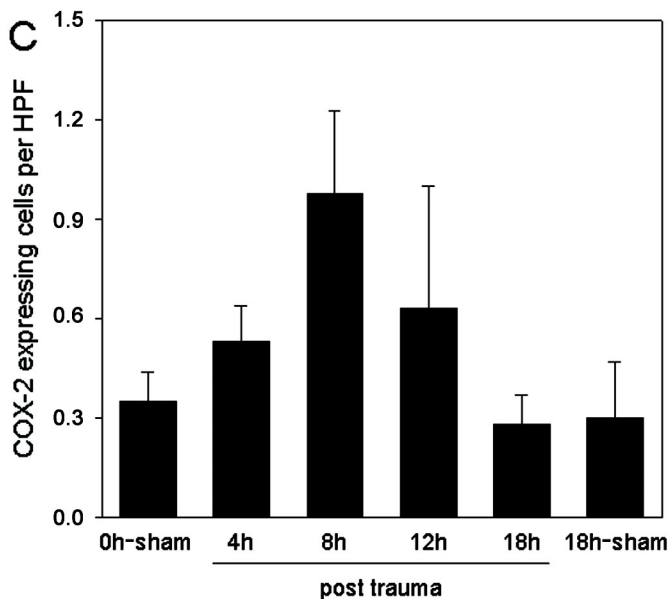
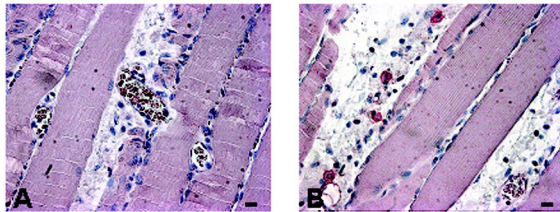


Fig. 2  
Immunohistochemical staining of cyclooxygenase (COX)-2 expression in skeletal muscle tissue without trauma (A) and at eight hours after closed soft-tissue injury (B). Note the COX-2 positive cells located in the perivascular connective tissue of injured muscle, while noninjured muscle shows minimal, if any, cellular immunoreactivity for COX-2. Scale bars represent 15  $\mu$ m. The bar graph (C) displays quantitative analysis of COX-2-expressing cells per high power field (HPF) in extensor digitorum longus muscle during the eighteen-hour time-period after trauma (four animals per time-point). The values are given as the mean and the standard error of the mean.

Protein expression was visualized by means of luminol-enhanced chemiluminescence (ECL Plus; Amersham Pharmacia Biotech, Freiburg, Germany) and exposure of the membrane to a blue light-sensitive autoradiography film (Kodak BioMax Light Film; Kodak Industrie, Chalon-sur-Saone, France). Signals were assessed densitometrically (Gel-Dokumentations-Systeme E.A.S.Y. Win32; Herolab GmbH, Wiesloch, Germany).

COX-1 and COX-2 protein expression was assessed in the two parecoxib groups and the saline-solution group at eighteen hours after trauma induction, and it was assessed at eighteen hours in the sham-treated animals of the control group. The kinetics of COX-1 and COX-2 expression were investigated with use of protein extraction from extensor digitorum longus tissue obtained from additional animals (five animals per time-point) that were killed at four, eight, twelve, and eighteen hours after the induction of trauma. Extensor digitorum longus muscle from animals without induction of trauma was harvested at either zero hours (the 0h-sham group) or eighteen hours (the 18h-sham group) and served as control tissue.

#### *Histology and Immunohistochemistry*

At the end of each experiment (eighteen hours after trauma), extensor digitorum longus muscle tissue was fixed in 4% phosphate-buffered formalin for two to three days and was then embedded in paraffin. From the paraffin-embedded tissue blocks, 4- $\mu$ m sections were cut and stained with hematoxylin-eosin for histological analysis. To assess the temporal profile of trauma-associated COX-2 expression, immunohistochemistry was performed in extensor digitorum longus muscle tissue of additional animals (four animals per time-point), which were killed at four, eight, twelve, and eighteen hours after trauma. Extensor digitorum longus muscle tissue from animals without trauma induction was harvested at either zero hours (the 0h-sham group) or eighteen hours (the 18h-sham group). COX-2 was detected by means of a goat polyclonal anti-COX-2 antibody (1:1000; Santa Cruz Biotechnology), followed by a donkey polyclonal anti-goat antibody (Santa Cruz Biotechnology) and counterstained with new fuchsin (Fuchsin Substrate-Chromogen System; Dako, Carpinteria, California) and haemalaun. Quantitative analysis was performed by counting the number of COX-2 positive cells in fifty consecutive high-power fields (400 times magnification).

#### *Statistical Analysis*

The results were given as the mean and the standard error of the mean. After proving the assumption of normality, comparisons between the experimental groups were performed by one-way analysis of variance, followed by the appropriate post hoc multiple comparison procedure, including Bonferroni correction (SigmaStat; Jandel, San Rafael, California). To assess the correlations between different microcirculatory parameters, Pearson product moment correlation analysis was used. Significance was set at  $p < 0.05$ .

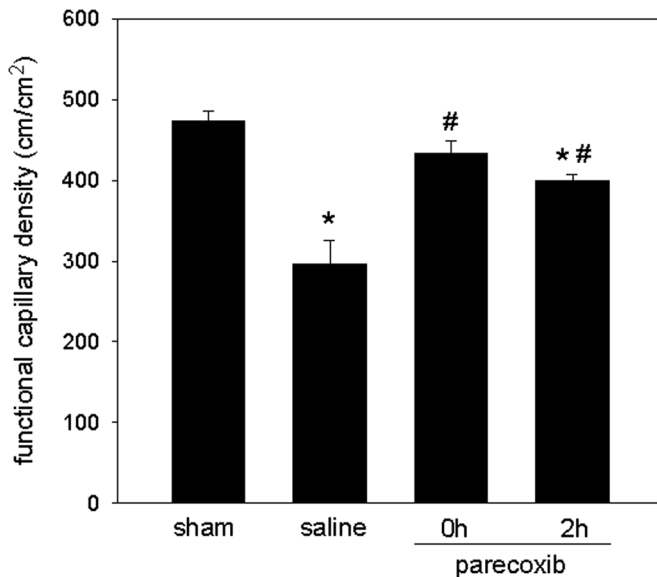


Fig. 3  
Functional capillary density of skeletal muscle tissue at eighteen hours after soft-tissue trauma and treatment with saline solution (seven animals) or parecoxib (fourteen animals). Parecoxib was applied either directly prior to trauma (parecoxib-0h) in seven animals or at two hours after trauma (parecoxib-2h) in seven animals. Seven animals without trauma served as controls (sham). The values are given as the mean and the standard error of the mean. The asterisk indicates a significant difference compared with the sham group ( $p < 0.05$ ). The pound sign indicates a significant difference compared with the saline solution-treated animals ( $p < 0.05$ ).

## Results

### Western Blot Analysis of COX-1 and COX-2 Expression in Skeletal Muscle Tissue

As illustrated by Western blot analysis of rat skeletal muscle tissue, controlled impact device-induced closed soft-tissue injury caused a transient increase in COX-2 protein expression with peak levels at eight hours and twelve hours after trauma induction, followed by a recovery to almost control levels at eighteen hours (Fig. 1, A and B). In line with this, animals assessed at eighteen hours after trauma did not differ with respect to COX-2 expression compared with sham-operated control animals regardless of being given saline solution or parecoxib before or after the injury (data not shown). Trauma induction was not only accompanied by an upregulation of the inducible isoform but also caused a pattern of COX-1 protein expression comparable with that seen for COX-2 protein (Fig. 1, C and D).

### COX-2 Immunohistochemistry of Skeletal Muscle Tissue

In parallel with the kinetics of COX-2 protein expression, cells in the perivascular connective tissue of injured muscle showed marked immunoreactivity for COX-2 (Fig. 2, A and B). Quantitative analysis of COX-2-expressing cells revealed an increase from four to twelve hours after trauma, with a threefold in-

crease at eight hours (Fig. 2, C), decreasing to essentially baseline at eighteen hours.

### Systemic Hemodynamics

Animals in the four experimental groups did not differ with respect to mean blood pressure or heart rate (see Appendix). Moreover, no differences were detected in hemoglobin, hematocrit, leukocyte count, and electrolytes among the groups. Of interest is the observation that animals treated with saline solution revealed a marked thrombocytopenia compared with those treated with parecoxib and those in the sham group (see Appendix).

### Microvascular Perfusion in Closed Soft-Tissue Injury

Closed soft-tissue trauma caused a substantial impairment in nutritive capillary perfusion, with mean value (and standard error of the mean) of  $296 \pm 30$  cm/cm<sup>2</sup>, whereas treatment with parecoxib, even when applied two hours after trauma, restored nutritive capillary perfusion up to almost physiological baseline values,  $474 \pm 11$  cm/cm<sup>2</sup> for the sham group,  $434 \pm 15$  cm/cm<sup>2</sup> for the parecoxib-0h group, and  $399 \pm 8$  cm/cm<sup>2</sup> for the parecoxib-2h group, as observed in the sham control animals (Fig. 3). In line with nutritive perfusion failure, high NADH autofluorescence of skeletal muscle tissue was observed after closed soft-tissue injury in saline solution-treated

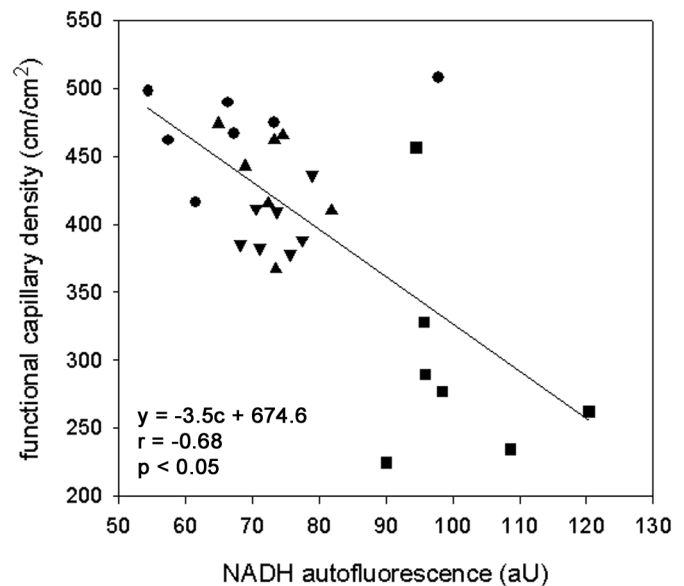


Fig. 4  
Pearson product-moment correlation analysis between values of functional capillary density and nicotinamide adenine dinucleotide (NADH) autofluorescence of skeletal muscle tissue at eighteen hours after trauma and treatment with saline solution (squares) in seven animals or parecoxib in fourteen animals. Parecoxib was applied either directly prior to trauma (triangles facing up) in seven animals or at two hours after trauma (triangles facing down) in seven animals. Seven sham control animals without trauma (circles) served as controls.  $r =$  regression coefficient.

**TABLE I Results of Intravital Fluorescence Microscopy with Assessment of Leukocyte and Thrombocyte Flow Behavior within Postcapillary Venules\***

	Sham	Saline Solution	Parecoxib-0h	Parecoxib-2h
Leukocyte rolling (%)	15 ± 3	47 ± 5†	19 ± 3‡	14 ± 2‡
Leukocyte adherence (n/mm <sup>2</sup> )	100 ± 20	854 ± 73†	184 ± 36‡	186 ± 32‡
Thrombocyte adherence (n/mm <sup>2</sup> )	0.8 ± 0.2	2.3 ± 0.5†	1.0 ± 0.1	0.8 ± 0.1‡

\*The values are given as the mean and the standard error of the mean. Intravital fluorescence microscopy with assessment of leukocyte and thrombocyte flow behavior within postcapillary venules was performed at eighteen hours after soft-tissue trauma and treatment with saline solution (seven animals) or parecoxib (fourteen animals). Parecoxib was applied either directly prior to trauma (parecoxib-0h; seven animals) or at two hours after trauma (parecoxib-2h; seven animals). Seven animals without trauma served as controls (sham). †Compared with the sham group, the difference was significant ( $p < 0.05$ ). ‡Compared with the saline solution-treated animals, the difference was significant ( $p < 0.05$ ).

animals, indicating pronounced tissue hypoxia (mean,  $100 \pm 4$  aU compared with  $68 \pm 5$  aU for the sham group). In contrast, animals treated with parecoxib exhibited a marked reduction of tissue NADH ( $73 \pm 2$  aU for the parecoxib-0h group and  $74 \pm 1$  aU for the parecoxib-2h group), which is in line with the concomitant improvement in capillary perfusion. Regression analysis revealed a significant inverse correlation between functional capillary density and NADH autofluorescence of skeletal muscle tissue with a regression coefficient of  $r = -0.68$  ( $p < 0.05$ ) (Fig. 4).

Capillaries were found to be significantly widened in traumatized skeletal muscle (mean,  $5.7 \pm 0.2$   $\mu\text{m}$ ) compared with nontraumatized sham controls (mean,  $4.8 \pm 0.1$   $\mu\text{m}$ ) ( $p < 0.05$ ). Capillary diameter was reduced to a mean of  $5.2 \pm 0.2$   $\mu\text{m}$  in the animals that received parecoxib prior to trauma. Parecoxib given after the injury was capable of completely restoring capillary diameter (mean,  $4.9 \pm 0.1$   $\mu\text{m}$  in the parecoxib-2h group compared with a mean of  $5.7 \pm 0.2$   $\mu\text{m}$  in the saline-solution group;  $p < 0.05$ ). Venular red blood-cell velocity was slightly decreased in the saline-solution-treated animals and the parecoxib-treated animals, but it was not significantly different from that in the sham control animals (data not shown) (analysis of variance,  $p = 0.11$ ).

#### *Inflammatory Cell Response in Closed Soft-Tissue Injury*

Soft-tissue trauma was characterized by an inflammatory cell response with significant ( $p < 0.05$ ) increases in leukocytes, both rolling along (threefold) and firmly attaching to the venular endothelium (eightfold). Parecoxib, given either prior to trauma or two hours after injury, effectively limited the inflammatory response with low numbers of leukocytes interacting with the venular endothelium, which was comparable with the numbers observed in sham control animals (Table I).

Following trauma, the saline solution-treated animals revealed enhanced intravascular thrombocyte accumulation, which was absent in the animals treated with parecoxib before or after injury (Table I). Intramuscular accumulation of leukocytes was significantly ( $p < 0.001$ ) correlated with that of thrombocytes ( $r = 0.62$ ).

#### **Discussion**

These results show that both preinjury and postinjury application of the selective COX-2 inhibitor parecoxib is effective in treating trauma-induced microcirculatory disturbances with almost complete restoration to normal by eighteen hours after the trauma in this animal model. These observations, together with the upregulation of COX-2 protein expression after skeletal muscle trauma, suggest a role for COX-2 in the response to soft-tissue injury.

#### *Closed Soft-Tissue Injury*

This model of closed soft-tissue injury mimics the characteristics observed clinically in patients experiencing high-energy trauma and demonstrates a marked decrease in capillary perfusion as well as a marked increase in leukocyte-endothelial cell interaction and microvascular permeability<sup>13</sup>. Besides direct tissue destruction caused by the impact itself, tissue damage results from traumatically induced inflammatory reactions, with tissue hypoxia being the most likely trigger. In line with this, injured muscle revealed a marked increase in tissue NADH autofluorescence, indicating pronounced tissue hypoxia. In general, the interruption of oxidative phosphorylation due to an inadequate oxygen supply is reflected by an increase in NADH levels<sup>22</sup>. NADH fluorimetry allows noninvasive investigation of organ metabolism, reflecting alterations in oxidative phosphorylation<sup>23</sup>. So far, enhanced NADH fluorescence caused by hypoxia has been monitored in rat liver tissue in vivo upon posts ischemic reperfusion and hemorrhagic shock<sup>21,24</sup>. We now demonstrate the strong inverse correlation between capillary perfusion and NADH fluorescence within traumatized skeletal muscle tissue. The insufficient oxygen supply can be attributed mainly to trauma-induced perfusion shutdown of individual capillaries, but it may in addition be due to capillary vasomotor dysfunction<sup>25</sup>, as indicated in the present study by extreme dilatation of these microvascular segments. Although the mechanisms of capillary diameter control in skeletal muscle tissue are incompletely known, it is reasonable to speculate that pericytes, endothelial cells, and the endothelin-nitric oxide system also control vascular diameter in muscular tissue, as has been shown for hepatic and pancreatic tissue<sup>26,27</sup>.

The results of this study extend our previous obser-

vations by demonstrating that injured muscle shows both leukocytic and thrombocytic sequestration. In this study, intraorgan thrombocyte accumulation after injury was severe enough to be associated with systemic thrombocytopenia. It has been reported that peripheral soft-tissue trauma causes massive intrapulmonary trapping of thrombocytes<sup>28,29</sup>, but, to our knowledge, sequestration of platelets within the injured tissue itself has not been previously demonstrated. Since platelets generate an array of proinflammatory mediators and oxygen radicals, they, like leukocytes, might be regarded as both mediator and effector cells<sup>30</sup>. This is further supported by the fact that, in the present study, the accumulation of thrombocytes strongly correlates with that of leukocytes.

#### COX-2 Inhibition in Closed Soft-Tissue Injury

Our data showing the strong ability of parecoxib to limit features of microvascular and inflammatory tissue damage implicate COX-2 as a potential mediator of soft-tissue injury. This view is underscored by the transient upregulation of COX-2, as shown by the time-course studies with use of both Western blot analysis and immunohistochemistry. Comparably, COX-2 has been reported to be upregulated in surgery-associated paraspinal muscle injury, but peak levels were not reached before three days<sup>31</sup>.

Although the present study exclusively focused on the inhibition of the inducible COX-2 isoform in soft-tissue injury, there is evidence that the contribution of each isoform to the prevention or development of disease is more complex than originally described. For example, one study has demonstrated that COX-1 inhibition equals that of COX-2 in efficacy to attenuate lipopolysaccharide-induced hepatic injury<sup>32</sup>. That study and other reports<sup>33,34</sup> have challenged the current paradigm of a selective role of COX-2 in the inflammatory response of tissue to injury. The present observation that soft-tissue trauma caused an increase in COX-1 protein as well as COX-2 suggests that COX-1 may be involved in the response of soft tissue to injury.


Besides their proinflammatory activities, prostaglandins have been shown to be beneficial in the resolution of tissue injury and inflammation. For example, prostacyclin exerts potent antiaggregatory and antiadhesive properties. Thus, inhibition of COX-2 as the predominant prostaglandin endoperoxide synthase not only may be of benefit but also may result in augmentation of the inflammatory response. Accordingly, it has been shown that superfusion of mesenteric venules with the COX-2 inhibitor, celecoxib, promotes leukocyte adherence<sup>35</sup>. Moreover, inhibition of COX-2 exacerbated inflammation-associated colonic injury in colitis models<sup>36</sup> and in both liver and bowel injury upon resuscitation from hemorrhagic shock<sup>37</sup>. However, COX-2 inhibitors have also been used successfully to reduce inflammation, as evidenced by attenuation of ischemic<sup>38</sup> and traumatic brain injury<sup>39</sup>, postischemic liver injury<sup>40,41</sup>, and pancreatitis-associated local and remote organ injury<sup>42,43</sup>. We now report that the acutely injured muscle benefits from immediate COX-2 inhibition, whether it is administered before or after trauma. The observation that preinjury and postinjury admin-

istration of parecoxib provided nearly identical efficacy suggests that COX-2 exerts its deleterious effects not earlier than two hours after trauma in this animal model. This suggests that there might be a therapeutic window to allow for successful postinjury treatment.

Parecoxib-induced reduction of leukocyte response within the injured tissue is presumably due to a reduction in endothelial ICAM (intercellular adhesion molecule)-expression, as this has been shown for the COX-2 inhibitor meloxicam in diabetic retinopathy<sup>44</sup>. Reduced leukocyte adherence in outflow venules of parecoxib-treated animals may be associated with a lower resistance to flow due to a higher cross-sectional area<sup>45</sup>, which, in turn, may indirectly support better capillary perfusion. Moreover, reduced leukocyte adherence goes along with less blood viscosity<sup>46</sup>, which additionally improves microvascular flow conditions.

In summary, the protective effect of COX-2 inhibition implies that COX-2 contributes to trauma-induced soft-tissue injury. COX-1 could also be targeted in order to limit tissue injury, but this approach is hampered by the multiple side effects exerted by the commonly available nonselective COX inhibitors. Thus, selective COX-2 inhibitors exhibiting low side effects may be of superior therapeutic value in protecting the microcirculation and preserving skeletal muscle from secondary inflammatory tissue damage following closed soft-tissue injury.

#### Appendix

 A table presenting the hemodynamic and hematologic parameters measured in all four study groups is available with the electronic versions of this article, on our web site at [jbjs.org](http://jbjs.org) (go to the article citation and click on "Supplementary Material") and on our quarterly CD-ROM (call our subscription department, at 781-449-9780, to order the CD-ROM). ■

Philip Gierer, MD  
Thomas Mittlmeier, MD  
Reingart Bordel  
Georg Gradl, MD  
Brigitte Vollmar, MD

Departments of Experimental Surgery (P.G., R.B. and B.V.) and Trauma and Reconstructive Surgery (P.G., T.M. and G.G.), University of Rostock, Schillingallee 70, 18055 Rostock, Germany. E-mail address for B. Vollmar: [brigitte.vollmar@med.uni-rostock.de](mailto:brigitte.vollmar@med.uni-rostock.de)

Klaus-Dieter Schaser, MD  
Department of Trauma and Reconstructive Surgery, Charité, Campus Virchow, Augustenburger Platz 1, Humboldt University, 13353 Berlin, Germany

The authors did not receive grants or outside funding in support of their research or preparation of this manuscript. They did not receive payments or other benefits or a commitment or agreement to provide such benefits from a commercial entity. No commercial entity paid or directed, or agreed to pay or direct, any benefits to any research fund, foundation, educational institution, or other charitable or nonprofit organization with which the authors are affiliated or associated.

doi:10.2106/JBJS.C.01510

## References

1. Buckwalter JA. Pharmacological treatment of soft-tissue injuries. *J Bone Joint Surg Am.* 1995;77:1902-14.
2. Laing DR, Dalley DR, Kirk JA. Ice therapy in soft tissue injuries. *NZ Med J.* 1973;78:155-8.
3. Cohn BT, Draeger RI, Jackson DW. The effects of cold therapy in the postoperative management of pain in patients undergoing anterior cruciate ligament reconstruction. *Am J Sports Med.* 1989;17:344-9.
4. Brooks PM, Day RO. Nonsteroidal antiinflammatory drugs—differences and similarities. *N Engl J Med.* 1991;324:1716-25. Erratum in: *N Engl J Med.* 1991;325:747.
5. Vane JR, Bakhle YS, Botting RM. Cyclooxygenases 1 and 2. *Annu Rev Pharmacol Toxicol.* 1998;38:97-120.
6. Dubois RN, Abramson SB, Crofford L, Gupta RA, Simon LS, Van De Putte LB, Lipsky PE. Cyclooxygenase in biology and disease. *FASEB J.* 1998;12:1063-73.
7. Andrews JR. Current concepts in sports medicine: the use of COX-2 specific inhibitors and the emerging trends in arthroscopic surgery. *Orthopedics.* 2000;23(7 Suppl):S769-72.
8. Berger RG. Intelligent use of NSAIDs—where do we stand? *Expert Opin Pharmacother.* 2001;2:19-30.
9. Elder CL, Dahners LE, Weinhold PS. A cyclooxygenase-2 inhibitor impairs ligament healing in the rat. *Am J Sports Med.* 2001;29:801-5.
10. Endo K, Sairyo K, Komatsubara S, Sasa T, Egawa H, Yonekura D, Adachi K, Ogawa T, Murakami R, Yasui N. Cyclooxygenase-2 inhibitor inhibits the fracture healing. *J Physiol Anthropol Appl Human Sci.* 2002;21:235-8.
11. Stichtenoth DO, Frolich JC. The second generation of COX-2 inhibitors: what advantages do the newest offer? *Drugs.* 2003;63:33-45.
12. Sokal RR, Rohlf FJ. *Biometry: the principles and practice of statistics in biological research.* 2nd ed. San Francisco: Freeman; 1981.
13. Schaser KD, Vollmar B, Menger MD, Schewior L, Kroppenstedt SN, Raschke M, Lubbe AS, Haas NP, Mittlmeier T. In vivo analysis of microcirculation following closed soft-tissue injury. *J Orthop Res.* 1999;17:678-85.
14. Dixon CE, Clifton GL, Lighthall JW, Yaghai AA, Hayes RL. A controlled cortical impact model of traumatic brain injury in the rat. *J Neurosci Methods.* 1991;39:253-62.
15. Lighthall JW, Dixon CE, Anderson TE. Experimental models of brain injury. *J Neurotrauma.* 1989;6:83-97.
16. Tynl K, Budreau CH. A new preparation of rat extensor digitorum longus muscle for intravital investigation of the microcirculation. *Int J Microcirc Clin Exp.* 1991;10:335-43.
17. Vollmar B, Slotta JE, Nickels RM, Wenzel E, Menger MD. Comparative analysis of platelet isolation techniques for the in vivo study of the microcirculation. *Microcirculation.* 2003;10:143-52.
18. Seifert J, Messmer K. Validity of blood volume determinations in hemorrhagic shock in rats. *Eur Surg Res.* 1971;3:306-16.
19. Mittlmeier T, Vollmar B, Menger MD, Schewior L, Raschke M, Schaser KD. Small volume hypertonic hydroxyethyl starch reduces acute microvascular dysfunction after closed soft-tissue trauma. *J Bone Joint Surg Br.* 2003;85:126-32.
20. Gierer P, Vollmar B, Schaser KD, Andreas C, Gradl G, Mittlmeier T. Efficiency of small-volume resuscitation in restoration of disturbed skeletal muscle microcirculation after soft-tissue trauma and haemorrhagic shock. *Langenbecks Arch Surg.* 2004;389:40-5.
21. Vollmar B, Burkhardt M, Minor T, Klauke H, Menger MD. High-resolution microscopic determination of hepatic NADH fluorescence for in vivo monitoring of tissue oxygenation during hemorrhagic shock and resuscitation. *Microvasc Res.* 1997;54:164-73.
22. Ince C, Coremans JM, Bruining HA. In vivo NADH fluorescence. *Adv Exp Med Biol.* 1992;317:277-96.
23. Chance B, Cohen P, Jobsis F, Schoener B. Intracellular oxidation-reduction states in vivo. *Science.* 1962;137:499-508.
24. Glanemann M, Vollmar B, Nussler AK, Schaefer T, Neuhaus P, Menger MD. Ischemic preconditioning protects from hepatic ischemia/reperfusion-injury by preservation of microcirculation and mitochondrial redox-state. *J Hepatol.* 2003;38:59-66.
25. Menger MD, Rucker M, Vollmar B. Capillary dysfunction in striated muscle ischemia/reperfusion: on the mechanisms of capillary “no-reflow.” *Shock.* 1997;8:2-7.
26. Menger MD, Vollmar B. [Impact of microcirculatory dysfunction on manifestation of postischemic liver injury]. *Chir Gastroenterol.* 2002;18(Suppl 1):46-51. German.
27. Vollmar B, Menger MD. Microcirculatory dysfunction in acute pancreatitis. A new concept of pathogenesis involving vasomotion-associated arteriolar constriction and dilation. *Pancreatol.* 2003;3:181-90.
28. Heideman M, Kaijser B, Gelin LE. Complement activation and hematologic, hemodynamic, and respiratory reactions early after soft-tissue injury. *J Trauma.* 1978;18:696-700.
29. Blomquist S, Thorne J, Elmer O. Different effects of bleeding and soft-tissue trauma on pulmonary platelet trapping in pigs. *J Trauma.* 1989;29:866-72.
30. Klinger MH. Platelets and inflammation. *Anat Embryol (Berl).* 1997;196:1-11.
31. Lu K, Liang CL, Chen HJ, Chen SD, Hsu HC, Chen YC, Hsu FF, Cho CL. Nuclear factor-kappaB-regulated cyclooxygenase-2 expression in surgery-associated paraspinal muscle injury in rats. *J Neurosurg Spine.* 2003;98:181-7.
32. Katagiri H, Ito Y, Ishii K, Hayashi I, Suematsu M, Yamashina S, Murata T, Narumiya S, Kakita A, Majima M. Role of thromboxane derived from COX-1 and -2 in hepatic microcirculatory dysfunction during endotoxemia in mice. *Hepatology.* 2004;39:139-50.
33. Schwab JM, Beschoner R, Meyermann R, Gozalan F, Schluessener HJ. Persistent accumulation of cyclooxygenase-1-expressing microglial cells and macrophages and transient upregulation by endothelium in human brain injury. *J Neurosurg.* 2002;96:892-9.
34. Loftin CD, Tiano HF, Langenbach R. Phenotypes of the COX-deficient mice indicate physiological and pathophysiological roles for COX-1 and COX-2. *Prostaglandins Other Lipid Mediat.* 2002;68-69:177-85.
35. Muscara MN, Vergnolle N, Lovren F, Triggler CR, Elliott SN, Asfaha S, Wallace JL. Selective cyclooxygenase-2 inhibition with celecoxib elevates blood pressure and promotes leukocyte adherence. *Br J Pharmacol.* 2000;129:1423-30.
36. Reuter BK, Asfaha S, Buret A, Sharkey KA, Wallace JL. Exacerbation of inflammation-associated colonic injury in rat through inhibition of cyclooxygenase-2. *J Clin Invest.* 1996;98:2076-85.
37. Tsukada K, Hasegawa T, Tsutsumi S, Kuwano H. Roles of cyclooxygenase-2 in tissue injury during hemorrhagic shock. *Shock.* 2000;13:392-6.
38. Nakayama M, Uchimura K, Zhu RL, Nagayama T, Rose ME, Stetler RA, Isakson PC, Chen J, Graham SH. Cyclooxygenase-2 inhibition prevents delayed death of CA1 hippocampal neurons following global ischemia. *Proc Natl Acad Sci USA.* 1998;95:10954-9.
39. Cernak I, O'Connor C, Vink R. Inhibition of cyclooxygenase 2 by nimesulide improves cognitive outcome more than motor outcome following diffuse traumatic brain injury in rats. *Exp Brain Res.* 2002;147:193-9.
40. Sunose Y, Takeyoshi I, Ohwada S, Tsutsumi H, Iwazaki S, Kawata K, Kawashima Y, Tomizawa N, Matsumoto K, Morishita Y. The effect of cyclooxygenase-2 inhibitor FK3311 on ischemia-reperfusion injury in a canine total hepatic vascular exclusion model. *J Am Coll Surg.* 2001;192:54-62.
41. Ito Y, Katagiri H, Ishii K, Kakita A, Hayashi I, Majima M. Effects of selective cyclooxygenase inhibitors on ischemia/reperfusion-induced hepatic microcirculatory dysfunction in mice. *Eur Surg Res.* 2003;35:408-16.
42. Foitzik T, Hotz HG, Hotz B, Wittig F, Buhr HJ. Selective inhibition of cyclooxygenase-2 (COX-2) reduces prostaglandin E2 production and attenuates systemic disease sequelae in experimental pancreatitis. *Hepatogastroenterology.* 2003;50:1159-62.
43. Song AM, Bhagat L, Singh VP, Van Acker GG, Steer ML, Saluja AK. Inhibition of cyclooxygenase-2 ameliorates the severity of pancreatitis and associated lung injury. *Am J Physiol Gastrointest Liver Physiol.* 2002;283:G1166-74.
44. Jousseaume AM, Poulaki V, Mitsiades N, Kirchhof B, Koizumi K, Dohmen S, Adamis AP. Nonsteroidal anti-inflammatory drugs prevent early diabetic retinopathy via TNF-alpha suppression. *FASEB J.* 2002;16:438-40.
45. House SD, Lipowsky HH. Leukocyte-endothelium adhesion: microhemodynamics in mesentery of the cat. *Microvasc Res.* 1987;34:363-79.
46. Chien S. Role of blood cells in microcirculatory regulation. *Microvasc Res.* 1985;29:129-51.